The electrical behaviour of C4-FN/CO2 (5%/95%) with varying humidities and operating conditions

By

Ewout van Veldhuizen

To obtain the degree of Master of Science in Electrical Engineering,
at the Delft University of Technology.
To be defended publicly on Thursday 8th of June 2023.

Supervisor:	Dr. Ir. Mohamad Ghaffarian Niasar Ir. André Lathouwers
Thesis Committee:	Prof. Ir. Peter Vaessen Dr. Ir. Mohamad Ghaffarian Niasar Dr. Ir. Milos Cvetkovic Ir. André Lathouwers

Delft University of Technology

Acknowledgments

The work that has been performed in this research has been made possible through the effort of many people. Therefore I would like to thank the following people for supporting me during this master thesis project;

The technicians of the High Voltage Lab of TU Delft: *Ir. Paul van Nes, Ir. Imke Splinter* and *Wim Termorshuizen*.
Paul van Nes and *Imke Splinter*, who helped and guided me through the experiments in the lab and who explained much about the different High Voltage equipment in the lab.
Wim Termorshuizen, who crafted all the test cells and electrodes that I used during this research.

The supervisors/professors of the High Voltage group: *Prof. Ir. Peter Vaessen, Dr. Ir. Mohamad Ghaffarian Niasar* and *Fellow André Lathouwers,* who guided me along the journey of performing experiments in the High Voltage Lab, asking important questions which answers improved the quality of the research.

And a special thanks to *PhD student Christian Mier Escurra* who helped and guided me with his knowledge about partial discharges through the partial discharge measurements.

Summary

A goal of the Paris Agreement (2021) is to reduce the greenhouse gas emissions by at least 40% by 2030 compared to 1990. Therefore SF6 is being phased out as insulation gas in Medium Voltage (MV) and High Voltage (HV) applications and needs to be replaced with a more eco-friendly insulation gas. A Fluoronitrile gas mixture shows the most promise as this replacement, especially for HV applications. TenneT has multiple pilots with this new gas, among them a Gas Insulated Line (GIL) in Meeden. However there are still some problems with this particular GIL. Multiple electrical breakdowns have occurred during a Site Acceptance Test (SAT). TenneT hypothesizes that too much humidity in the insulation gas is responsible for the electrical breakdowns. This master thesis has as objective to test and to examine the hypothesis of TenneT, i.e. examining the electrical behaviour of a Fluoronitrile gas mixture with varying humidities and operating conditions.

The objective of this master thesis is met by answering research questions that investigated the AC insulation performance of a Fluoronitrile gas mixture with a varying amount of humidity in the gas. Also the AC insulation performance of a humid Fluoronitrile gas mixture at different operating pressures is investigated. Furthermore, the partial discharge (PD) behaviour of corona in a Fluoronitrile gas mixture is investigated. This is achieved by comparing the Partial Discharge Inception Voltage (PDIV), the Phase Resolved Partial Discharge (PRPD) pattern and some of the PD characteristics (e.g. rise time, fall time) of corona in a dry and humid Fluoronitrile gas mixture.

The findings of the experimental work confirm the hypothesis of TenneT. Humidity does influence the electrical behaviour of a Fluoronitrile gas mixture. An increase in the amount of humidity in the gas results in a decrease of the AC insulation performance. This also applies to higher operating pressures, although the influence of humidity on the AC insulation performance decreases as the operating pressure increases. The PD behaviour of corona in a Fluoronitrile gas mixture is also affected by the presence of humidity in the gas. The PRPD pattern and PD characteristics of corona in a Fluoronitrile gas mixture differ with the presence of much humidity in the gas, as the charge of the corona discharges in a humid Fluoronitrile gas mixture are larger. The PDIV however did not change with the presence of much humidity in the gas.

The results of this master thesis will help TenneT, and other users, with the transition to a Fluoronitrile gas mixture. TenneT can now think of (extra) mitigating measures to prevent high amounts of humidity in HV equipment. Therefore preventing electrical breakdowns as a consequence of high humidity levels in the Fluoronitrile gas mixture.

Index

List of definitions and abbreviations

Word	Definition
Absorbed (moisture)	Water molecules that permeate into materials. The degree to which water permeates is dependent on the structure and type of the material.
AC	Alternating current.
Adsorbed (moisture)	Water molecules that adhere to and accumulate on the surfaces of solids.
BD(s)	Breakdown(s).
Breakdown behaviour of C4-FN/CO2 (5%/95%)	Shows the behaviour of the breakdown strength of C4-FN/CO2 (5%/95%) over a variation of a parameter.
CDF	Cumulative Density Function is represented by $F_X(x) = P(X \leq x)$, where the right side represent the probability that the random variable X takes on a value less than or equal to x. The boundary of the probability is [0,1] where 0 equals 0% and 1 equals 100%.
Characteristic impedance	Characteristic impedance is determined by the geometry and materials of the transmission line and is not dependent on its length.
CT	Current transformer.
DC	Direct current.
Desorption (moisture)	Releasing water molecules from a material.
Delta	The difference between the minimum and maximum measured breakdown voltage of C4-FN/CO2 (5%/95%) during an experiment, where an experiment consisted out of 10 breakdown repetitions.
Discontinuity	A change in impedance of the circuit.
Dry	Gas with extremely low dewpoint temperature, e.g. <-50°C.
Electrical Breakdown	A phenomenon which occurs when insulation is stressed over its maximum withstand capabilities. An electrical breakdown creates a conductive path between two conductors when $E_{applied} > E_{max\ of\ insulation}$.
Enclosure	Metallic pipe constructure of High Voltage equipment. To contain the insulation gas in the HV equipment.
Fall time	The time taken for the amplitude of a pulse to fall from 90% to 10% of its maximum amplitude.
Flushing	A process in which a gas is blown through an object. To rid the object of certain external properties, e.g. humidity or gas particles.
Humid	Gas with certain dewpoint temperature that is higher than the dewpoint temperature of the dry gas, e.g. >-50°C.
Humidity	Gaseous state of water.
HV	High Voltage.
Hydrolysis	Any chemical reaction in which a molecule of water breaks one or more chemical bonds.
Intrinsic electric breakdown strength	Is the breakdown strength of a material if all interfering effects are prevented. Those effects are caused by impurities in the material.
Moisture	Liquid state of water.
η-factor	Field utilization factor. It can summarise simple electric field configurations.
PD(s)	Partial Discharge(s).
PDIV	Partial Discharge Inception Voltage. Is the voltage at which discharges with a certain amplitude start occurring at a steady rate.
PRPD pattern	Phase Resolved Partial Discharge pattern. The partial discharges placed in the phase of the applied voltage.

Phase Ø	Phase of applied voltage at the time of partial discharge pulse occurrence. The phase angle is expressed in degrees (°).
Ppmv	Used to specify an amount of humidity in a gas mixture. Depends on the pressure of the gas and the water vapor partial pressure.
Primary side	The low voltage side of a transformer (in this thesis).
Pulse repetition rate n	Ratio between the total number of partial discharge pulses recorded in a selected time interval and the duration of this time interval.
Retention time	In chromatography it is the interval between the injection of a sample and the detection of substances in that sample.
Rise time	The time taken for the amplitude of a pulse to rise from 10% to 90% of its maximum amplitude.
Secondary side	The high voltage side of a transformer (in this thesis).
U_{50}	Corresponds to the applied voltages which gives a 50% probability of producing a breakdown between electrodes.
UBD	Breakdown Voltage.

1 Introduction

This chapter gives an introduction of the research that is performed in this report. The first section introduces the research topic by providing background information. The second section describes the motivation of this research. Afterwards the research objective and the appurtenant research questions are given. The last section outlines the structure of the report.

1.1 Background information

The electrical grid is the largest machine made by humans. The electrical grid contains a variety of High Voltage (HV) equipment. Some of that HV equipment uses an insulation gas. Examples of such equipment are: Circuit Breaker (CB), Gas Insulated Switchgear (GIS) and a Gas Insulated Line (GIL). This insulation gas has to have certain specific electrical properties. For many decades, even up to today, that insulation gas is SF6. SF6 has excellent electrical properties but is a strong greenhouse gas, i.e. SF6 has a high Global Warming Potential (GWP) of 23.500. This means that one kilogram of SF6 absorbs the same heat as 23.500kg of CO2 based on a 100-year period. A goal of the Paris Agreement (2021) is to reduce the greenhouse gas emissions by at least 40% by 2030 compared to 1990 [1]. Therefore SF6 is being phased out and a new insulation gas is needed. The new insulation gas must have similar electrical properties as that of SF6 but a much lower GWP.

A lot of research has been done in finding a new insulation gas. Fluoronitrile, abbreviated with C4-FN, shows the most promise as this new insulation gas, especially for HV applications [2]. Fluoronitrile has a GWP of roughly 9% of the GWP of SF6. Furthermore, C4-FN is used as a gas mixture often mixed with CO2 in the molar ratio of <20% C4-FN and >80% CO2. This reduces the GWP of the insulation gas in HV applications over 99%. 3M has developed C4-FN/CO2 (3,5%/96,5%) under the commercial name 3M Novec™ 4710 insulation gas. GE has developed C4-FN/CO2 (5%/95%) under the commercial name g^3, which stand for Green Gas for Grid.

1.2 Motivation

TenneT has multiple pilots of C4-FN containing gases, among them a GIL in Meeden. Multiple electrical breakdowns (BDs) occurred in that GIL during the Site Acceptance Test (SAT). The inside of the GIL in Meeden was inspected after the failed SAT. The inspection discovered that the inside of the GIL contained some unknown crystals. Research has shown that those crystals are formed if there is too much humidity in the insulation gas[3]. TenneT thinks that there is a link between the electrical breakdowns and the high amounts of humidity as well. The hypothesis of TenneT is that too much humidity in the insulation gas is responsible for the electrical breakdowns.

1.3 Research objective and research questions

The hypothesis of TenneT is to be tested in this master thesis. The research objective is to examine:

"The electrical behaviour of C4-FN/CO2 (5%/95%) with varying humidities and operating conditions"

Two research stages A and B, each with two research questions, have been devised to meet the research objective. The four research questions are:

Phase A – How does humidity affect the AC insulation performance of C4-FN/CO2 (5%/95%)?

[A-1] How is the AC breakdown strength of C4-FN/CO2 (5%/95%) influenced by different humidities?
[A-2] How does humidity affect the AC breakdown strength of C4-FN/CO2 (5%/95%) at different operating pressures?

Phase B – How does humidity affect the Partial Discharge behaviour of corona in C4-FN/CO2 (5%/95%)?

[B-3] How does humidity affect the partial discharge behaviour of corona in C4-FN/CO2 (5%/95%)?
[B-4] How does humidity affect the characteristics of a corona discharge in C4-FN/CO2 (5%/95%)?

1.4 Structure of the report

This report contains six chapters and three appendices. The introduction on this master thesis is given in the first chapter. The second chapter delineates the research. Chapter three covers the literature study of this master thesis. The literature study gives elaborate background information on the delineated topics of the second chapter. The fourth chapter describes all the methods and equipment that are involved in answering the four research questions. Some of the equipment and methods that are explained in the fourth chapter needed to be created, refined or examined. The process of creating, refining and examining certain methods and equipment is elaborately explained in appendix A. The fifth chapter answers each of the four research questions separately by explaining the findings and results of the performed experiments. The last chapter gives concise answers to each of the research questions and the conclusion of this research. It also covers the recommendations for further investigation of the electrical behaviour of C4-FN/CO2 (5%/95%).

2 Delineating the research topic

The unrefined thesis objective was: *"Investigate the effect of humidity on Fluoronitrile".* The Fluoronitrile gas mixture is to be used inside HV equipment. The gas has therefore many specific requirements. The effect of humidity can consequently be very broad. Certain conditions have to be delineated in order to successfully investigate the thesis objective. This chapter delineates the research on the Fluoronitrile gas mixture to a more specific thesis objective.

2.1 Delineating the electrical function of the Fluoronitrile gas mixture

There are a number of requirements that have to be met in order for a gas mixture to be used for insulation inside HV equipment, especially for a GIS. The gas in some part of a GIS must be an good electrical *interrupter* for the arcs that will be created inside the circuit breakers and switches. The gas inside a GIS must also be an good electrical *insulator* to accommodate the high voltage.
This research focuses only on the electrical insulation capabilities of the Fluoronitrile gas mixture and not the current interrupting capabilities of the Fluoronitrile gas mixture.

2.2 Delineating the electrical behaviour that is to be examined

The Fluoronitrile gas mixture must be able to operate normally under different electrical stresses. There are a number of tests to investigate the electrical insulation behaviour of the Fluoronitrile gas mixture. The Fluoronitrile gas mixture is labelled as a good electrical insulator only if it passes all the different test. These tests include: AC/DC voltage test, lightning impulse voltage test, switching impulse voltage test and Very Fast Transients (VFT) [4].

There is often a lot of electrical activity before an electrical breakdown in AC or DC. This electrical activity can be monitored by measuring the activity of partial discharges.
This research focuses on the AC voltage test on the Fluoronitrile gas mixture and also on a small part of the partial discharge activity in the Fluoronitrile gas mixture.

2.3 Delineating the effect of humidity

Only the effect of the gaseous state of water on the electrical insulation performance of the Fluoronitrile gas mixture is considered in this research. The effect of the other states, i.e. solid and liquid, are not considered in this research.

The Fluoronitrile gas mixture can decompose due to unwanted electrical activity and create various by-products. Examples of unwanted electrical activity are: partial discharges, breakdown and arcing. Water can react with some of the by-products of the Fluoronitrile gas mixture and form corrosive by-products[5]. These corrosive by-products will have an effect on the HV equipment which can also in turn influence the electrical insulation performance of the gas mixture.
This research only focuses on the direct influence of humidity on the electrical performance of the Fluoronitrile gas mixture.

2.4 Summary

This chapter delineated the thesis objective. This thesis has now a refined thesis objective. The thesis objective is to examine: *"the effect of humidity on the electrical insulation performance of the Fluoronitrile gas mixture*". This is achieved by examining:

- The effect of humidity on the AC breakdown strength of the Fluoronitrile gas mixture.
- The effect of humidity on the partial discharge activity in the Fluoronitrile gas mixture.

3 Literature study

The previous chapter delineated the specific requirements of the investigation on the effect of humidity on the electrical insulation performance of a Fluoronitrile gas mixture. The delineation resulted in three specific requirements that are taken into account for this research. This chapter gives some background information on those three requirements;

1. Humidity inside HV equipment, discussed in section 3.1.
2. Electrical behaviour of Fluoronitrile that is to be examined, discussed in section 3.2.
3. Electrical insulation performance of Fluoronitrile, discussed in section 3.3.

3.1 Humidity inside HV equipment

This section explains the origin of humidity in HV equipment. In this section a GIS is used as example of HV equipment. First, the origin of water inside a GIS is explained. Afterwards it is explained where the humidity inside a GIS originates from. Lastly, some data is shown on humidity measurements inside a GIS.

3.1.1 Origin of water inside HV equipment

There are different mechanisms on how water can penetrate a GIS [6]:

1. Water can infiltrate into a GIS through leaking points, created by corrosion on the enclosure. The water will creep into the enclosure despite the pressure difference between the atmosphere and the insulation gas inside the enclosure.
2. Water can permeate through the rubber seals between enclosure compartments.
3. Water can originate from a bad installed cable termination.
4. Water desorption from the GIS itself, i.e. the conductor, the spacer and the internal surface of the enclosure.

Research has shown that the moisture inside a GIS is mainly caused by mechanism four, the ab- and adsorption of water into and onto the GIS components. The root of mechanism four happens during the fabrication, storage, transport and installation of the GIS components. During which period, depending on the surroundings, water can be ab- and adsorbed from the surrounding into and onto the GIS components [6]. The GIS components, especially spacers, will absorb and desorb the moisture during temperature fluctuations. The temperature fluctuations are caused by the operation of the GIS. The cause for the temperature fluctuations during operation will be explained in the next section, i.e. section 3.1.2.

The other mechanisms do not significantly contribute to the increase in moisture inside a GIS [6]. By using an absorbing media, like desiccants cannisters or molecular sieves, the amount of moisture in a GIS can be limited[6,7].

3.1.2 Origin of humidity inside HV equipment

The previous section explained that moisture will always be present inside a GIS. Water can also be present in other states, e.g. gas (i.e. humidity). This depends on two conditions.

1. **Dewpoint temperature of the insulation gas:**
   Whether a molecule will be in its gaseous, liquid or solid state will depend on the characteristics of the molecule and its environment. The dewpoint is one of the characteristics. A molecule will transform from its gaseous state into a liquid state if the temperature of the molecule is equal to or lower than its dewpoint temperature. The dewpoint temperature is a product of the temperature of the gas and the relative humidity of the gas [8].

2. **The temperature of the insulation gas:**
    a. The operating pressure inside a GIS:
    A deviation in the pressure correspond to a deviation in the temperature. This is shown by the ideal gas law, $PV = nRT$. Where P is pressure [Pa], V is volume [m^3], n is the amount of substance [mol], R is the universal gas constant and T is temperature [K]. The ideal gas law says that the pressure and temperature must change accordingly if V, R and n are constant, i.e. P_1/T_1 must be equal to P_2/T_2.
    b. Ambient temperature:
    A GIS can be installed indoor or outdoor. The ambient temperature is often in a stable range. i.e. around room temperature, if a GIS is installed indoor. The ambient temperature is the temperature of the atmosphere around the GIS if a GIS is installed outdoor. That means that the temperature can vary a lot and the variations depend on the location of the GIS, i.e. the climate.
    c. Operating temperature:
    A GIS can have a high (continuous) current (>kA) depending on the load conditions. This current will heat the conductor which will heat the gas.

    Figure 3.1 shows a temperature profile of an outdoor experimental GIS set-up. The current is $4000A_{RMS}$ for 17 hours and $0A_{RMS}$ for 7 hours. The temperature of the insulation gas varied between the temperature of the conductor and the (bottom of the) enclosure, i.e. 60°C and 20°C. The 60°C was a consequence of the operating temperature and the 20°C was a consequence of the ambient temperature.

Moisture will turn into humidity if the temperature is high enough and the dewpoint temperature low enough. This humidity will ultimately be mixed with the insulation gas.

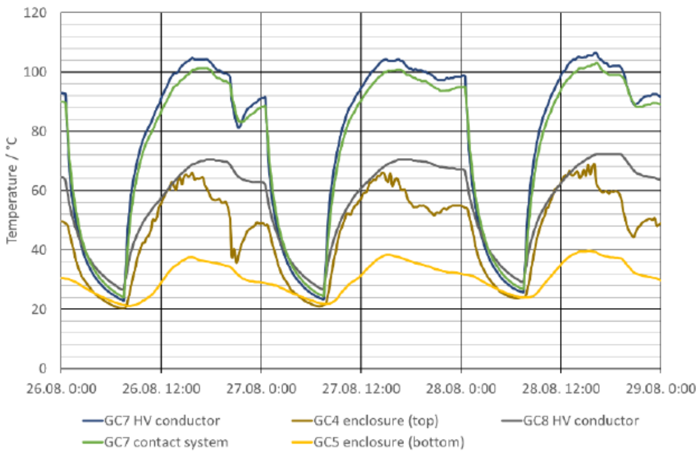

Figure 3.1 Temperature profile of an experimental GIS set-up [9].

3.1.3 Humidity measurement inside a GIS

There are different units to identify the amount of humidity. The most used and recommended unit is Parts Per Million by Volume (ppmv). This is an ideal unit since it is only dependents on the dewpoint temperature and pressure of the gas. Manufactures of GIS and different standards (IEC and CIGRE) all have different limits concerning humidity. The humidity is allowed to vary between circa 150 ppmv and 840 ppmv, depending on operating voltage and pressure [6,9].

Figure 3.2 shows four different scenario's in which the humidity is measured. Subfigure a and b show the importance of a desiccant, like a molecular sieve, to minimize the amount of humidity in a GIS.

Subfigure c and d show a comparison between humidity in the summer and winter days. The figures emphasizes the effect of the temperature on the amount of humidity. In the summer days the temperature is higher, which results in more moisture desorption of the material, which ultimately increases the amount of humidity. It is to be noted that only humidity is measured and no moisture, since the measuring method only is able to measure the gaseous form of water [7].

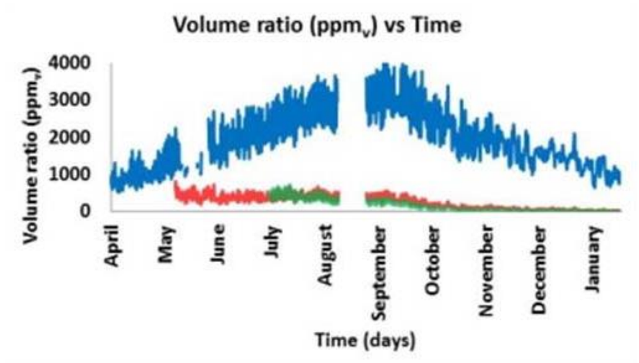

a) Humidity measured over 256 days with and without molecular sieve(s).

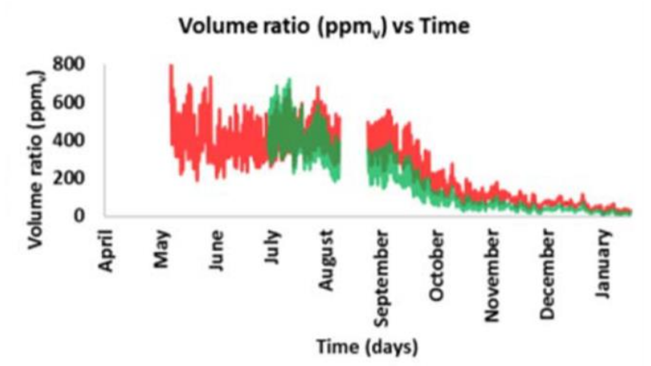

b) A more detailed overview of the measured humidity with molecular sieve(s) over 256 days.

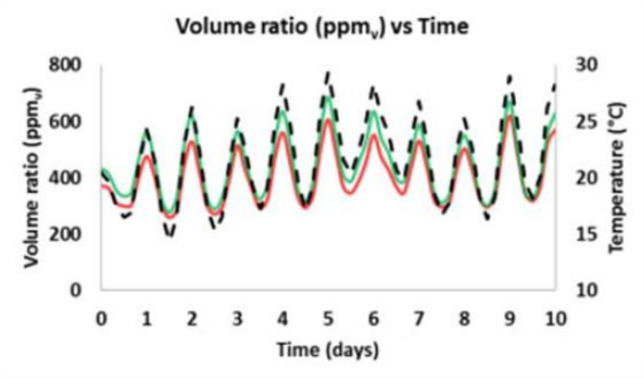

c) Humidity measured during summer days.

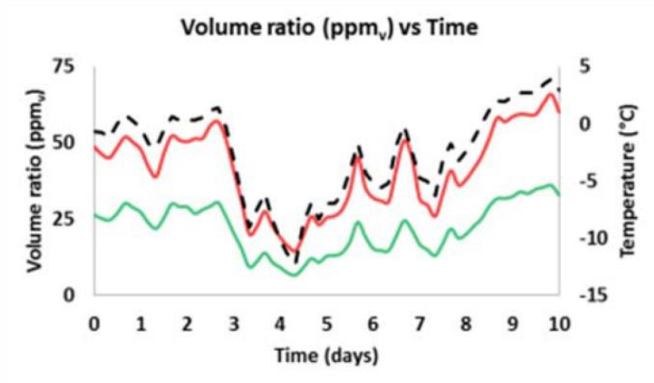

d) Humidity measured during winter days.

---- = ambient temperature ---- = without molecular sieve ---- = with one molecular sieve ---- = with two molecular sieves

Figure 3.2 Different amounts of humidity measured over different periods of time. With a similar climate found in Canada [7]. The gap in the measurements was caused by an error in the measuring equipment. The temperature is the ambient temperature as it is an outdoor GIS.

3.2 The electrical behaviour of Fluoronitrile that is to be examined

This section explains the electrical behaviour that is to be examined during this research, i.e. AC breakdown and partial discharges. The first section gives a short overview of partial discharges. It is explains how partial discharges arise, describes the different kind of partial discharges and describes different methods with which the partial discharges can be measured. The last section explains the requirements for an breakdown in AC.

3.2.1 Partial Discharges

What is a partial discharge?

A partial discharge is a localized dielectric breakdown that does not completely bridge the space between two electrodes. Partial discharges happen as a result of localized stress in a dielectric insulation. Partial discharges in HV equipment will over a long time cause degradation of the insulation material. The partial discharge activity is therefore a good diagnostic signal for assessing the condition of the insulation inside the HV equipment [10].

How is a partial discharge created?

A partial discharge is initiated by an initial available electron. This electron can come from different mechanisms, for example come from radiation (e.g. radio-active or cosmic). The electron travels from the cathode to anode, due to the electric field. The electron will be accelerated by the electric field, gaining kinetic energy (W). The kinetic energy can be calculated wit $W\ [eV] = eE\lambda$, where e is the charge of an electron [C], E is the electric field [V/m] and λ is the mean free path [m]. A number of things can happen if the electron collides with an atom/molecule. Two of them are ionization and attachment, together they form the effective ionization factor.

A successful ionization can be seen as: $A + e \rightarrow A^{+} + 2e$. The electron liberates an electron from atom/molecule A, giving it a positive charge. A successful attachment can be seen as: $A + e \rightarrow A^{-}$. The electron is absorbed by atom/molecule A, giving it a negative charge.

Successful ionizations cause an avalanche and the process repeats itself. These avalanches cause a leakage current. Therefore partial discharges can be measured by measuring the leakage current [10].

The book *"Industrial High voltage"* by *F.H. Kreuger* explains with more detail the creation and occurrence of partial discharges [11].

Different kind of partial discharges

A partial discharge will originate at a location with electric field enhancement. There are many sources which cause an electric field enhancement [12]. These Partial discharge sources can be classified into 3 categories [10]. There are other factors, besides the defect source, which affect partial discharge generation [2]. Table 3.1 gives an overview on these different parameters. Elaborate information on these parameters can be found in their respective reference paper.

Partial discharge sources [12]	Free metal particles defect, insulator gap defect, metal protrusion defect, moving particle, floating electrode and insulator metal pollution.
Partial discharge categories [18]	Internal partial discharge, surface partial discharge and corona partial discharge
Factors affecting partial discharge generation [2]	Electrode geometry, contamination geometry, electrode surface roughness and the properties of the insulation material

Table 3.1 An overview on different parameters related to creation of partial discharges.

Each partial discharge source has its own characteristics, such as; magnitude, phase, rate and rise/fall time, etc. This makes it possible to recognize partial discharges by examining their characteristics.

Measuring methods of partial discharges

There are different methods for measuring partial discharges. These methods can be divided into two categories. Table 3.2 gives an overview of these different methods. Partial discharges in this research are measured according to the conventional method, i.e. IEC60270 [13]. The unconventional methods are not used during this research and are therefore not explained. The unconventional methods are explained in CIGRE brochure D1.33 [14]. The IEC60270 is called the conventional method because it is a well-established measuring method for factory and laboratory testing. Figure 3.3 shows a typical circuit for measuring partial discharges conform the IEC60270.

Conventional method [13]	**Unconventional methods [14]**
- IEC60270	- Electromagnetic - Optical - Acoustic - Chemical

Table 3.2 Different methods to measure partial discharges.

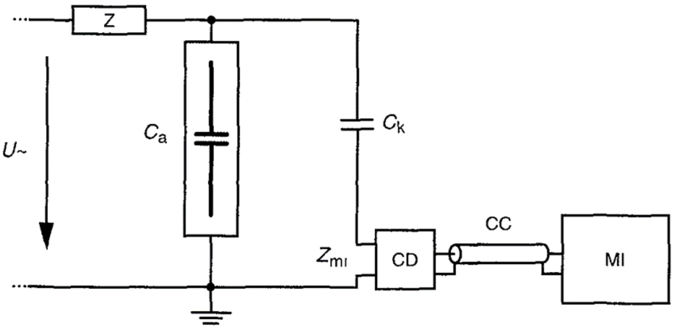

U~ = supply voltage
Z = input impedance
C_k = coupling capacitor
C_a = test object
CC = connecting cable
CD = coupling device
MI = measuring instrument

Figure 3.3 A typical PD measurement circuit conform IEC60270 [13].

The coupling capacitor ensures that partial discharges will circulate and makes it therefore possible to measure the partial discharges. It is important to choose the coupling capacitor around the same value as the test object, to achieve optimum sensitivity for the measurement.
The coupling device is usually a four-terminal network (quadripole) that converts the input currents to output voltage signals and measures the applied voltage and phase.
The input impedance makes sure that the PD pulses do not circulate back to the source side, but will circulate through the coupling capacitor. It also serves as a current limiter in case of a breakdown.

The conventional method allows the measurement of many partial discharge characteristics. All of these characteristics can be found in IEC60270 [13]. In this research the PRPD pattern of a metal protrusion defect (corona) in the Fluoronitrile gas mixture was measured. Therefore, several characteristics were measured; the pulse repetition (n), the charge (q) and the phase of the applied voltage (Ø). An example of a PRPD pattern of corona is visible on Figure 3.4.

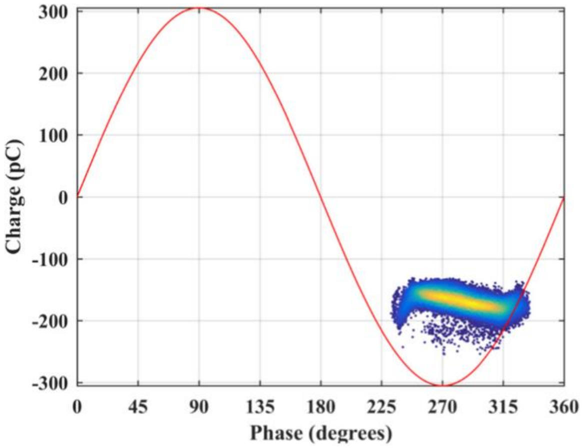

Figure 3.4 A typical PRPD pattern of corona measured in SF6 [15].

3.2.2 AC breakdown

In section 3.2.1 it was explained that an initial electron in an electric field can cause an avalanche. An avalanche can only create partial discharges. An avalanche cannot create a breakdown on its own. A feedback process is required in order to create a complete breakdown between the electrodes. The kind of feedback process depends on the mechanism which started the partial discharge [11].

For example, the ϒ-process is needed as feedback to create a breakdown in gases where the start mechanism is the Townsend mechanism. In the ϒ-process an ion collides with the cathode and releases a new electron. These electrons are called secondary electrons and cause new avalanches. There is an electrical breakdown if there are enough electrons between the electrodes [11].

3.3 Electrical insulation performance of Fluoronitrile

In general, the electrical insulation performance of an electrical system does not only depend on the insulation gas, but also depends on other factors. The insulation performance is determined by the following aspects;

1. The electrical properties of the insulation gas.
2. Field configuration (uniform, quasi-uniform and non-uniform electric fields).
3. Electrode surface roughness.
4. Shape and polarity of applied voltage.

This section only explains the first point, i.e. the electrical properties of the insulation gas. The electrical properties of the insulation gas depends on a couple parameters. The following parameters are elaborated in this section;

1. The electric strength of Fluoronitrile.
2. The gas composition of the Fluoronitrile gas mixture.
3. The chemical stability of the Fluoronitrile gas mixture.

A small section, section 3.3.4, discusses the formation of the crystals in a Fluoronitrile gas mixture and the effect of those crystals on the electrical properties of the Fluoronitrile gas mixture.

It is to be noted that (pure) Fluoronitrile is abbreviated to C4-FN. A gas mixture of Fluoronitrile and carbon dioxide is abbreviated to C4-FN/CO2 (*xx*%/*yy*%). (*xx*%/*yy*%) is the specific molar concentration of the gas mixture, i.e. *xx*% Fluoronitrile and *yy*% carbon dioxide.

3.3.1 The electric strength of the Fluoronitrile gas mixture

Table 3.3 shows a comparison of some important parameters of C4-FN and SF6 in their purest form. C4-FN is a more electronegative gas compared to SF6. Therefore C4-FN is a better electrical insulator compared to SF6 at equal pressure and temperature.

The electronegativity of a gas is directly related to the effective ionization coefficient. Section 3.2.1 explained that the effective ionization coefficient is related with the ionization and attachment of electrons. The initial electron travels from cathode to the anode and creates $\alpha \cdot dx$ new electrons due to successful ionizations. Some of these electrons do not gain sufficient energy and $\eta \cdot dx$ electrons are re-absorbed in the gas molecules due to unsuccessful ionizations. This results in an effective ionization of $\alpha_{eff} = \alpha - \eta$.

Figure 3.5 shows the reduced effective ionization coefficient against the reduced electric field strength of different gases or gas mixtures. The reduced electric field strength can be calculated with Equation 3-1 where U_{BD} is the breakdown voltage [V], d is the distance between the electrodes [m], K_B is the Boltzmann constant, T is the temperature [K], p is the pressure [Pa] and N is the density of the gas [15].

The electric strength of different gas mixtures can easily be compared by comparing their critical reduced electric field strength. The critical reduced electric field strength $(E/N)_{cr}$ is where the reduced effective ionization coefficient of zero, i.e. the ionization is equal to the attachment. It can be seen from Figure 3.5 that $(E/N)_{cr}$ of C4-FN is much higher compared to the $(E/N)_{cr}$ of SF6. This means that C4-FN needs a much stronger electric field to have an equal effective ionization coefficient as that of SF6. The same principle applies to C4-FN/CO2 (3,7%/96,3%) and SF6. The $(E/N)_{cr}$ of C4-FN/CO2 (3,7%/96,3%) is lower than the $(E/N)_{cr}$ of SF6. Therefore, a breakdown in C4-FN/CO2 (3,7%/96,3%) will require a lower voltage compared to a breakdown in SF6. This can also be seen in Figure 3.6.

$$\frac{E}{N}\,(Td) = \frac{U_{BD}}{d} \cdot \frac{k_B \cdot T}{p} \cdot 10^{21}$$

Equation 3-1

Property \ Gas	100% SF6	100% C4-FN
Chemical formula	SF6	$(CF_3)_2CFCN$
Relative electric strength (% of SF6)	1	>2
Boiling point [°C]	-50,8	-4,7
Global Warming Potential (GWP)	23.500	~2100
Atmospheric Lifetime [years]	3200	30

Table 3.3 Properties of pure (100%) SF6 and pure (100%) C4-FN [2,16].

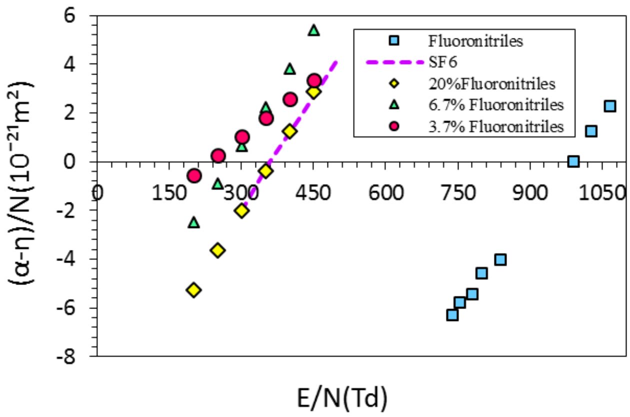

Figure 3.5 Density-reduced effective ionization coefficient, (α-η)/N, as a function of E/N for the C4-FN/CO2 mixtures and SF6 [2].

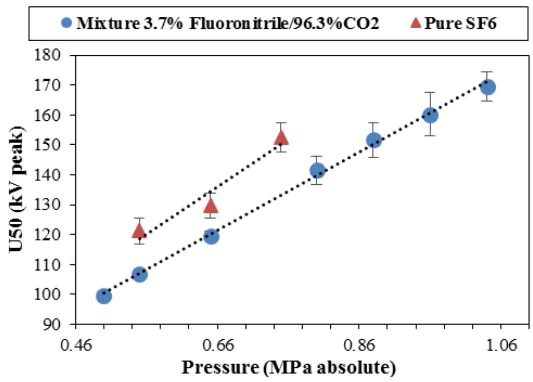

Figure 3.6 AC breakdown voltages of C4-FN/CO2 (3,7%/96,3%) and pure SF6 as function of pressure for a 5mm sphere-plane electrode gap configuration [2].

Despite its excellent electrical insulation properties, the insulation gas will not be pure C4-FN. A mixture of C4-FN with natural gases is used, the reason will be given in the next section, i.e. section 3.3.2. These natural gases have a low electric strength, which will decrease the overall electric insulation strength of the gas mixture. For example, at 420 kV a mixture of C4-FN/CO2 (5%/95%) will reach 70 % of the electric insulation strength of pure SF6 at the same pressure [2].

Two things can be done to give of C4-FN/CO2 (*xx*%/*yy*%) the same electric strength as that of SF6;

- Increase the pressure of the gas mixture.
  The effect of the operating pressure on the breakdown strength can be seen on Figure 3.6. The pressure (p) has an direct effect on the kinetic energy (W) of an electron during an avalanche, $W = eE\lambda :: E/p$. Increasing the pressure decreases the free path of an electron, resulting in lower kinetic energy. Therefore decreasing the chance on a successful collision. The voltage needs to be increased in order for the electron to gain enough energy to cause a successful collision [11].
- Increase the percentage of C4-FN present in the gas mixture.
  Figure 3.7 shows that an increase of C4-FN in a gas mixture of will result in a higher breakdown strength.

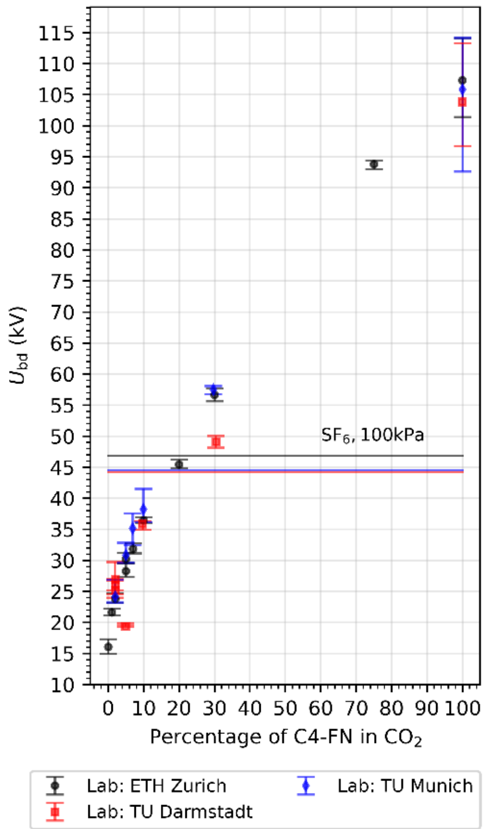

Figure 3.7 Synergy scan of a mixture of C4-FN in CO2 at 100 kPa compared with SF6 at 100 kPa (horizontal lines) for AC breakdowns in an uniform arrangement [2].

3.3.2 The gas composition of the Fluoronitrile gas mixture

Section 3.3.1 mentioned that the insulation gas will not be pure C4-FN. Pure C4-FN is not suitable for various operating conditions, because the boiling temperature of C4-FN is relatively low, i.e. -4,7 °C. This means that the gas below that temperature will liquify at which it is no electrical insulator anymore. Which makes it unsuitable for GIS operation since the minimum ambient temperature for a GIS can range from -50°C to -5°C, depending on the location (indoor/outdoor/special application in cold countries) [17]. Therefore the electric insulation gas has to be a mixture of C4-FN with other natural gases.

Natural gases, like N2 and CO2, have a lower boiling temperature and will thus decrease the overall boiling temperature of a C4-FN gas mixture. CO2 is chosen as carrier for the C4-FN gas mixture making it more reliable for lower ambient temperatures [2]. The mixture can also contain some O2. O2 is added in the CB's to reduce the amount of decomposition products due to (heavy) arc interruption [2]. The decomposition products can cause sooting, which increases the possibility of an electrical breakdown. Adding these natural gases makes it possible to have a larger application range of C4-FN in HV equipment. For example, a gas mixture of C4-FN/O2/CO2 (5%/5%/90%) at 0,6 MPa will have a liquefaction temperature of -27,1°C [2]. Also the negative effects of the gas, like toxicity, GWP, etc., become smaller.
The precise amount of concentration of the Fluoronitrile gas mixture depends on the manufacturer.

3.3.3 The chemical stability of the Fluoronitrile gas mixture

An excellent property of SF6 is that the gas is able to recombine to its original form after it is decomposed, unfortunately this is not the case for C4-FN. C4-FN is also far less stable compared to SF6, this can be noticed when comparing the atmospheric lifetime of the gases.

C4-FN inside a GIS will, just like SF6, decompose when it is exposed to (too) large quantities of energy. There are multiple occasions when (too) large quantities of energy are present inside a GIS. For example, during an arc, caused by an unsuccessful current interruption, or a breakdown or a partial discharge. These arc temperatures can range from several degrees Celsius to thousands of degrees Celsius [11,18,19]. The gas can decompose due to direct electron impact or thermal dissociation[5].

The decomposition of C4-FN/CO2 gas mixtures under AC breakdown has been researched [5]. In this research the gas experienced 2000 breakdowns. Figure 3.8a shows the gas composition before the breakdowns and Figure 3.8b shows the gas composition after the 2000 breakdowns. Perfluorocarbon gases, gases which are comprised of carbon and fluor, were found to be the main decomposition products of the gas mixture. Figure 3.9 shows the electric strength of some of the decomposition products. It can be concluded that most of the by-products still have a higher electric strength compared to SF6, but lower than C4-FN. This means that the electric strength after a number of breakdowns will decrease. This is slightly visible on Figure 3.10, where the breakdown voltage after 2000 breakdowns slightly decreases.

However, the deterioration of the overall electrical insulation performance should be still acceptable if the volume is large enough and if there is a gas flow inside the enclosure to move the gas around.

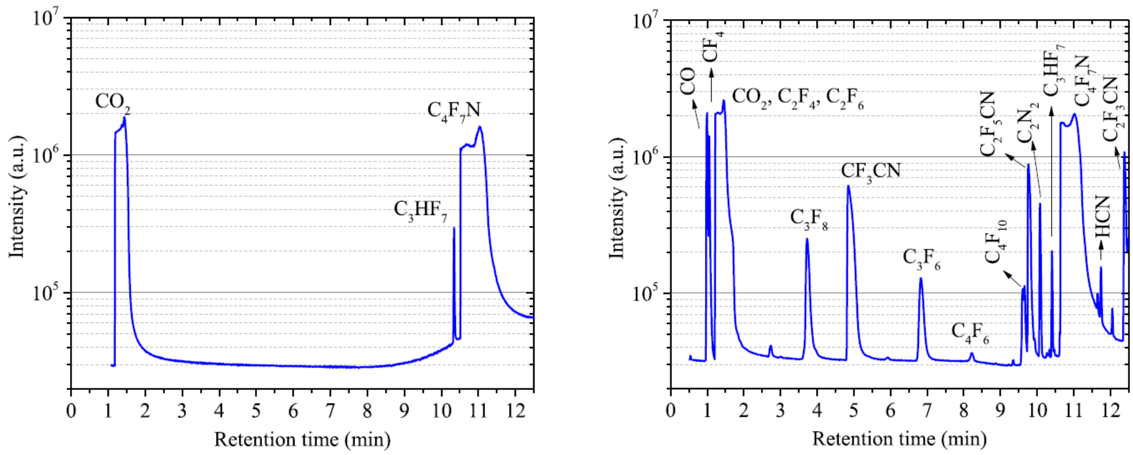

a) before the breakdown *b) after the breakdown*

Figure 3.8 Gas chromatogram of the gas mixture (C4-FN/CO2 13,3%/86,7%) before and after multiple breakdowns [5].

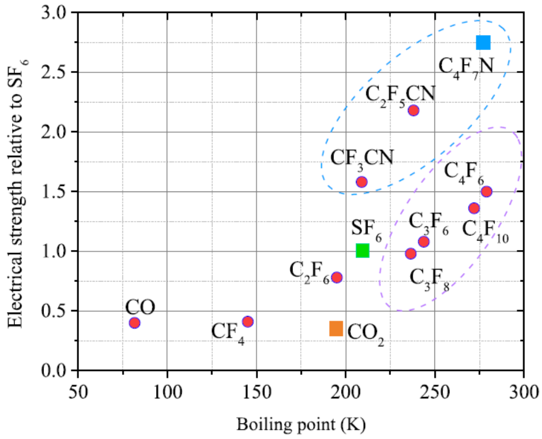

Figure 3.9 The electric strength of the main decomposition products [5].

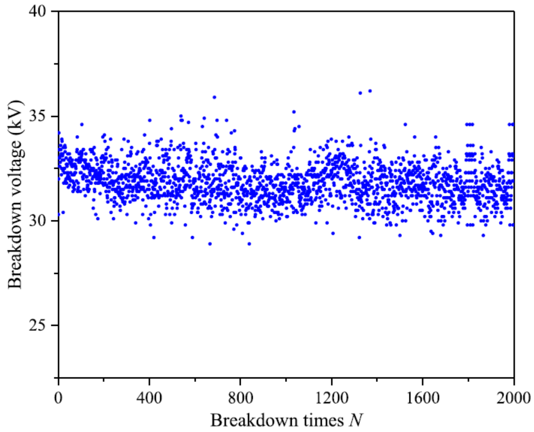

Figure 3.10 The recorded breakdown voltages in the experiment [5].

3.3.4 Crystals found in the Fluoronitrile gas mixture

Research has shown that too much humidity inside the Fluoronitrile gas mixture can create crystals [3]. These crystal require a long time and 'extreme' operating conditions to form. The crystals are formed through a process called hydrolysis. The hydrolysis of C4-FN is a known phenomenon, it is a multi-step chemical reaction that initiates when H2O reacts with C4-FN. Depending on the (operating) conditions the reactions can stop at different steps, i.e. molecules like amide, dimer and many others. All these by products are solid or can solidify under ambient temperature. The solid by-products are often referred to as crystals as they have a similar appearance.

The long-term behaviour of C4-FN mixtures and the formation of crystals has been researched by performing a large number of experiments [3]. A number of experiments were performed to investigate the creation of these crystals under normal operating conditions. There were no crystals to be found at the end of these experiments. Another experiment was created where the hydrolysis reaction was forced. To force the hydrolysis the experiment had far-stretched operating conditions, such as: 7 bar_{abs}, humidity at 10.000 ppmv and a temperature of 80 °C for 2000 hours. The result of the forced hydrolysis can be seen on Figure 3.11. Another experiment was performed with a Voltage Transformer (VT). The VT in that experiment had an applied voltage of 1,25xU_n for 800 days. The compartments of the VT had a humidity of <2000 ppmv. Unlike the other test where hydrolysis was forced by far-stretched operating conditions, the long term test of the VT with more normal operating conditions also produced crystals. Those crystals can be seen on Figure 3.12. However, there was no clear correlation discovered between the measured humidity and the formation of crystals in this test.
Based on the data collected from the experiments, the temperature and the have a large influence on the formation of the crystals.

The crystals that were created during some experiments were conserved for new experiments. These new experiments investigated the effect that these crystals can have on the electrical behaviour of the insulation gas. The breakdown behaviour and partial discharge activity was examined.

- The breakdown experiments proved that the breakdown voltages are not affected by the presence of the solid by-products, i.e. the crystals.
- The partial discharge experiments proved that the solid by-products, i.e. the crystals, do not cause any partial discharge activity.

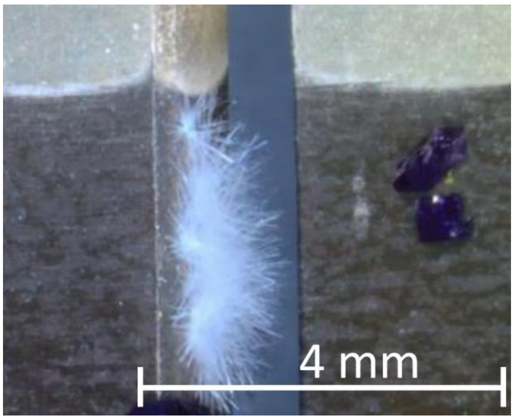

Figure 3.11 Crystals found on the contacts after experiment with far-stretched operating conditions was performed [3].

Figure 3.12 Crystals found in the VT after 800 days at 1,25x Un [3].

3.4 Summary

Chapter 2 delineated the thesis objective. This was done by delineating three topics, these topics were:

1. Humidity inside HV equipment
2. Electrical behaviour of Fluoronitrile that is to be examined
3. Electrical insulation performance of Fluoronitrile

This chapter provided background knowledge on the three different topics:

1. The amount of humidity inside a GIS is observed to vary. For example, humidity inside a GIS is the highest during the summer months and the lowest during the winter months. Humidity inside a GIS originates from moisture inside the GIS. There are different mechanisms for moisture penetration into a GIS. The most common mechanism is the water desorption from the GIS itself, i.e. the conductor, the spacer and the internal surface of the enclosure. The state of the water, i.e. liquid or gaseous, depends on temperature and the dewpoint temperature of the insulation gas.
2. Electrons in an electric field can cause a collision with other atoms/molecules. A number of phenomena can happen as a result. Two important phenomena are attachment and ionization. Together they form the effective ionization coefficient. The effective ionization coefficient causes electrical activity inside HV equipment. This includes partial discharges and AC breakdowns.
3. Pure Fluoronitrile is a better electrical insulator than SF6. Pure Fluoronitrile has an electric strength of more than two times SF6. However, the boiling temperature of pure Fluoronitrile is around -5°C at atmospheric pressure. This entails that pure Fluoronitrile is not suited for all HV applications. Therefore Fluoronitrile is mixed with natural gases, like CO2. This reduces the electrical insulation strength but ensures a larger application range of C4-FN in HV equipment. As an example, the Fluoronitrile gas mixture will be a mixture of C4-FN/CO2 (5%/95%), i.e. a gas mixture of C4-FN and CO2 with a molar ratio of 5% and 95% respectively.

4 The structure of the experiments: test cells, circuits and methods

This chapter explains all the things that are involved in the experiments that have been performed during the research. The first section is a further refinement of chapter two and shapes four research questions. Each research question has its own individual approach that is also explained. The second section explains everything about the equipment that is used during this research. The third section covers the methods that are used during this research. The last section explains the circuits that are used during this research.

4.1 The research questions and their approach

Chapter 2 delineated and refined the thesis objective. The refined thesis objective is to examine: *"the effect of humidity on the electrical insulation performance of the Fluoronitrile gas mixture*". This is achieved by examining:

- The effect of humidity on the AC breakdown strength of the Fluoronitrile gas mixture.
- The effect of humidity on the partial discharge activity in the Fluoronitrile gas mixture.

Based upon these two topics, four research questions were devised to meet the thesis objective. Each of the four research questions has its own individual approach. An approach consists out of multiple experiments.

The four research questions are divided into two phases, the phases are related to the two topics. Phase A examines the effect of humidity on the AC insulation performance of C4-FN/CO2 (5%/95%). This is examined by investigating the AC breakdown behaviour of humid C4-FN/CO2 (5%/95%) in three different electric field configurations, i.e. uniform, quasi-uniform and non-uniform. Phase B examines the partial discharge behaviour of corona in humid C4-FN/CO2 (5%/95%). The research questions and approaches of phase A are summarized in Table 4.1. The research question and approaches of phase B are summarized in Table 4.2.

Phase A – How does humidity affect the AC insulation performance of C4-FN/CO2 (5%/95%)?

Question 1:	How is the AC breakdown strength of C4-FN/CO2 (5%/95%) influenced by different humidities?
Approach:	Examine the electrical breakdown strength of C4-FN/CO2 (5%/95%) with different humidities. The results will be mapped into a graph, showing the correlation between the humidity and breakdown voltages.
Question 2:	How does humidity affect the AC breakdown strength of C4-FN/CO2 (5%/95%) at different operating pressures?
Approach:	Examine the electrical breakdown strength of C4-FN/CO2 (5%/95%) with a specific humidity at different pressures. This is done in two stages. The results of both stages will be mapped into one graph. The graph shows if the correlation between the breakdown voltages and humidity, found in question 1, still holds for different operating pressures. The first stage: Examine the AC breakdown strength of dry C4-FN/CO2 (5%/95%) at different operating pressures. The second stage: Examine the AC breakdown strength of humid C4-FN/CO2 (5%/95%) at different operating pressures.

Table 4.1 Summary of the updated research questions and related experiments to examine the electrical breakdown behaviour of humid C4-FN/CO2 (5%/95%).

Phase B – How does humidity affect the Partial Discharge behaviour of corona in C4-FN/CO2 (5%/95%)?

Question 3:	How does humidity affect the partial discharge behaviour of corona in C4-FN/CO2 (5%/95%)?
Approach:	Compare the Partial Discharge Inception Voltage (PDIV) and the Phase Resolved Partial Discharge (PRPD) pattern of corona in dry and humid C4-FN/CO2 (5%/95%).
Question 4:	How does humidity affect the characteristics of a corona discharge in C4-FN/CO2 (5%/95%)?
Approach:	Compare and analyse the waveform of multiple corona partial discharges in dry and humid C4-FN/CO2 (5%/95%).

Table 4.2 Summary of the updated research questions and related experiments to examine the PD behaviour of humid C4-FN/CO2 (5%/95%).

All the experiments done in phase A and B are performed in the High Voltage Laboratory of TU Delft. The results of the experiments, which are performed to answer the four research questions, are given in chapter five.

There were a lot of known-unknowns before the start of the research. These known-unknowns needed to be converted to known-knowns to ensure that the experiments and their results are reliable, reproducible and replicable. The process of the conversion of the known-unknowns into known-knowns is described in appendix A. The known-unknowns and their solution/conclusion are briefly repeated in this chapter at the relevant sections. The reader is encouraged to read appendix A as the appendix gives an elaborate and detailed description and solution of the conversion of known-unknowns to known-knowns. Appendix A discusses the following known-unknowns;

1. Are the electrode configurations described CIGRE Brochure 849 D1 feasible for this research?
2. What are the damaging effects to the electrodes caused by the breakdowns and what are the mitigating measures that can be taken?
3. What is the maximum breakdown strength the enclosure of the test cell, i.e. at what voltage will the air outside the enclosure break down?
4. How can the humidity of C4-FN/CO2 (5%/95%) be altered?

4.2 The different equipment that is used

This section describes the different test cells that are used during this research. The first section describes the test cell that is used to examine the AC breakdown behaviour of humid C4-FN/CO2 (5%/95%). The second section describes the test cell that is used to examine the partial discharge behaviour of corona in humid C4-FN/CO2 (5%/95%). Lastly the electrodes that are used to mimic different electric field configurations are discussed.

4.2.1 The test cells to examine the AC breakdown behaviour of humid C4-FN/CO2 (5%/95%)

There are two test cells to examine the AC breakdown behaviour of humid C4-FN/CO2 (5%/95%). Both cells are identical except for the height of the test cell. The two test cells have a different breakdown voltage, i.e. the voltage at which the air around the test cell breaks down, due to the difference in height. The small test cell has a breakdown strength of circa 90kV_{peak} and the large test cell has a breakdown strength of circa 190kV_{peak}. The small test cell is used for the experiments of research question A-1. A photo of the small test cell is shown in Figure 4.1. The long test cell is used for the experiments of research question A-2. A photo of the long test cell is shown in Figure 4.2.
The creation process of the two test cells is described in appendix A, section A.3. The test cells are equipped with a relative pressure meter to monitor the pressure of the insulation gas inside the test cell. The test cells have two female DILO connections in order to flush the test cell. The need and function of the flushing is explained in section 4.3.1.

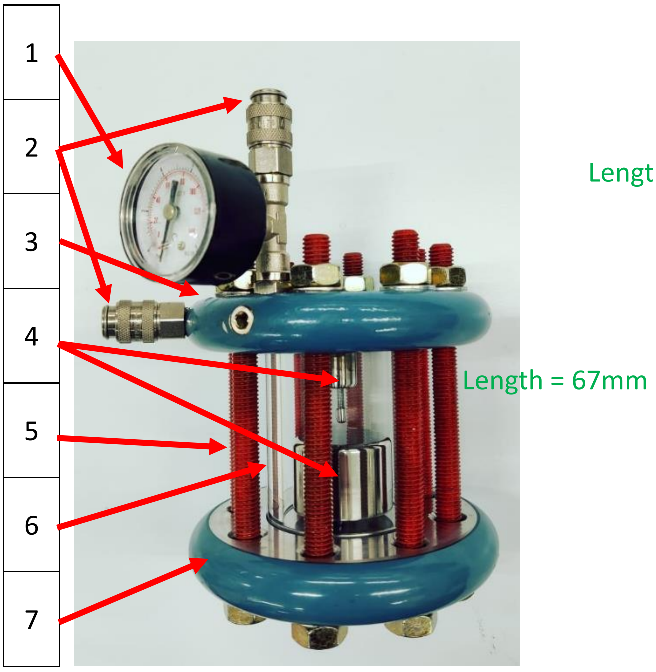

Figure 4.1 The initial small test cell to examine the breakdown behaviour of C4-FN/CO2 (5%/95%).

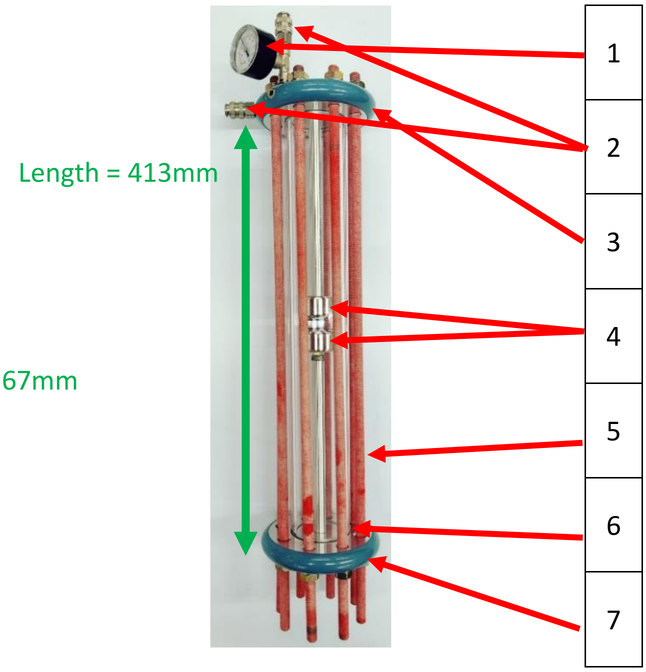

Figure 4.2 The second, longer, test cell to examine the breakdown behaviour of C4-FN/CO2 (5%/95%).

Nr.	Description
1	Relative pressure meter.
2	Female DILO connection to serve as the in-/outlet of the gas.
3	Top plate of the test cell, made of aluminium.
4	Electrodes to form a specific electric field configuration. The electrodes in the large test cell are connected to the top and bottom plate with aluminium rods of circa 14cm.
5	Glasfiber reinforced plastic screw threads to keep the test cell pressure tight. Which allows testing with higher pressures up to 20+ bar_{abs}.
6	PMMA cylinder, to contain the insulation gas. There are O-rings between the top/bottom plate and cylinder to prevent leakage of the gas.
7	Bottom plate of the test cell, made of aluminium.

4.2.2 The test cell to examine the partial discharge behaviour of corona in humid C4-FN/CO2 (5%/95%)

There is one test cell to examine the Partial Discharge behaviour of corona in humid C4-FN/CO2 (5%/95%). A photo of this test cell is visible on
Figure 4.3. The PDIV, PRPD pattern and a multiple waveforms of corona will be measured in this test cell.

Optimal measurements of the PD waveform

There are some requirements to get an optimal measurement of the waveform of a high frequency partial discharge. Those requirements must be fulfilled in order to accurately measure the waveform of PD's which is invaluable for a detailed analysis of the PD characteristics. The two requirements are:

1. Reflection coefficient Γ = 0.
   Reflection can happen anywhere in the circuit where there is a discontinuity. Γ can be calculated with Equation 4-1, where Z_0 is the characteristic line impedance and Z_L is the load impedance. When Γ = 0 the incident signal experiences no reflection and the incident signal is the transmitted signal.

$$\Gamma = \frac{Z_L - Z_0}{Z_L + Z_0}$$

Equation 4-1

   To reach a reflection coefficient of 0, all impedances need to be matched. An oscilloscope with an input impedance of 50Ω is able to measure high frequency signals. Therefore the needle has to mimic a 50Ω impedance. The 50Ω impedance of the needle is based on the design of a coaxial transmission line, Z_0. The equation of Z_0 is given as Equation 4-2, where ε_r is the relative permittivity of the dielectric between the inner and outer conductor [20]. The characteristic impedance of 50Ω is created in the bottom plate of the test cell. This was already made for the PhD research of *Christian Mier Escurra*. This is reused for this research with his permission.
   The transmission line between the PD source (50Ω needle) and measuring instrument (50Ω oscilloscope) also needs to have a characteristic impedance of 50Ω to avoid reflection.

$$Z_0 = \frac{138}{\sqrt{\varepsilon_r}} log_{10} \frac{d_{outer\ conductor}}{d_{inner\ conductor}}$$

Equation 4-2

2. Compact measuring circuit.
   A transmission line also has a resistive impedance, besides a characteristic impedance, as a transmission line is not an ideal conductor. Losses will occur and will attenuate the signal due to the resistive part of the transmission line. Therefore the transmission line needs to be as short as possible, to avoid as much attenuation of the PD signal as possible. Attenuation will compromise the details of the PD waveshape.
   To further decrease the size of the measuring circuit, a coupling capacitor is included in the test cell. The coupling capacitor is the test cell itself, i.e. the top plate and the bottom plate of the test cell.

The test cell has to be free of partial discharges up to a certain voltage to ensure that the only PD activity measured is that of the corona phenomena caused by the needle. The test cell is constructed with plastic parts instead of metal parts, e.g. plastic nuts instead of metal nuts, to minimize any PD activity.

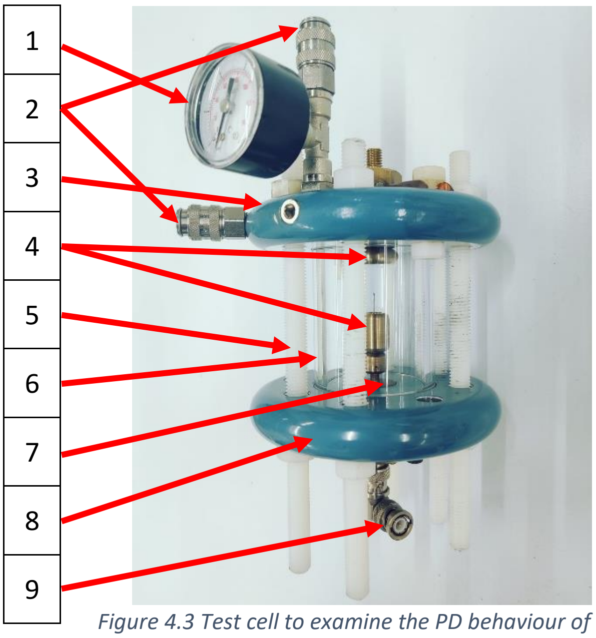

Figure 4.3 Test cell to examine the PD behaviour of C4-FN/CO2 (5%/95%).

Nr.	Description
1	Relative pressure meter.
2	Female DILO connection to serve as the in-/outlet of the gas.
3	Top plate of the test cell, made of aluminium.
4	Plate – needle electrode configuration, to simulate a sharp protrusion on the electrode.
5	Plastic screw threads to keep the test cell pressure tight.
6	PMMA cylinder, to contain the insulation gas. There are O-rings between the top/bottom plate and cylinder to prevent leakage of the gas.
7	Casted epoxy ring to give the needle a coaxial characteristic impedance of 50Ω.
8	Bottom plate of the test cell, made of aluminium.
9	Male BNC connector.

4.2.3 The electrodes to mimic three different electric field configurations

This section discusses the electrode configurations to mimic three different electric field configurations and explains the gap distance between the electrodes. Lastly it is described how breakdowns can affect the measurement of the breakdown voltages of C4-FN/CO2 (5%/95%).

Three different electric field configurations that are examined

Three sets of electrodes are designed to simulate three simple but different electric field configurations. The design of the electrodes is done in COMSOL. The design process is elaborately explained in appendix A, section A.1.

The three different electric field configurations have their own field utilization factor η. The η-factor summarizes general information on the arrangement of the electrodes that simulate a specific electric field. The formula for the η-factor is given as Equation 4-3, where *U* is the applied voltage and *d* is the distance between the electrode. The three different electric field configurations are:

- An uniform electric field, η = 1. This is realized with two Rogowski electrodes. Through the use of the Rogowski electrodes it can be examined what the effect of humidity is on the intrinsic electric breakdown strength of C4-FN/CO2 (5%/95%).
- A quasi-uniform electric field, η ≈ 0,6. This is realized with a sphere (r_{sphere} = 2mm) and a plate electrode. Through the use of sphere – plate combination it can be examined if humidity affects the electric breakdown strength of C4-FN/CO2 (5%/95%) under the influence of small electric field disturbance.
- A non-uniform electric field, η ≈ 0,08. This is realized with a needle and a plate electrode. Through the use of needle – plate combination it can be examined if humidity affects the electric breakdown strength of C4-FN/CO2 (5%/95%) in an concentrated electric field.

The η-factor is unitless and is calculated through COMSOL. The η-factor based upon a gap distance of 5,00mm and an applied voltage of $5kV_{peak}$.

$$\eta = \frac{\frac{U}{d}}{maximum\ electric\ field\ strength}$$

Equation 4-3

Ensuring a constant gap distance of 5,0mm

It is extremely important to keep a constant gap distance (5,0mm) between the electrodes during the experiments. A deviation of the gap distance greatly affects the breakdown voltage of C4-FN/CO2 (5%/95%). Two rules are followed to ensure a constant gap distance of 5,0mm during all the experiments. The reasons for these rules are elaborately explained in appendix A, section A.1. The rules are:

1. Use a constant torque of 30cmkg on the nuts during assembly. This results in the same distance between the top and bottom of the test cell and thus a constant gap distance.
2. Complement the thread which connects the electrodes to the test cell with washers and nuts. To give all the electrodes the same effective height.

The effect of breakdowns on the breakdown voltage of C4-FN/CO2 (5%/95%)

The effect of breakdowns on the electrodes and on the breakdown voltage of C4-FN/CO2 (5%/95%) is examined. The discharge energy released during a breakdown, although limited, damages the electrodes. The damage and the effects thereof are examined for all the electric field configurations. The investigation on the effect of breakdowns on the electrodes is elaborately explained in appendix A, section A.2. The results of the investigation are presented in Table 4.3. Table 4.3 shows if the breakdown voltage of C4-FN/CO2 (5%/95%) is affected by the state of the electrodes.

Only the breakdown voltage of C4-FN/CO2 (5%/95%) in a uniform electric field is affected by the state of the electrodes. The surface roughness of the Rogowski electrodes is increased due to the occurrence of multiple breakdowns. An increased surface roughness gives rise to a local enhancement of the electric field and can create an early breakdown. The early breakdown results in a lower breakdown voltage of C4-FN/CO2 (5%/95%) [15, 38, 39]. The delta of the measured breakdown voltages of C4-FN/CO2 (5%/95%) keeps increasing after each experiment if the surface roughness of the Rogowski electrodes is not treated. Delta is the difference between the minimum and maximum measured breakdown voltage of C4-FN/CO2 (5%/95%) during an experiment.

The Rogowski electrodes need to be polished after each experiment to reduce the surface roughness of the electrodes. Polishing the Rogowski electrodes limits the delta of the measured breakdown voltages of C4-FN/CO2 (5%/95%) during an experiment.

The effect of different polishing methods to reduce the surface roughness of the Rogowski electrodes is examined. The results of the different polishing methods conclude that the delta of the breakdown voltages of C4-FN/CO2 (5%/95%) in an uniform electric field can be limited to <10kV_{peak}. The electrodes are sanded with waterproof sanding paper with a grit of P1200 and afterwards polished with 'brasso koperglans' to limit the delta <10kV_{peak}.

Field configuration	Breakdown voltage of C4-FN/CO2 (5%/95%)
Uniform	Affected by unpolished electrodes, delta increases after each experiment. Delta of 10kV_{peak} in first experiment increases to 24kV_{peak} in fifth experiment.
Quasi-uniform	Not affected by unpolished electrodes, delta does not increase after each experiment. Delta remains below 2kV_{peak}.
Non-uniform	Not affected by unpolished electrodes, delta does not increase after each experiment. Delta remains below 1,5kV_{peak}.

Table 4.3 The examined effect of multiple breakdowns on the breakdown voltage of C4-FN/CO2 (5%/95%). Experiments performed below 1,2 bar_{abs}. Delta is the difference between the minimum and maximum measured breakdown voltage of C4-FN/CO2 (5%/95%) during an experiment.

4.3 The different used methods

This section explains the different methods that are used to make the required test conditions and to perform the test in a repeatable, reproducible and replicable way. First, the creation of different operating conditions for the C4-FN/CO2 (5%/95%) is discussed. Afterwards, the methods used to examine the breakdown behaviour, partial discharge behaviour and the partial discharge characteristics are described.

4.3.1 Method to create different operating conditions

A special designed 'mixing vessel' is used to create humid C4-FN/CO2 (5%/95%). This mixing vessel was created during the PhD research of Andreas Purnomoadi which was publicised in 2020 [6]. Multiple sensors can be connected to the mixing vessel to monitor and control all the different properties of the gas. All the connections, with their functions, are shown in Figure 4.4. Figure 4.4 shows a grey switch that is connected to the test cell. The grey switch is added to the test cell to prevent gas from escaping during the decoupling of the test cell from the mixing vessel.

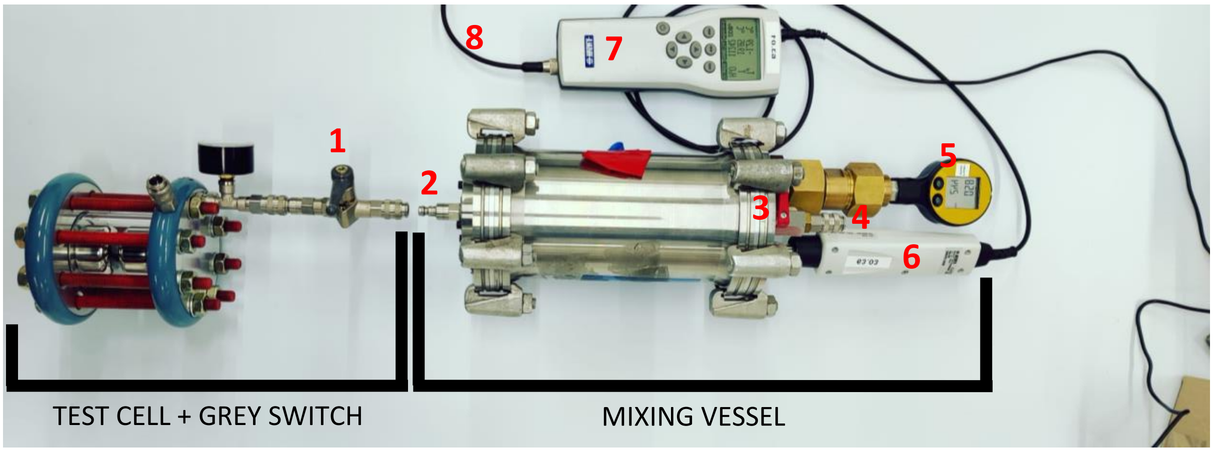

Figure 4.4 The set-up to create humid C4-FN/CO2 (5%/95%).

Nr.	Description
1	Grey switch created to control the gas flow from the mixing vessel to the test cell
2	Male DILO connection to connect the grey switch on the test cell to the mixing vessel
3	Red switch to control the gas flow from the gas tank into the mixing vessel
4	Female DILO connection acting as the inlet for the gas into the mixing vessel
5	Digital pressure sensor KELLER LEO 2, used to monitor the pressure inside the mixing vessel
6	Humidity probe DMP74B, used to measure the humidity inside the mixing vessel
7	Handheld dewpoint meter DM70, used to read out the humidity measurement by the DMP74B probe
8	Connection of the humidity probe DMP74B to the handheld dewpoint meter DM70

Humidity sensor

There are a lot of sensors to measure the humidity of a gas (mixture). For this research multiple sensors have been examined. The different sensors which were examined are shortly discussed in appendix A, section A.4. The sensor which is chosen for this research is the handheld dewpoint meter DM70 with the DMP74B probe from Vaisala. The DMP74B probe contains a hygroscopic polymer film. The capacitance of the hygroscopic polymer film will change due to the humidity. By measuring the capacitance of the hygroscopic polymer film it is possible to know the humidity of the gas mixture.

Pressure sensor

The digital pressure sensor KELLER LEO 2 is able to measure the pressure in the range from $0bar_{abs}$ to $30bar_{abs.}$

Creating humid C4-FN/CO2 (5%/95%)
Altering the humidity of C4-FN/CO2 (5%/95%) is based on the principle of combining gaseous water with dry C4-FN/CO2 (5%/95%). The gaseous water is created by injecting demineralized water into the vacuumized mixing vessel. The demineralized water is injected into the mixing vessel by the means of a syringe and connection piece. The connection piece makes it possible to connect a syringe to the inlet of the mixing vessel. Water vaporizes in vacuum at -50°C and creates the gaseous water. Dry C4-FN/CO2 (5%/95%) is added to the gaseous water inside the mixing vessel to create humid C4-FN/CO2 (5%/95%). Photos of the inlet of the mixing vessel, the connection piece and syringe are visible in Figure 4.5, Figure 4.6 and Figure 4.7 respectively

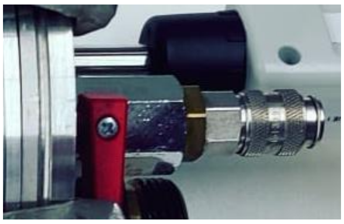

Figure 4.5 A zoom-in of the red switch controlling the inlet flow of the gas into the mixing vessel.

Figure 4.6 The connection piece which enables the syringe to inject the water into the mixing vessel.

Figure 4.7 The syringe used to inject the water. 1,0mL syringe with 100 marks.

The process of creating humid C4-FN/CO2 (5%/95%) is based on a simple principle but optimized through trial and error. The optimization process and the physics behind the creation of humid C4-FN/CO2 (5%/95%) is in detail explained in appendix A, section A.4.

The steps of the optimized procedure are:
1. The grey switch is mounted on top of the test cell.
2. The test cell with the grey switch is connected to the mixing vessel.
3. The grey switch and the red switch (near the inlet of the mixing vessel) are opened.
4. The entire set-up is evacuated to 0,4mbar$_{abs}$. The *Dilo Economy Series L057R01 service cart* is used for evacuating. The minimum evacuation limit for non-SF6 gases is 0,4mbar$_{abs}$.
5. The entire set-up is flushed with N2 to dry the set-up.
6. The entire set-up is evacuated to 0,4mbar$_{abs}$.
7. The entire set-up is flushed with dry C4-FN/CO2 (5%/95%). A lot of N2 particles are still present in the entire set-up because the entire set-up is evacuated to 0,4mbar$_{abs}$ and not 0bar$_{abs}$. Flushing with C4-FN/CO2 (5%/95%) replaces the remaining N2 particles with C4-FN/CO2 (5%/95%).
8. The entire set-up is evacuated to 0,4mbar$_{abs}$.
9. The grey switch is closed.
10. A certain amount of demineralized water is sucked into the syringe.
11. The syringe with water is weighed up to 3 decimals.
12. The connection piece is weighed up to 3 decimals.
13. The syringe is tightly connected to the connection piece.
14. The connection piece (with syringe) is connected to the inlet of the mixing vessel.
15. The red switch is opened allowing water to get sucked into the evacuated mixing vessel of 0,4mbar$_{abs}$. Water vaporizes in 0,4mbar$_{abs}$ at circa -30 °C, creating the gaseous water.
16. The syringe with water is weighed up to 3 decimals.
17. The connection piece is weighed up to 3 decimals.
18. Check if the required amount of water is evaporated. If not repeat steps 10 to 14.
19. C4-FN/CO2 (5%/95%) is added until the desired pressure is reached.
20. Wait until the mixing is stabilized, circa 20 minutes.

21. Check the final humidity on the handheld dewpoint meter DM70. If the desired humidity is not achieved, restart the procedure at step 3.
22. Open the grey switch to transfer the created humid C4-FN/CO2 (5%/95%) from the mixing vessel to the test cell.
23. Close the grey switch.
24. Decouple the test cell *with* the closed grey switch from the mixing vessel.
25. Gas mixture is ready for testing.

Unit to indicate humidity
Section 3.1.3 explained that the most common and used unit to indicate humidity is ppmv. This unit only depends on the dewpoint temperature and the pressure of the gas [8]. The dewpoint temperature of dry C4-FN/CO2 (5%/95%) is circa -55°C. A dewpoint of -55°C corresponds to a humidity of 35ppmv at 1 bar_{abs}.
The formula to calculate the humidity (in ppmv) with the dewpoint temperature and pressure can be found in appendix A, section A.4. Appendix A, section A.4, also describes the relationship between the humidity in ppmv and the amount of (injected) water.

4.3.2 Method to measure the AC breakdown voltage of C4-FN/CO2 (5%/95%)
The breakdown voltage of C4-FN/CO2 (5%/95%) is measured according to the ASTM-D-2477 standard [40]. Other papers in which gases were researched, provided extra insight to form a good and complete testing method [21-25]. A document is made in which all the details of the experiments could be documented. This document makes it possible to perform repeatable, reproducible and replicable experiments. This document is added as appendix B.

The IEC60243-1 prescribes that at least 5 breakdown repetitions must be made in order to determine the breakdown voltage/electric strength [21]. The number of breakdown repetitions is chosen as 10, to make a good and reliable mean. The applied voltage for the breakdown experiments is increased with a steady rate of 1-5kV_{peak}/s up to 80% of the roughly measured breakdown voltage. During the last 20% the applied voltage is increased with a rate of 0,5kV_{peak}/s [40]. Three consecutive breakdown repetitions are performed to get a rough value of the breakdown voltage. During these three consecutive breakdown repetitions the applied voltage is increased with a rate of rise of 2-4kV_{peak}/s. Between the (10) breakdown repetitions a waiting time of three minutes is implemented. This is done as to minimize the influence of the already conducted breakdowns on the consecutive breakdowns. As there is a possibility that a breakdown decomposed the gas, altering the composition and thus the dielectric strength of the gas between the electrodes.

Preventing the negative consequences of applying high voltage
The sharp contour of DILO connections on the top of the test cell can cause corona discharges depending on the applied voltage. There are two reasons that these corona discharges are unwanted:
1. The corona discharges can lead to an early breakdown on the outside of the enclosure of the test cell, lowering the breakdown strength of the test cell.
2. The corona discharges create ozone and high frequency noise, both harmful to humans. The higher the applied voltage, the stronger the corona discharges.

Two corona shield are added to the test circuit to prevent high and strong levels of corona discharges. The test circuit will be explained in section 4.4.1. A photo of the two shield are visible on Figure 4.8. The top corona shield surrounds the entire top of the test cell. The top of the test cell and the top corona shield have the same potential, creating a potential difference of 0V and thus preventing the occurrence of corona discharges. The bottom shield has the same potential as the bottom of the test cell and is used to spread the electric field over a larger surface reducing the electric field intensity.

Figure 4.8 Added corona shields to mitigate corona discharges caused by the sharp contour of the DILO connections.

4.3.3 Method to measure the partial discharge behaviour

The PDIV and PRPD pattern are measured to examine the PD behaviour of corona in C4-FN/CO2 (5%/95%). The PDIV and PRPD pattern are measured according to the IEC60270 standard [13]. Other papers in which the PDIV and PRPD pattern were researched, provided extra insight to form a good and complete test method [26,27].
The PDIV is measured by increasing the applied voltage with a steady rate of rise of $1kV_{peak}/s$. The PDIV is the voltage at which discharges start to generate with a constant rate and constant amplitude. The PRPD pattern is measured at least 20% above the PDIV to generate enough partial discharge activity.

It is important that the test cell (without electrodes) and circuit are PD free in order to be sure that the partial discharges that are measured originate from the designated PD source, i.e. the needle in the test cell. The test cell will therefore be tested without electrodes to make sure that the test cell, and circuit, are PD free up to $15kV_{peak}$. The $15kV_{peak}$ is a rough overestimation of the PDIV of corona in C4-FN/CO2 (5%/95%) at $1bar_{abs}$. The literature study found that the PDIV of corona in C4-FN/CO2/O2 (5%/unknown%/unknown%) at $1bar_{abs}$ is roughly $9kV_{peak}$ [28]. Because of the different contributing factors to the inception voltage of partial discharges an overestimated PDIV of $15kV_{peak}$ is assumed for this research.

The PD analyser is calibrated before the start of the experiments. This is to ensure that the PD analyser displays the correct level of charge originating from the partial discharges.

4.3.4 Method to measure the partial discharge characteristics

The characteristics of corona discharges in C4-FN/CO2 (5%/95%) are examined by measuring the waveform of the partial discharges [20]. The waveform is measured at 10% above the PDIV. The applied voltage is never above 50% of the breakdown voltage of C4-FN/CO2 (5%/95%) in the non-uniform electric field configuration. The PDIV and the breakdown voltage are known due to earlier measurements. 100 partial discharge signals, i.e. waveshapes, are sampled and analysed in Matlab.

4.3.5 Safety measurements

According to the safety datasheet of C4-FN the gas is labelled as a hazard gas [29]. The "Acute Toxicity (inhalation): category 4" identification is of particular importance. The safety datasheet discloses that C4-FN is harmful if inhaled. It causes respiratory tract irritation and can cause frostbite through skin contact. A risk assessment is made based upon the safety datasheet and mitigating measures were created to perform the experiments in a safe and responsible way. The risk assessment is added as appendix C. Filling or removing C4-FN/CO2 (5%/95%) from the test cell is always done inside a fume hood, to minimize the risk of inhalation.

4.4 Circuits

In this section three circuits that are used throughout this research are explained. The first circuit is used for measuring the AC breakdown strength of C4-FN/CO2 (5%/95%) under different operating conditions. The second circuit is for measuring the PD behaviour of corona in C4-FN/CO2 (5%/95%) by examining the Phase Resolved Partial Discharge (PRPD) pattern and the Partial Discharge Inception Voltage (PDIV). The third circuit is used to measure the PD waveform to examine various PD characteristics in C4-FN/CO2 (5%/95%).

4.4.1 Circuit to examine the AC breakdown behaviour of C4-FN/CO2 (5%/95%)

A circuit is set up in accordance with the IEC60060-1 to measure the breakdown strength of C4-FN/CO2 (5%/95%) [4]. The circuit is shown in Figure 4.9. A power supply ① is connected to a variac ② to regulate the voltage. An overcurrent protection ③ is connected between the output of the variac and an inductor ④. The inductor is connected in series with the primary side of the step up transformer ⑤. The secondary side of the step up transformer is connected in parallel to the test cell ⑧ and a capacitive voltage divider ⑨. A voltage measurement device ⑩ is connected in parallel to the capacitive voltage divider to measure the applied voltage to the test cell. The circuit also contains an resistor ⑦ and a fast tripping circuit ⑥ to limit the discharge energy.

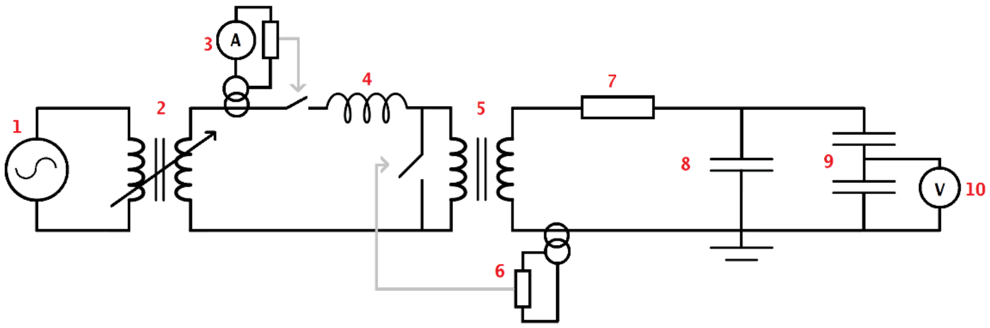

Figure 4.9 Circuit to examine the breakdown strength of C4-FN/CO2 (5%/95%).

Power supply ①

The power supply is the 0930HVI-1/9f supply of the High Voltage lab. The power supply has an fixed output voltage of $230V_{RMS}$ 50Hz with an rated current of $80A_{RMS}$. A photo of the power source is visible on Figure 4.10.

Variac ②

The variac is used to control the primary side of the step up transformer. The variac is used to transform the fixed output voltage of the power supply to a desired voltage. The variac is rated for an output voltage of 0 – $525V_{RMS}$ and has a rated power of 25kVA. A photo of the variac is visible on Figure 4.11. The output of the variac will however not be above $230V_{RMS}$ as the source connected to the input has a fixed voltage of $230V_{RMS}$.

Overcurrent protection ③

The overcurrent protection is used to protect the equipment against high currents. The overcurrent protection is set to trip at $40A_{RMS}$ at which it opens a switch disconnecting the equipment from the power supply.

The step up transformer ⑤

The step up transformer is an Emil Haefely & Cie. AG. type TEOS 200/100. The transformer can transform voltage $500V_{RMS}/200kV_{RMS}$ and a has a rated power of 100kVA. The step up transformer is used to step up the low adjustable output voltage of the variac to a high voltage. A photo of the step up transformer is visible on Figure 4.12.

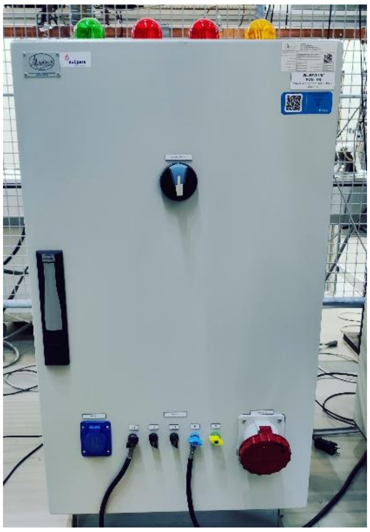

Figure 4.10 Power source used for BD experiments.

Figure 4.11 Variac used to regulate the applied voltage in the BD experiments.

Figure 4.12 the step up transformer to step up the low regulated voltage to high voltage.

The inductor ④ + fast tripping circuit ⑥ + The resistor ⑦

The resistor, inductor and the fast tripping circuit are used to limit the energy which is released during a breakdown. The released energy during a breakdown can:

1. Damage the electrodes, which can increase the electric field and lead to an early breakdown.
2. Decompose the gas, which can lower the dielectric strength of the insulation gas and lead to an early breakdown.

The released energy must be limited to mitigate these effects. The released energy can be calculated with $E = p \cdot t = V \cdot I \cdot t$. The voltage is the breakdown voltage, which will vary during the experiments. The voltage will thus not be limited. Therefore the current and time must be as small as possible to reduce the released energy.

<u>Limiting the current of a breakdown</u>

A 1kΩ resistor is used to limit the current and to create a low-pass filter with the capacitance of the circuit. The low-pass filter protects the step up transformer from transient (over)voltages when a breakdown occurs. The reflected transient (over)voltage over the transformer creates stress on the windings of the transformer. A large resistor is however not used as the current becomes too small to trigger the tripping circuit.

The inductor is used to create a series resonant circuit. The resonance creates two benefits.

1. The voltage on the primary side of the step up transformer is higher than the output voltage of the variac.
2. The breakdown current is limited. The impedance of the circuit will be increased during a breakdown as the resonance will change due to a short in the capacitive test object. The increased impedance limits the breakdown current.

The inductor is a HTT 1 phase series reactor type GEIN 210 / 3.6 – 2. Rated at 201kVAR and 2010V_{RMS}. A photo of the inductor is visible on Figure 4.13.

<u>Limiting the time of a breakdown</u>

A fast tripping circuit is used to limit the time of a breakdown and prevent consecutive breakdowns from occurring. The tripping circuit is realised with a Current Transformer (CT). The CT will measure a transient in the current and sends a signal to a box which shorts the primary side of the step up transformer to earth. The applied voltage on the test cell will be removed due to the short.

Test cell ⑧
The test cell is one of the two test cells designed to examine the breakdown behaviour of C4-FN/CO2 (5%/95%), as is described in section 4.2.1.

Capacitive voltage divider ⑨ + voltage measurement ⑩
The capacitive voltage divider is a Emil Haefely & Cie. AG. Basel of 400pF rated for 400kV$_{rms}$ at 50Hz. The capacitive voltage divider is used to measure the applied voltage over the test cell. The measured voltage is converted with a 2114:1 Volt ratio. A photo of the capacitive voltage divider is visible on Figure 4.14. The converted voltage by the capacitive voltage divider is read from the digital measuring instrument DMI 551 of Haefely.

Maximum stress of the circuit
The circuit of the breakdown experiments has been calculated to its maximum stress, i.e. the allowed operating current and voltage where the equipment will not be damaged.

- Maximum current:
    - The primary side of the step up transformer is rated for 200A$_{RMS}$.
    - The variac is rated for 50A$_{RMS}$.
    - The inductor is rated for 100A$_{RMS}$.

    This means the allowed maximum operating current is the rated current for the variac. A 20% safety factor is implemented as some of the equipment in the circuit is 70+ years old. The overcurrent protection is set at 40A$_{RMS}$ to prevent any damage to the (old) equipment.
- Maximum voltage:
  The maximum operating voltage on the secondary side of the step up transformer is the maximum breakdown voltage of the enclosure of the large test cell, which is circa 190kV$_{peak}$.
    - The secondary side of the step up transformer is rated for 280kV$_{peak}$. 190kV$_{peak}$ corresponds to roughly 70% of the rated output voltage.
    - The capacitive voltage divider is rated for 564kV$_{peak}$. 190kV$_{peak}$ corresponds to roughly 34% of the rated output voltage.

  190kV$_{peak}$ on secondary side of the step up transformer corresponds to 475V$_{peak}$ on the primary side of the step up transformer. The voltage on the primary side of the transformer is roughly 6x the output voltage of the variac due to the resonance.
    - The variac is rated for 742V$_{peak}$. The maximum output voltage of the variac will be 80V$_{peak}$, which is equivalent to 46% of its capacity.
    - The inductor is rated for 2.834V$_{peak}$. The maximum voltage across the inductor will be 400V$_{peak}$, which is equivalent to 15% of its capacity.

In case of a breakdown there will be a higher transient current compared to the normal operating current. The transient current is still below the calculated maximum current of 40A$_{RMS}$. Furthermore, the tripping circuit will limit the time the transient current flows through the circuit, further reducing the possibility to damage the equipment.

Figure 4.13 Inductor used to create resonance with the capacitive test cell.

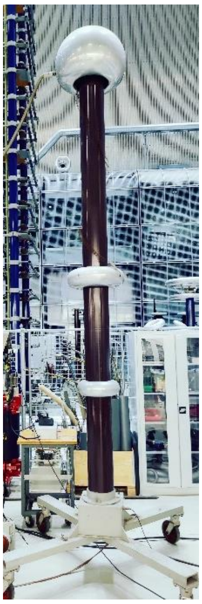

Figure 4.14 Capacitive voltage divider used to measure the applied voltage over the test cell.

4.4.2 Circuit to examine the partial discharge behaviour of C4-FN/CO2 (5%/95%)

A circuit is set up in accordance with the IEC60270 to measure the PD behaviour of corona C4-FN/CO2 (5%/95%) [13]. The PDIV and the PRPD pattern are measured to examine the PD behaviour of corona in C4-FN/CO2 (5%/95%), as described in 4.3.3. The circuit is shown in Figure 4.15.

The circuit of Figure 4.15 is realized with a lot of the same equipment that is used in the circuit of Figure 4.9 in which the breakdown strength of C4-FN/CO2 (5%/95%) is examined. This applies to: the power supply ①, the variac ②, the overcurrent protection ③, the inductor ④, the step up transformer ⑤, the fast tripping circuit ⑥, the resistor ⑦, the capacitive voltage divider ⑨ and the voltage measurement device ⑩.
The new equipment is a coupling capacitor ⑪ connected in parallel to the test cell ⑧. A coupling device ⑫ is connected in series with the coupling capacitor and the ground. A PD analyser ⑬ is connected to the coupling device to visualize the measured information of the Partial Discharges.

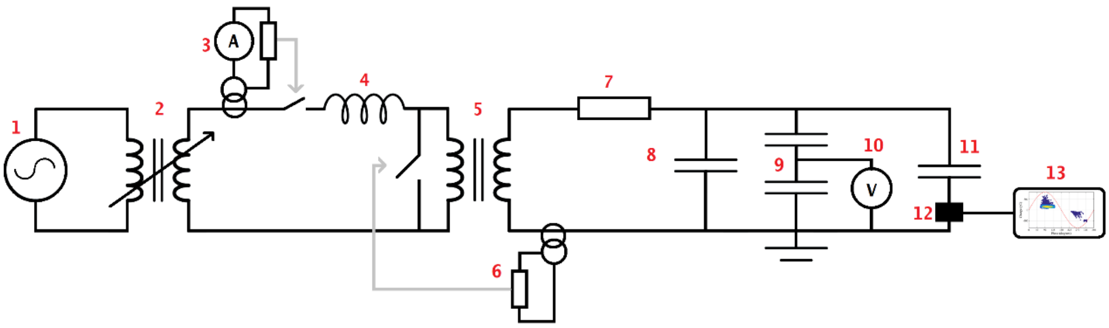

Figure 4.15 Circuit to examine the PD behaviour of corona in C4-FN/CO2 (5%/95%).

Resistor ⑦

The resistor has still the functions as is explained in section 4.4.1. In this circuit the resistor also has the function to stop the Partial Discharges from traveling back to the source of the circuit. This ensures that the Partial Discharges run through the coupling capacitor and the coupling device.

Test cell ⑧
The test cell designed to examine the partial discharge behaviour of C4-FN/CO2 (5%/95%), as is described in section 4.2.2, is used.

Coupling capacitor ⑪
The coupling capacitor is a 1000pF rated for 100kV$_{RMS}$ of Haefely. The coupling capacitor is used to make a loop in which the Partial Discharges can travel. A photo of the coupling capacitor is visible on Figure 4.16.

Coupling device ⑫
The AKV type 568 quadripole is used as coupling device. It has a bandwidth of 50kHz – 5MHz and is rated for 500kV$_{RMS}$ and 0,5A$_{RMS}$. The coupling device is used to measure the information on the Partial Discharges.

The coupling device has two output channels which carry information on the partial discharges. One output channel carries information on the charge/current of the Partial Discharges. The other output channel is the low output voltage of a capacitive voltage divider inside the coupling device. This low output voltage is used to synchronise the Partial Discharges to the phase of the applied voltage. Both channels are connected to the PD analyser. A photo of the coupling device is visible on Figure 4.17.

PD analyser ⑬
The PD analyser is a DDX 9101 of Tettex instruments. It has an adjustable bandwidth of 20kHz-500kHz. The PD analyser combines the information of the Partial Discharges and synchronises them with the applied voltage. This creates the Phased Resolved Partial Discharge Pattern.

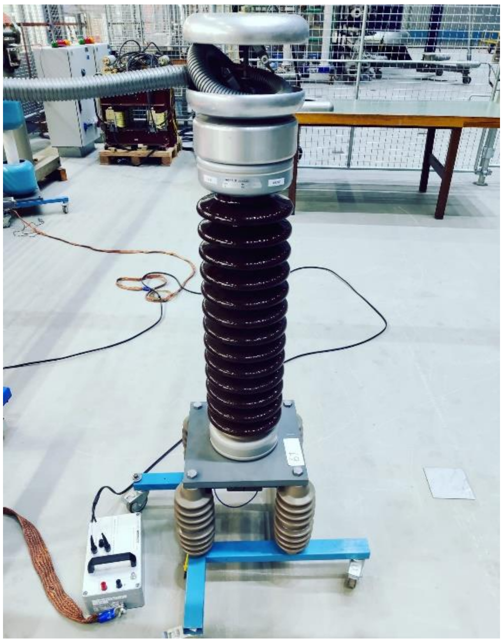

Figure 4.16 Coupling capacitor used to make a loop in which the Partial Discharges can travel. (The device left on the floor is a quadripole.)

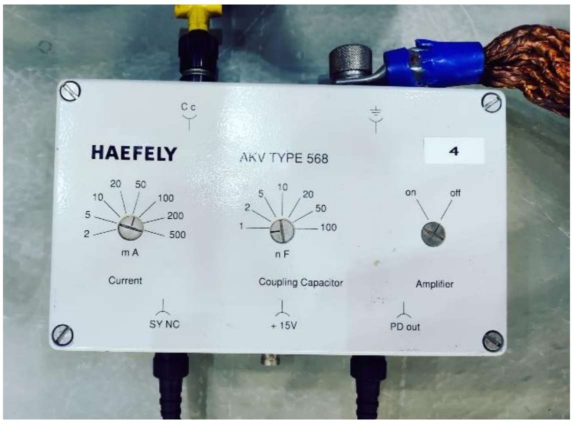

Figure 4.17 Coupling device used to extract information on the Partial discharges.

Maximum stress of the circuit

The equipment has been calculated to its maximum stress, i.e. the allowed operating current and voltage where the equipment will not be damaged. This circuit uses three new pieces of equipment in addition to the same equipment that is used in the circuit to examine the breakdown strength of C4-FN/CO2 (5%/95%).

- Maximum current:
  The maximum current is already calculated in section 4.4.1. By upholding that same maximum current, i.e. 40 A_{RMS}, the new equipment is within the limits of their capacity as well.
- Maximum voltage:
  The PRPD pattern is measured at least 20% above the PDIV. In section 4.3.3 the PDIV of corona in C4-FN/CO2 (5%/95%) at 1bar_{abs} is overestimated at 15kV_{peak}. 20% above the overestimated PDIV corresponds to 18kV_{peak}.
  The maximum voltages are already calculated in section 4.4.1. 18kV_{peak} is roughly 10% of the maximum voltage that is measured in the circuit to examine the breakdown strength of C4-FN/CO2 (5%/95%). This entails that the voltage on the equipment, including the three new pieces, are within the limits of their capacity.

4.4.3 Circuit to examine the waveform of corona partial discharges in C4-FN/CO2 (5%/95%)

The circuit shown in Figure 4.18 is used to measure the waveforms of corona discharges in C4-FN/CO2 (5%/95%). A voltage source ① is connected to a variac ② to regulate the output voltage. An overcurrent protection ③ is connected between the output of the variac and the primary side of the step up transformer ④. A resistor ⑤ is connected in series with the secondary side of the step up transformer for protection. The test cell ⑧ and a capacitive voltage divider ⑥ are connected in parallel to the secondary side of the step up transformer.
The test cell is connected to an oscilloscope ⑪ through a transmission line ⑨. An overvoltage protection ⑩ is placed in the middle of the transmission line to serve as a touch-safety protection. A voltage measurement device ⑦ is connected in parallel to the capacitive voltage divider to measure the applied voltage to the test cell. Figure 4.19 shows a photo of the circuit for examining the PD waveform.

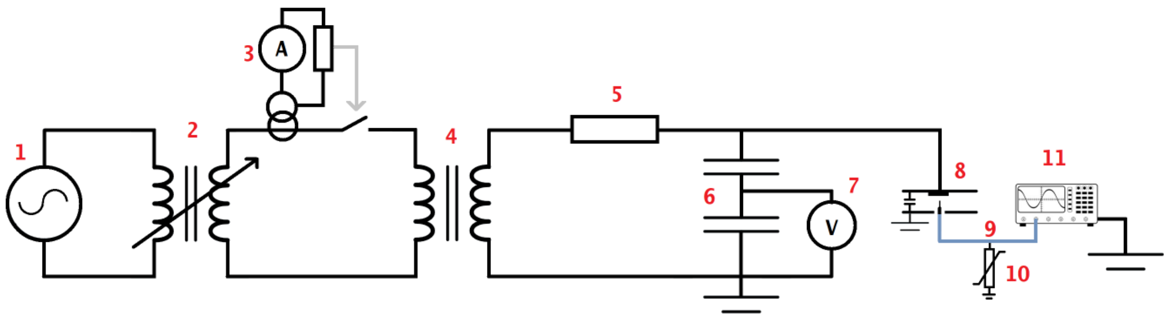

Figure 4.18 Circuit to examine the PD characteristics of C4-FN/CO2 (5%/95%).

Voltage source ①

The voltage source is a 230V_{RMS} 50Hz power socket.

Variac ②

The variac is used to control the primary side of the step up transformer. The variac is used to transform the fixed output voltage of the voltage source to a desired voltage. The variac can produce an output voltage of 0 – 280V_{RMS} and a maximum output current of 8A_{RMS}. A photo of the variac is shown on Figure 4.20.

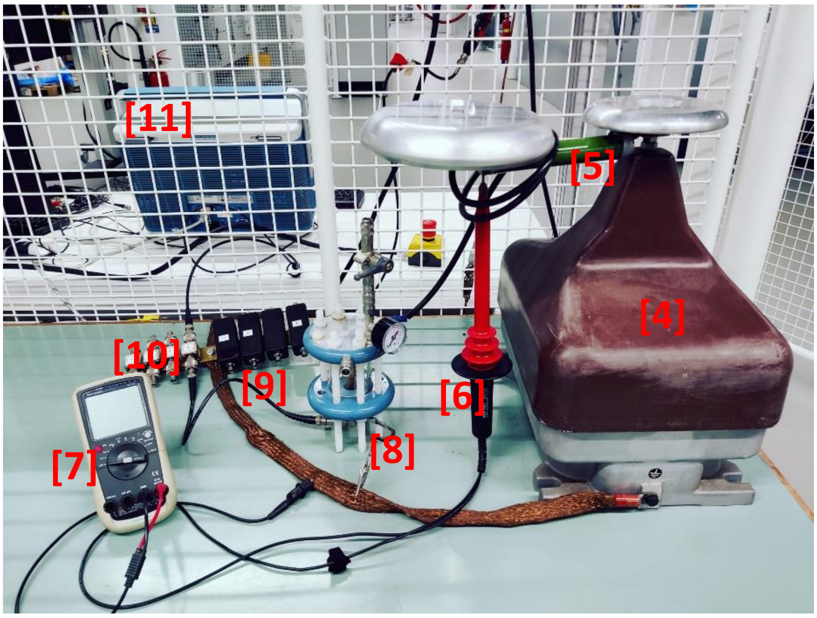

Figure 4.19 Photo of the circuit to examine the PD characteristics of corona in C4-FN/CO2 (5%/95%). The metal disks mitigate possible corona discharges.

Overcurrent protection ③
The overcurrent protection is used to protect the equipment against too much current. The overcurrent protection is set to trip at 0,7A_{RMS} at which it opens a switch disconnecting the equipment from the voltage source. A photo of the overcurrent protection is shown on Figure 4.20.

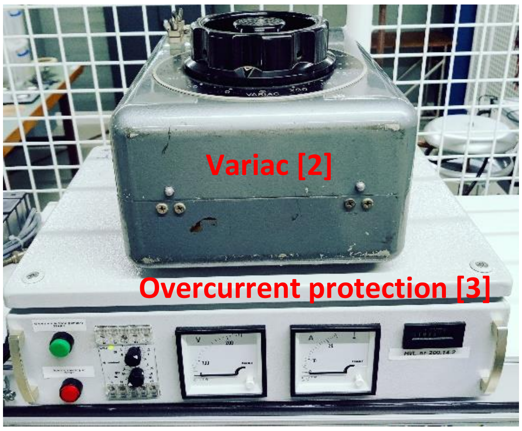

Figure 4.20 The variac and safety box used in the circuit to examine the PD characteristics of corona in C4-FN/CO2 (5%/95%).

Step up transformer ④
The step up transformer is used to step up the low adjustable output voltage of the variac to a high voltage. The transformer can transform voltage 60V_{RMS}/20kV_{RMS} and a has a rated power of 50VA.
The maximum voltage on the primary side of the step up transformer (60V_{RMS}) is lower than the maximum voltage of the variac (230V_{RMS}). There is not a different variac available with a lower output voltage. The output voltage of the variac is not allowed to be over 60V_{RMS}, as to prevent damage to the step up transformer.

Resistor ⑤
A resistor of 5kΩ is used to limit the current in case of an electrical breakdown.

Voltage divider ⑥ + voltage measurement device ⑦
A resistive voltage divider is used to measure the applied voltage over the test cell. The resistive voltage divider is an AC/DC high voltage probe of VOLTCRAFT rated for 28kV$_{RMS\ AC}$. The measured voltage is converted with a 1000:1 Volt ratio. The converted voltage by the voltage divider is read from a multimeter. The maximum applied voltage across the multimeter is 600V$_{RMS}$.

Test cell ⑧
The test cell designed to examine the partial discharge behaviour of C4-FN/CO2 (5%/95%), as is described in section 4.2.2, is used.

Transmission line ⑨ with overvoltage protection ⑩ + oscilloscope ⑪
The needle with characteristic impedance of 50Ω is connected with a transmission line to the 50Ω input of an oscilloscope. The transmission line is a 50Ω coaxial cable. The overvoltage protection serves as safety protection in case the oscilloscope is floating (floating potential). The overvoltage is a surge arrestor which connects the applied voltage to ground if the applied voltage is above 90V$_{RMS}$. The oscilloscope is a Tektronix DPO 7354C. The oscilloscope has maximum bandwidth of 3,5GHz at 50Ω input impedance. The maximum input voltage of the oscilloscope while using the 50Ω input impedance is 5V$_{RMS}$.

Maximum stress of the circuit in which the PD characteristics are examined
The circuit has been calculated to its maximum stress, i.e. the allowed operating current and voltage where the equipment will not be damaged.

- Maximum current:
    - The primary side of step up transformer is rated for 0,83A$_{RMS}$.
    - The variac is rated for 8A$_{RMS}$.

  This means the allowed maximum current is the rated current of the step up transformer, i.e. 0,83A$_{RMS}$. To prevent any damage to the equipment, i.e. the variac and step up transformer, the overcurrent protection is set at 0,7A$_{RMS}$.
- Maximum voltage:
  The waveshape of the corona PD is measured at 10% above the PDIV. In section 4.3.3 the PDIV of corona in C4-FN/CO2 (5%/95%) at 1bar$_{abs}$ is overestimated at 15kV$_{peak}$. 10% above the overestimated PDIV corresponds to 16,5kV$_{peak}$.
    - The secondary side of the step up transformer is 28kV$_{peak}$. 16,5kV$_{peak}$ corresponds to roughly 60% of the rated output voltage.
    - The voltage divider is rated for 40kV$_{peak}$. 16,5kV$_{peak}$ corresponds to roughly 41% of the rated output voltage.

  16,5kV$_{peak}$ measured by the voltage probe gives a low voltage output of 16,5V$_{peak}$.
    - The multimeter is rated for 846V$_{peak}$. 16,5V$_{peak}$ corresponds to 2% of the rated voltage.

  16,5kV$_{peak}$ on secondary side of the step up transformer corresponds to 50V$_{peak}$ on the primary side of the step up transformer.
    - The variac is rated for 394V$_{peak}$. 50V$_{peak}$ corresponds to roughly 13% of the rated output voltage.

4.5 Summary

Chapter 2 delineated and refined the thesis objective and created two topics that were going to be investigated. This chapter converted these two topic into four research questions. The four research question can be divided into two phases, i.e. the delineated topics from chapter 2. Each of the four research questions has its own approach. An approach consists out of multiple experiments. An experiment consists generally out of 10 breakdown repetitions. The research question that were devised to meet the thesis objective are;

Phase A – How does humidity effect the AC insulation performance of C4-FN/CO2 (5%/95%)?

[A-1] How is the AC breakdown strength of C4-FN/CO2 (5%/95%) influenced by different humidities?

[A-2] How does humidity affect the AC breakdown strength of C4-FN/CO2 (5%/95%) at different operating pressures?

Phase B – How does humidity affect the Partial Discharge behaviour of corona in C4-FN/CO2 (5%/95%)?

[B-3] How does humidity affect the partial discharge behaviour of corona in C4-FN/CO2 (5%/95%)?

[B-4] How does humidity affect the characteristics of a corona discharge in C4-FN/CO2 (5%/95%)?

Phase A is examined in three different electric field configurations: uniform, quasi-uniform and non-uniform. Phase B is examined in the non-uniform electric field configuration. Three sets of electrode pairs were designed in COMSOL to acquire the three different electric field configuration with a specific field utilization factor.

5 Results of the experiments

This chapter discusses the results of the experiments which were performed in order to answer the four research question. Each research question is elaborately and separately answered in one section. Each section shows the results of the experiments that are performed. Conclusion are drawn based on those results, thereby answering each research question.

5.1 Phase A – question 1

The research question is: How is the AC breakdown strength of C4-FN/CO2 (5%/95%) influenced by different humidities?
The AC breakdown strength is measured by measuring the AC breakdown voltages. The breakdown strength is examined in all three electric field configurations, at low pressures, i.e. ≤ 1,2 bar_{abs}. Investigating the effect of humidity at these lower pressures allowed for a very high humidity up to 15.000ppmv. The pressure of the gas in each electric field configuration is chosen at a specific value, the reason is twofold;

1. The effect of humidity on the breakdown strength of C4-FN/CO2 (5%/95%) at different pressures is examined in the second research question, i.e. A – 2. Therefore of no importance during this question.
2. The digital voltage measurement device, described in section 4.4.1, did not display the voltage continuously. Sometimes it showed a blank display, possibly because it switch to a different voltage range. As a consequence the measured voltage was not displayed for several kilovolts. This is avoided by choosing a pressure at which the breakdown voltages were not near the 'blank display value'.

The measured breakdown behaviour of C4-FN/CO2 (5%/95%) at a varying humidity is shown in Figure 5.1, Figure 5.2 and Figure 5.3 for the uniform, quasi-uniform and non-uniform electric field configuration respectively. The conclusion on the correlation between the effect of humidity and the breakdown strength of C4-FN/CO2 (5%/95%) is given after the data is analysed, i.e. in section 5.1.2. The data is analysed to provide more conclusive data over the correlation between the amount of humidity and the electrical breakdown strength. The analysed breakdown behaviour of C4-FN/CO2 (5%/95%) with a varying humidity is shown in Figure 5.4, Figure 5.5 and Figure 5.6 for the uniform, quasi-uniform and non-uniform electric field configuration respectively.

Figure 5.9 shows the relative breakdown behaviour of the three different examined electric field configurations. By comparing the relative breakdown behaviour it possible to make a conclusion on how the electric field configuration influences the effect of humidity on the electrical breakdown strength of C4-FN/CO2 (5%/95%).

Information about the graphs

- Each dot in the graphs represents an experiment consisting out of 10 breakdown repetitions.
- The vertical bars show the range of the minimum and maximum measured breakdown voltage of C4-FN/CO2 (5%/95%). The dot is the average breakdown voltage of the 10 breakdown repetitions.
- The horizontal bars show a 5% deviation of the measured humidity. The dewpoint reading of the gas was stable after waiting 20 minutes. However, when the gas was inserted into the test cell the (stable) dewpoint temperature deviated. The deviation was always in the range of 5%.
- The distance between the electrode was kept constant at 5,0mm for all the experiments.
- The pressure of the humid C4-FN/CO2 (5%/95%) gas mixture was for all the experiments in one electric field configuration identical, up to 2 decimals.

5.1.1 Measured data

Uniform electric field configuration

Figure 5.1 shows the correlation between the breakdown behaviour of C4-FN/CO2 (5%/95%) and the presence of humidity in an uniform electric field configuration. The program Excel made a trendline based upon the results of the experiments. A logarithmic trendline showed the best fit through the measured results, implying that there is logarithmic correlation between the amount of humidity and the electrical breakdown strength of C4-FN/CO2 (5%/95%) in an uniform electric field configuration. The coefficient of determination of the trendline is given by R^2, $R^2 = 1$ implies that the trendline has an excellent fit with the data and $R^2 = 0$ implies that trendline has no fit with the data. The trendline is UBD [kV] = -1,762 ln (humidity [ppmv]) + 40,905 and has a coefficient of determination of $R^2 = 0{,}9351$.

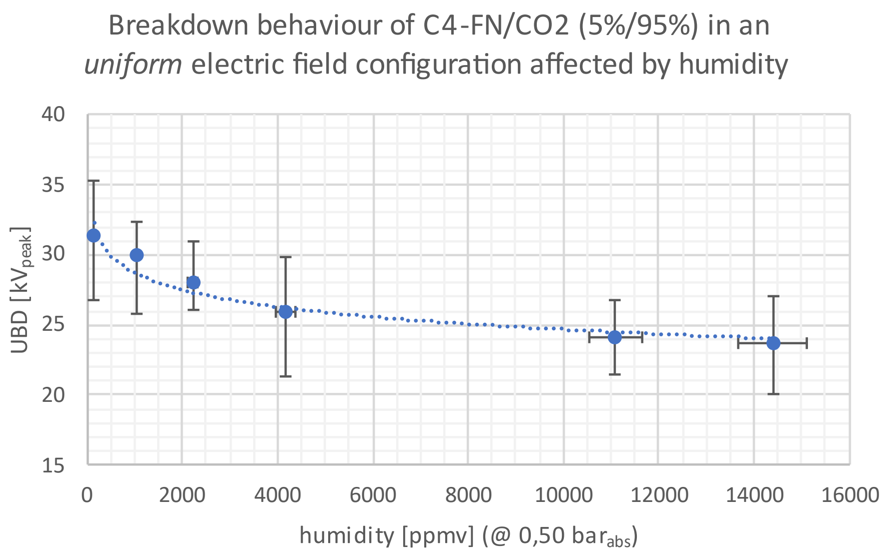

Figure 5.1 Breakdown strength of C4-FN/CO2 (5%/95%) in an uniform electric field affected by humidity.

Quasi-uniform electric field configuration

Figure 5.2 shows the correlation between the breakdown behaviour of C4-FN/CO2 (5%/95%) and the presence of humidity in a quasi-uniform electric field configuration. The program Excel made a trendline based upon the results of the experiments. A logarithmic trendline showed the best fit through the measured results, implying that there is logarithmic correlation between the amount of humidity and the electrical breakdown strength of C4-FN/CO2 (5%/95%) in a quasi-uniform electric field configuration. The coefficient of determination of the trendline is given by R^2, $R^2 = 1$ implies that the trendline has an excellent fit with the data and $R^2 = 0$ implies that the trendline has no fit with the data. The trendline is UBD [kV] = -1,217 ln (humidity [ppmv]) + 28,375 and has a coefficient of determination of $R^2 = 0{,}9499$.

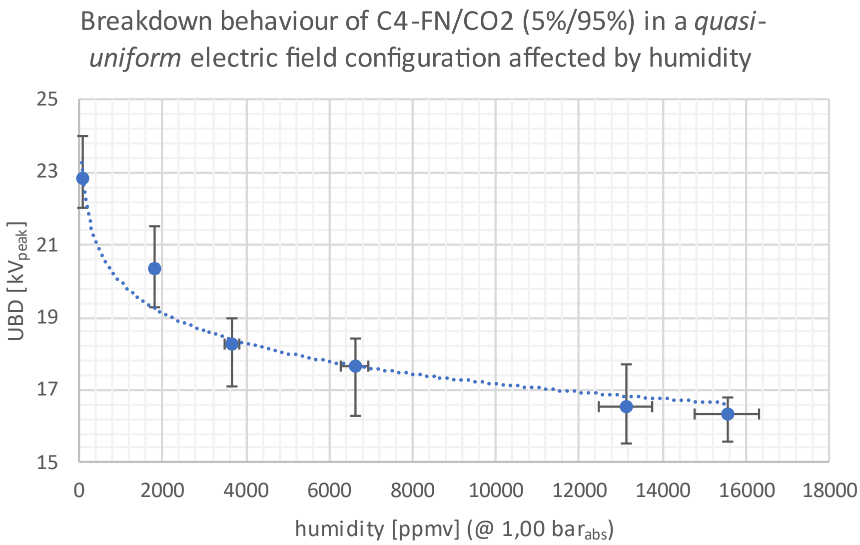

Figure 5.2 Breakdown strength of C4-FN/CO2 (5%/95%) in a quasi-uniform electric field affected by humidity.

Non-uniform electric field configuration

Figure 5.3 shows the correlation between the breakdown behaviour of C4-FN/CO2 (5%/95%) and the presence of humidity in a non-uniform electric field configuration. The program Excel made a trendline based upon the results of the experiments. A linear trendline showed the best fit through the measured results, implying that there is linear correlation between the amount of humidity and the electrical breakdown strength of C4-FN/CO2 (5%/95%) in a non-uniform electric field configuration. The coefficient of determination of the trendline is given by R^2, $R^2 = 1$ means that the trendline has an excellent fit with the data and $R^2 = 0$ means that the trendline has no fit with the data. The trendline is UBD [kV] = $-2x10^{-5}$ · (humidity [ppmv]) + 21,515 and has a coefficient of determination of $R^2 = 0{,}9491$.

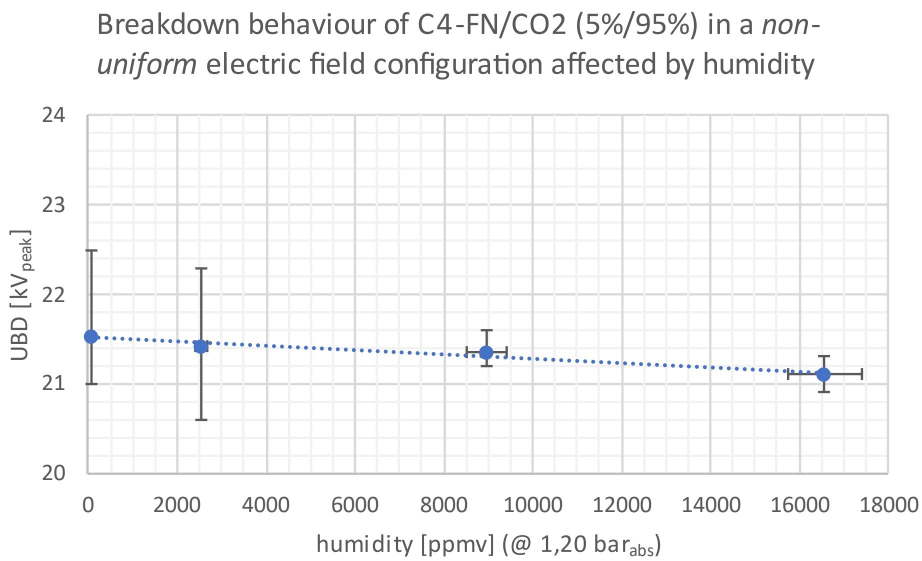

Figure 5.3 Breakdown strength of C4-FN/CO2 (5%/95%) in a non-uniform electric field affected by humidity.

5.1.2 Analysed data

Some of the datapoints with their error bars overlap with each other in Figure 5.1, Figure 5.2 and Figure 5.3. This makes it difficult to draw solid conclusions over the measured results. Therefore the data is statistically analysed to extract more reliable data out of the measured results. The statistical analysis is done in Matlab with the toolbox *"distributionFitter"*.

Electrical breakdowns can be analysed by placing a Weibull, Gumbell or (log)Normal distribution over the data [30]. The electrical breakdowns in this research are fitted to a normal distribution. The distribution gives information on certain parameters, like mean and deviation.
The Normal distributions did not accurately fit all the measured data, this is due to the limited number of breakdown repetitions that were performed during an experiment, i.e. 10 breakdown repetitions in one experiment.

The Normal distribution is used to create CDF plots with 95% confidence bounds for all experiments of phase A – question 1. The 95% confidence bounds are calculated with the mean and standard deviation of all the 10 breakdown repetitions. The statistical breakdown voltage U_{50} is determined from these CDF plots. The U_{50} of C4-FN/CO2 (5%/95%) in uniform, quasi-uniform and non-uniform electric fields are shown in Figure 5.4, Figure 5.5 and Figure 5.6 respectively. A smaller confidence bound indicates are more reliable analysis.

Information about the graphs

The same information about the graphs from section 5.1.1 applies here too, except there are two new additions/changes;

- The black vertical error bars now represent the 95% confidence bounds.
- The red bars represent the minimum and maximum measured breakdown voltage of C4-FN/CO2 (5%/95%). The red bars are added for comparison and to illustrate the improvement of the statistical analysis.

Answer to the research question in an uniform electric field configuration

Figure 5.4 shows the U_{50} of C4-FN/CO2 (5%/95%) in an uniform electric field configuration. It can be concluded that humidity *affects* the breakdown strength of C4-FN/CO2 (5%/95%) in an uniform electric field configuration. The breakdown behaviour shows a logarithmic correlation between the amount of humidity in the gas mixture and the breakdown strength of C4-FN/CO2 (5%/95%).

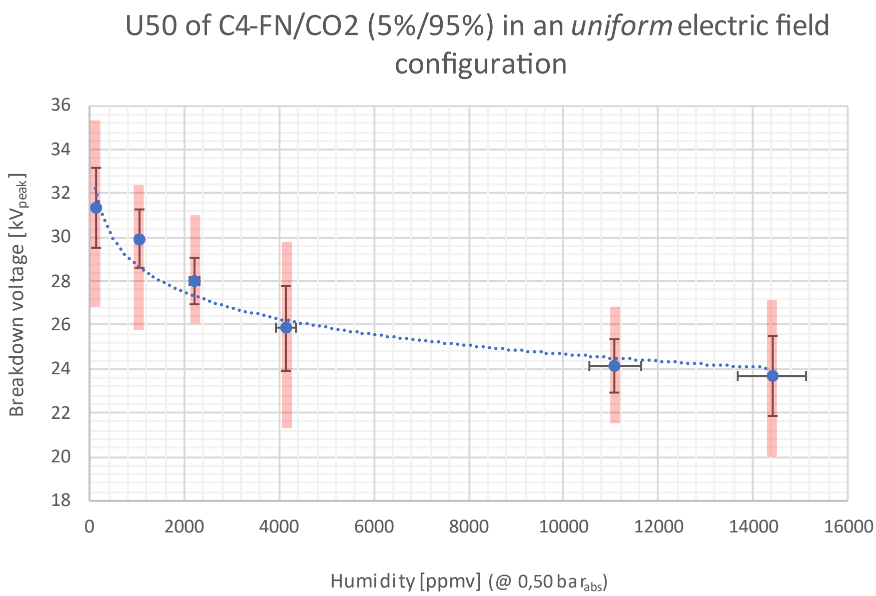

Figure 5.4 The statistical breakdown behaviour of C4-FN/CO2 (5%/95%) in an uniform electric field affected by humidity.

Answer to the research question in a quasi-uniform electric field configuration

Figure 5.5 shows the U_{50} of C4-FN/CO2 (5%/95%) in a quasi-uniform electric field configuration. It can be concluded that humidity *affects* the breakdown strength of C4-FN/CO2 (5%/95%) in an quasi-uniform electric field configuration. The breakdown behaviour shows a logarithmic correlation between the amount of humidity in the gas mixture and the breakdown strength of C4-FN/CO2 (5%/95%).

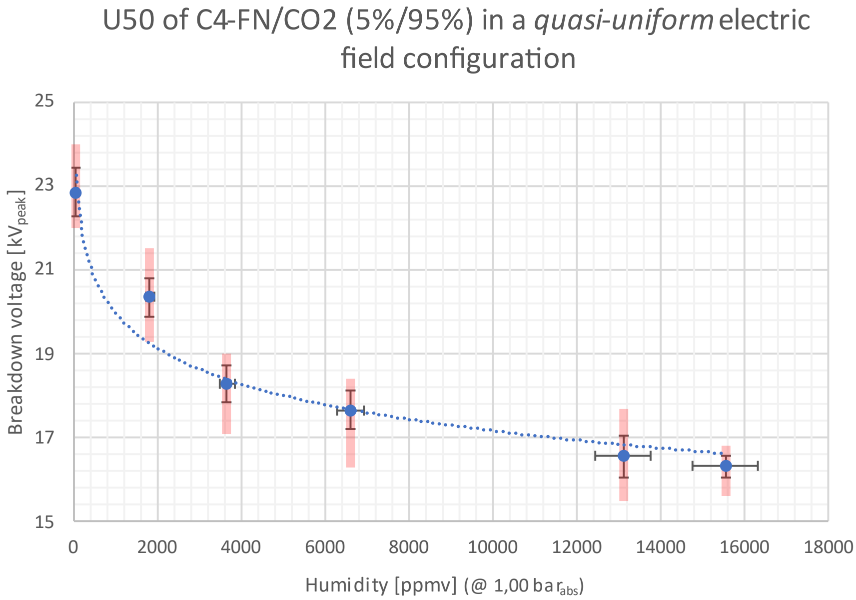

Figure 5.5 The statistical breakdown behaviour of C4-FN/CO2 (5%/95%) in a quasi-uniform electric field affected by humidity.

Answer to the research question in a non-uniform electric field configuration

Figure 5.6 shows the U_{50} of C4-FN/CO2 (5%/95%) in a non-uniform electric field configuration. It can be concluded that humidity *affects* the breakdown strength of C4-FN/CO2 (5%/95%) in a non-uniform electric field configuration. The influence of humidity on the breakdown behaviour in a non-uniform electric field configuration is however far less distinct compared to the breakdown behaviour of C4-FN/CO2 (5%/95%) in an uniform and a quasi-uniform electric field configuration. The breakdown behaviour shows a linear correlation between the amount of humidity in the gas mixture and the breakdown strength of C4-FN/CO2 (5%/95%).

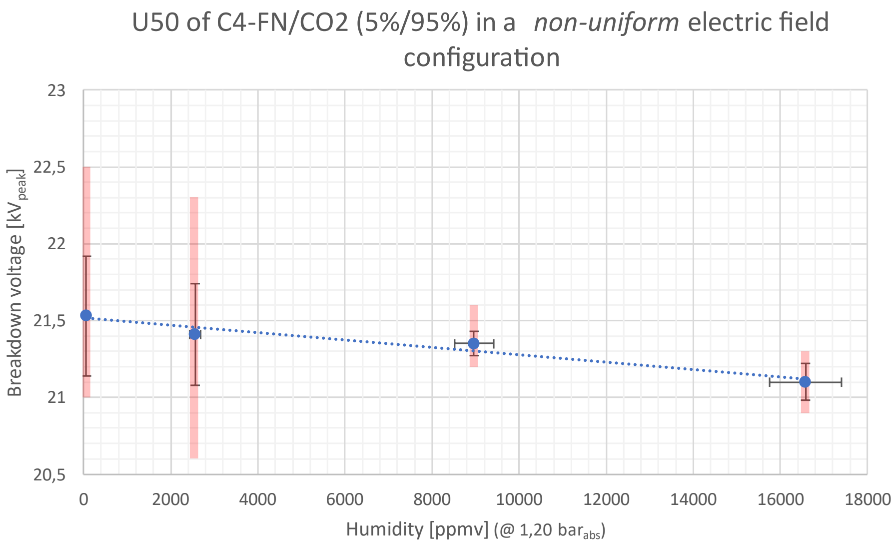

Figure 5.6 The statistical breakdown behaviour of C4-FN/CO2 (5%/95%) in a non-uniform electric field affected by humidity.

Hypothesis for the affected breakdown behaviour of C4-FN/CO2 (5%/95%) by humidity

A hypothesis has been made about the reason for the affected breakdown behaviour of C4-FN/CO2 (5%/95%) by humidity. It is hypothesized that C4-FN/CO2 (5%/95%) mixed with different humidities have different effective ionization coefficients (α_{eff}). An increase in humidity results in an increase of the effective ionization coefficient.

Numerical studies have shown that the α_{eff} of a gas can change with the presence of humidity [31-34]. In those studies the reduced ionization and reduced attachment coefficients have been calculated by solving the two-term Boltzmann equations. Figure 5.7 and Figure 5.8 show the reduced (effective) ionization coefficient ($\alpha_{(eff)}$/N [m^2]) against the reduced electric field strength (E/N [T_d]) [31,32]. The figures show that there are different α_{eff} coefficients for gases mixed with different humidities. Figure 5.7 shows that an *increase* in the humidity in air, *decreases* the α_{eff} coefficient. This allows a *higher* breakdown voltage. The opposite is true SF6. Figure 5.8 shows that an *increase* in the humidity in SF6, *increases* α_{eff}. This allows a lower breakdown voltage.

However, these different α_{eff} coefficients are not constant throughout different electric field configurations and all phenomena.

- Different electric field configurations:
  The effect of humidity in air on the AC breakdown voltage in uniform fields is negligible, but significant for quasi-uniform and non-uniform fields [33,34].
  This can also be concluded from the results of the experiments that were performed to answer research question A-1.
- Different phenomenon:
  The effect of humidity in SF6 on the flashover voltage can vary for different voltage phenomena. The effect of humidity in SF6 on the AC flashover voltage in a quasi-uniform field is significant, but negligible for positive lightning impulses [6].

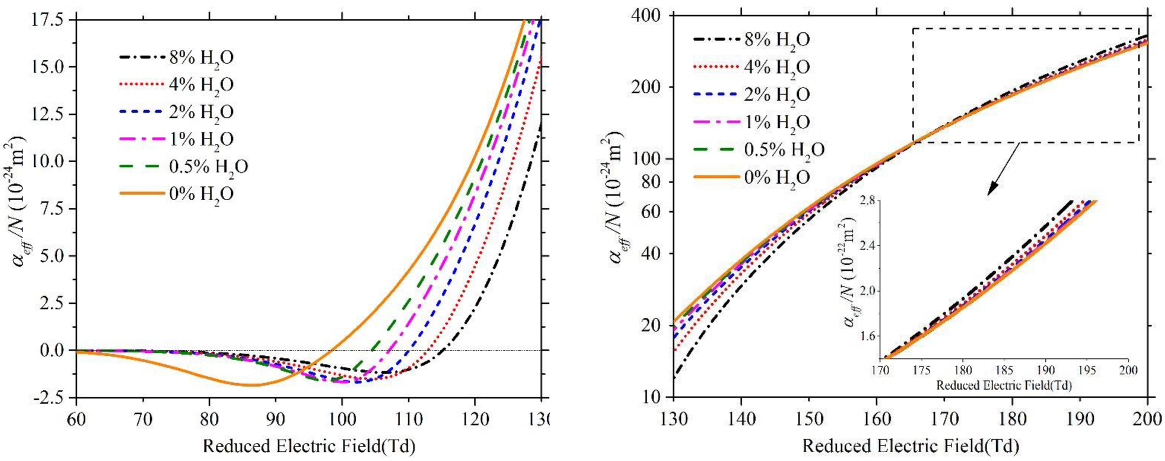

(a) *(b)*

Figure 5.7 α_{eff} for air mixed with humidity [32].
(a) α_{eff} for lower electric field strengths (b) α_{eff} for higher electric field strengths.

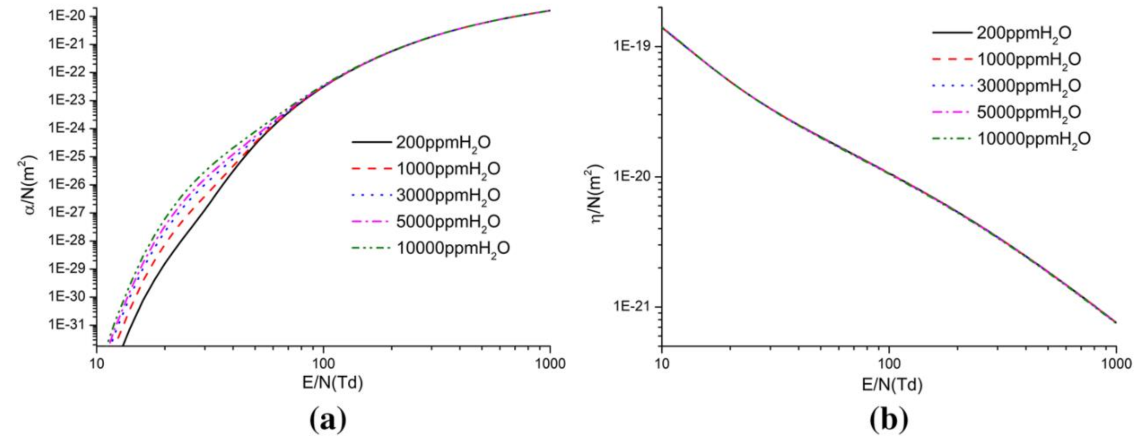

Figure 5.8 (a) α for SF6 mixed with humidity (b) η for humidity mixed with SF6. $\alpha_{eff} = \alpha - \eta$ [31].

5.1.3 Comparison between the behaviour of the breakdown strength of C4-FN/CO2 (5%/95%) in the different electric field configurations

The previous results indicated that the effect of humidity on the breakdown strength of C4-FN/CO2 (5%/95%) is also related to the electric field configuration, i.e. the η-factor. Therefore the relative breakdown behaviour of humid C4-FN/CO2 (5%/95%) in the three different electric field configurations are compared to each other. The relative breakdown behaviour is based on the trendlines discussed in section 5.1.1. The comparison is plotted and shown in Figure 5.9

However, the test were performed at different pressure. The pressure of C4-FN/CO2 (5%/95%) has to be equal in all the three different electric field configurations to make a proper comparison and an appropriate conclusion. A number of things were done to achieve this:

- Uniform electric field configuration: the breakdown behaviour of humid C4-FN/CO2 (5%/95%) was measured with three experiments at 1,00bar$_{abs}$.
- Non-uniform electric field configuration: the breakdown behaviour of humid C4-FN/CO2 (5%/95%) was originally measured at 1,20bar$_{abs}$. The breakdown behaviour at 1,20bar$_{abs}$ can for this instance be assumed to be (about) equal to the breakdown behaviour at 1,00bar$_{abs}$. This is based on the results from the experiments that were performed during research question A-2, see Figure 5.12.

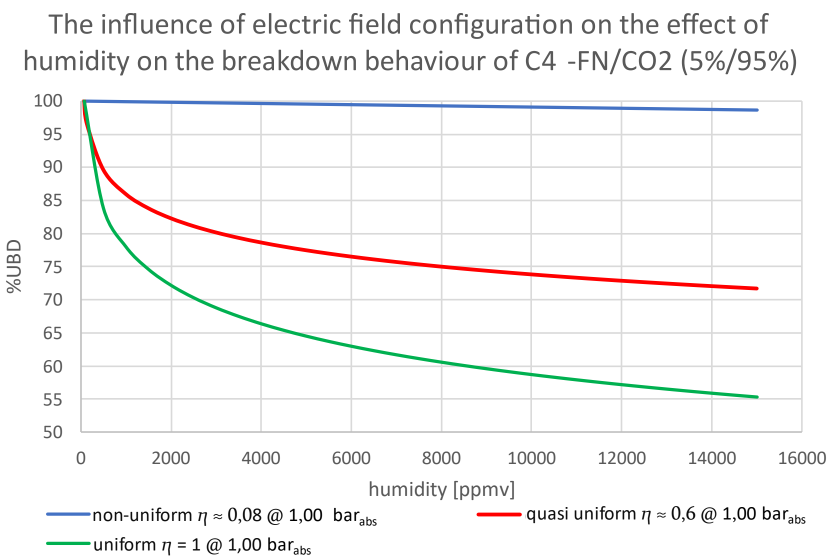

Figure 5.9 The comparison between the behaviour of the relative breakdown strength of C4-FN/CO2 (5%/95%) in the three different electric field configurations. This graph is based on the trendlines that Excel made through the results of the experiments.

From Figure 5.9 it can be concluded that the η-factor of the electric field also affects electrical breakdown behaviour of humid C4-FN/CO2 (5%/95%). The effect of humidity on the electrical breakdown behaviour of C4-FN/CO2 (5%/95%) shows a decreasing influence as the η-factor of the electric field decreases.

5.1.4 Answer to research question A – 1

There is a correlation between the breakdown behaviour of C4-FN/CO2 (5%/95%) and the presence of humidity in the gas mixture. The extent of the influence of humidity on breakdown strength of C4-FN/CO2 (5%/95%) depends on two factors:

1. <u>The amount of humidity present in the gas mixture.</u>
   The breakdown strength of C4-FN/CO2 (5%/95%) shows a decrease with an increase of humidity.
2. <u>The η-factor of the electric field configuration.</u>
   The effect of humidity on the breakdown behaviour of C4-FN/CO2 (5%/95%) decreases with a decreasing η-factor of the electric field configuration.

A hypothesis has been made about the reason for the affected breakdown behaviour of C4-FN/CO2 (5%/95%) by humidity. It is hypothesized that C4-FN/CO2 (5%/95%) mixed with different humidities have different effective ionization coefficients (α_{eff}). An increase in humidity results in an increase of the effective ionization coefficient. However, these different α_{eff} coefficients are not constant throughout different electric field configurations.

5.2 Phase A – question 2

The research question is: How does humidity affect the AC breakdown strength of C4-FN/CO2 (5%/95%) at different operating pressures?
This is examined in all three electric field configurations. The breakdown voltages of humid and dry C4-FN/CO2 (5%/95%) are measured at different operating pressures and are mapped into a graph. There are three different graphs, one graph for each electric field configuration. These graphs shows the correlation between the AC breakdown strength of (dry and) humid C4-FN/CO2 (5%/95%) and the operating pressure. The graphs will thus also conclude if the results of research question A – 1 (the effect of humidity on the breakdown behaviour of C4-FN/CO2 (5%/95%)) is constant throughout different operating pressures.
The breakdown behaviour of dry C4-FN/CO2 (5%/95%) serves as a reference for the comparison between the breakdown behaviour of dry and humid C4-FN/CO2 (5%/95%). The measured breakdown voltages of C4-FN/CO2 (5%/95%) are shown in Figure 5.10, Figure 5.11 and Figure 5.12.

The operating pressure is measured from 1 bar_{abs} to 7bar_{abs} with intervals of 2bar_{abs} where the humidity of humid C4-FN/CO2 (5%/95%) is kept constant between 2000-3000ppmv. However, the preferred maximum pressure of 7bar_{abs} for humid C4-FN/CO2 (5%/95%) could not be reached. In order to reach 7bar_{abs} in the test cell, the created humid C4-FN/CO2 (5%/95%) in the mixing vessel needed a pressure of 10$bar_{abs.}$ The 10bar_{abs} could not be reached due to the low pressure of the gas tank, i.e. <10bar_{abs}. The use of another gas tank of C4-FN/CO2 is avoided to keep a consistency of the used gas mixture. Table 5.1 shows the new maximum pressures of the humid C4-FN/CO2 (5%/95%) in the three different electric field configurations.

Electric field configuration	**New maximum operating pressure**
Uniform	6,85bar_{abs}
Quasi-uniform	6,55bar_{abs}
Non-uniform	6,30bar_{abs}

Table 5.1 The new maximum pressures of the humid C4-FN/CO2 (5%/95%) in the three different electric field configurations.

About the chosen value for the humidity of C4-FN/CO2 (5%/95%)

- The humidity of the of the gas at 7bar_{abs} is limited to <3000ppmv, due to the high operating pressure and low temperature of the gas. A higher humidity can be reached at 7bar_{abs} if the temperature of the gas mixture is increased. However, this will create the difficulty of keeping the gas the same high temperature at all times to prevent condensation of the humidity in the gas mixture. Due to lack of facilities and avoiding unnecessary hardship, the humidity is chosen to vary between 2000-3000ppmv.
- The humidity varies with a range of a 1000pmv as it is impossible to create a humidity of a certain value for multiple experiments. It is also extremely difficult to create a humidity in the range of 100ppmv.

5.2.1 Measured data

- Each dot in the graphs represents an experiment consisting out of 10 breakdown repetitions.
- The vertical bars show the range of the minimum and maximum measured breakdown voltage of C4-FN/CO2 (5%/95%). The dot is the average breakdown voltage of the 10 breakdown repetitions.
- During the performed experiments the distance between the electrode was kept constant at 5,0mm.

Answer to the research question in an uniform electric field configuration

Figure 5.10 shows the correlation between the effect of humidity on the breakdown behaviour of C4-FN/CO2 (5%/95%) and the operating pressure in an uniform electric field configuration. It can be concluded that the effect of humidity on the breakdown behaviour of C4-FN/CO2 (5%/95%) is not constant throughout different operating pressures. The effect of humidity on the breakdown behaviour of C4-FN/CO2 (5%/95%) in an uniform electric field configuration decreases as the operating pressure increases.

The average breakdown voltage of humid C4-FN/CO2 (5%/95%) at 6,85bar_{abs} is not equal to the average breakdown voltage dry C4-FN/CO2 (5%/95%) at 6,85bar_{abs}. Both trendlines intersect at 8bar_{abs} by assuming that the trendline through the datapoints follows the same path for higher operating pressures. This hints that the breakdown behaviour of C4-FN/CO2 (5%/95%) with a humidity of 2000-3000ppmv in a uniform electric field configuration is no longer affected by humidity at an operating pressure ≥ 8bar_{abs}.

It is interesting to mention that the breakdown voltage of humid C4-FN/CO2 (5%/95%) at 7bar_{abs} showed a conditioning effect. The breakdown voltage of humid C4-FN/CO2 (5%/95%) kept increasing from the first breakdown to the sixth breakdown, after which it was (more) constant. This effect was not observed at the lower operating pressures and a repetition of the experiment at 7bar_{abs}, with polished electrodes, showed the same conditioning effect.

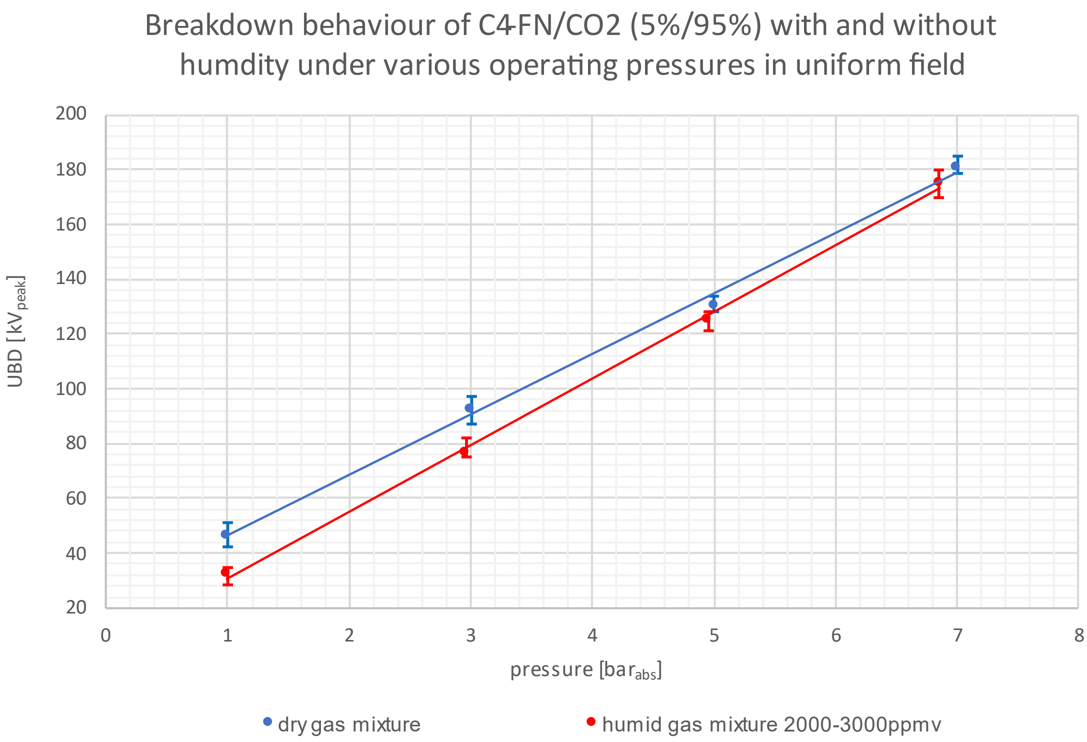

Figure 5.10 Breakdown strength of C4-FN/CO2 (5%/95%) with different humidities in an uniform electric field against increasing operating pressures.

Answer to the research question in a quasi-uniform electric field configuration
Figure 5.11 shows the correlation between the effect of humidity on the breakdown behaviour of C4-FN/CO2 (5%/95%) and the operating pressure in a quasi-uniform electric field configuration. It can be concluded that the effect of humidity on the breakdown behaviour of C4-FN/CO2 (5%/95%) is not constant throughout different operating pressures. The effect of humidity on the breakdown behaviour of C4-FN/CO2 (5%/95%) in a quasi-uniform electric field configuration decreases as the operating pressure increases.

The average breakdown voltage of humid C4-FN/CO2 (5%/95%) at 6,55bar_{abs} is the same as the average breakdown voltage dry C4-FN/CO2 (5%/95%) at 6,55bar_{abs}. This hints that the breakdown behaviour of C4-FN/CO2 (5%/95%) with a humidity of 2000-3000ppmv in a quasi-uniform electric field configuration is no longer affected by humidity at an operating pressure of ≥ 6,55bar_{abs}.

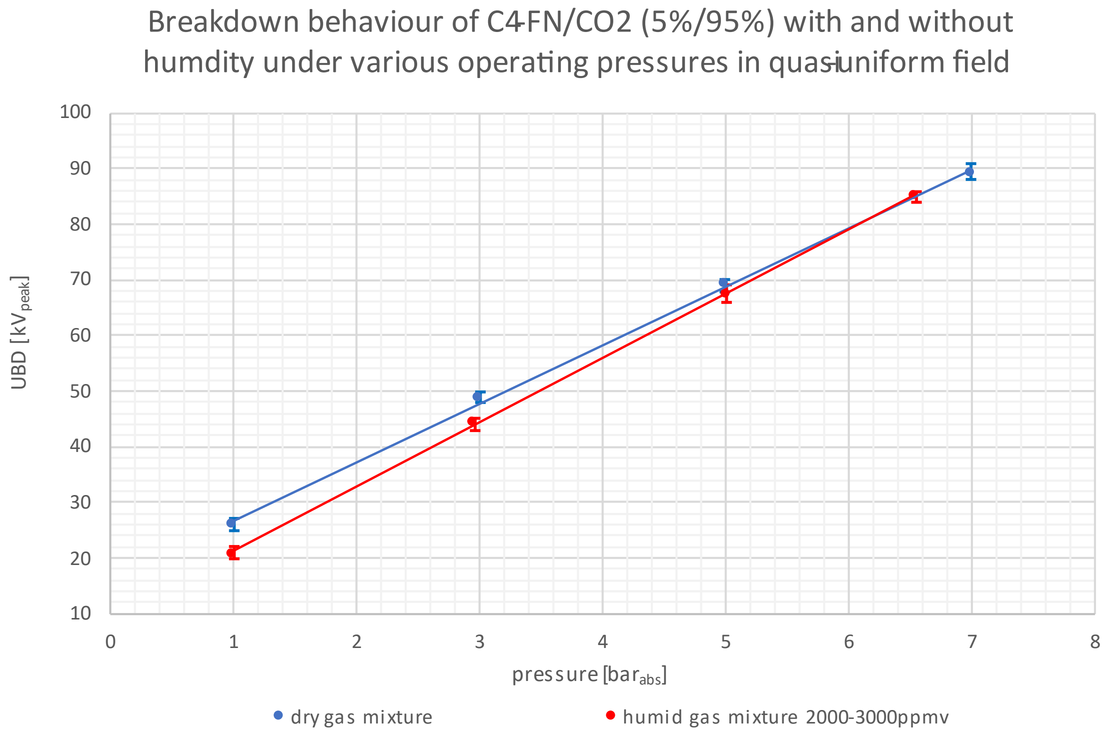

Figure 5.11 Breakdown strength of C4-FN/CO2 (5%/95%) with different humidities in a quasi-uniform electric field against increasing operating pressures.

Answer to the research question in a non-uniform electric field configuration
Figure 5.12 shows the correlation between the effect of humidity on the breakdown behaviour of C4-FN/CO2 (5%/95%) and the operating pressure in a non-uniform electric field configuration. The results from Figure 5.6 in section 5.1.2 showed that the effect of humidity on the breakdown voltage of C4-FN/CO2 (5%/95%) in a non-uniform electric field configuration is extremely small. Therefore it is difficult to see if the effect humidity on the breakdown strength of C4-FN/CO2 (5%/95%) decreases at higher operating pressures, like it does in an uniform and quasi-uniform electric field configuration.

It can be seen from Figure 5.12 that the effect of humidity on the breakdown strength of C4-FN/CO2 (5%/95%) is also barely present at higher operating pressures, except at 5bar_{abs}. At 5bar_{abs} there is an anomaly where the effect of humidity on the breakdown strength of C4-FN/CO2 (5%/95%) is extremely noticeable. A repetition of the experiment at 5bar_{abs} showed similar results.

The curves of the breakdown behaviour of dry and humid C4-FN/CO2 (5%/95%) differ because of the anomaly at 5bar$_{abs}$. This precludes a solid conclusion about the correlation between the effect of humidity on the breakdown behaviour of C4-FN/CO2 (5%/95%) and the operating pressure. A more detailed curve of the breakdown behaviour of dry and humid C4-FN/CO2 (5%/95%) would establish a solid conclusion about the correlation between the effect of humidity on the breakdown behaviour of C4-FN/CO2 (5%/95%) and the operating pressure in a non-uniform electric field configuration.

It is strongly believed that, based on the data available, the effect of humidity on the breakdown behaviour of C4-FN/CO2 (5%/95%) at different operating pressures in a non-uniform electric field configuration is negligible.

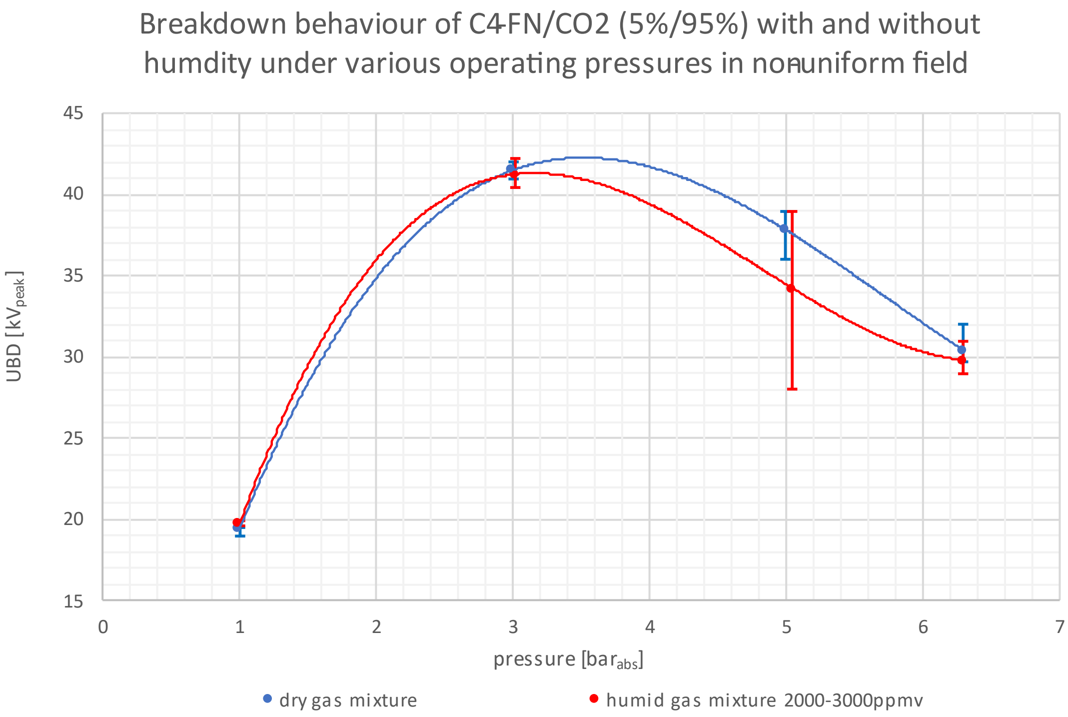

Figure 5.12 Breakdown strength of C4-FN/CO2 (5%/95%) with different humidities in a non-uniform electric field against increasing operating pressures.

Cause for the increase of the breakdown voltage of dry C4-FN/CO2 (5%/95%) by the increase of the operating pressure

In section 3.3.1 it is explained that an increase of the operating pressure results in an increase of the breakdown voltage. Figure 5.10 and Figure 5.11 show a linear correlation between the operating pressure and the breakdown strength in the uniform and quasi-uniform electric field configuration. However, Figure 5.12 shows a non-linear correlation between the breakdown voltage and the operating pressure in a non-uniform electric field configuration. The non-linear breakdown behaviour in a non-uniform electric field configuration is due to the properties of the insulation gas and the high electric field strength. The non-linear breakdown behaviour will likely change if the properties of the gas between the electrodes is are altered [35,36].

Hypothesis for the affected breakdown behaviour of humid C4-FN/CO2 (5%/95%) by the operating pressure

A hypothesis has been made about the affected breakdown behaviour of humid C4-FN/CO2 (5%/95%) by the operating pressure. This hypothesis is related to the earlier made hypothesis. Earlier it was hypothesized that C4-FN/CO2 (5%/95%) mixed with different humidities have different effective ionization coefficients (α_{eff}).

It is also hypothesized that an increase in the operating pressure results in an decrease between the variation of the dry and humid effective ionization coefficients.

5.2.2 Answer to research question A – 2

There is a correlation between the effect of humidity on the breakdown behaviour of C4-FN/CO2 (5%/95%) and different operating pressures. The extent of the influence of humidity on breakdown strength of C4-FN/CO2 (5%/95%) at different operating pressures depends on two factors;

1. <u>The operating pressure:</u>
   The effect of humidity on the breakdown behaviour of C4-FN/CO2 (5%/95%) decreases as the operating pressure increases.
2. <u>The η-factor of the electric field configuration:</u>
   The effect of humidity on the breakdown behaviour of C4-FN/CO2 (5%/95%) at different operating pressures decreases with a decreasing η-factor of the electric field configuration.

It is also hypothesized that the extent of the influence of humidity on breakdown strength of C4-FN/CO2 (5%/95%) at different operating pressures depends on the amount of humidity present in the gas mixture. A large amount of humidity present in C4-FN/CO2 (5%/95%) affects the breakdown strength of C4-FN/CO2 (5%/95%) more at a certain pressure compared to a smaller amount of humidity. This is based on the conclusion from research question A – 1, see section 5.1.4.

A hypothesis has been made about the reason for the decreasing effects of humidity on the breakdown behaviour of C4-FN/CO2 (5%/95%) at higher operating pressures. This hypothesis is related to the hypothesis made in section 5.1.4. There it was hypothesized that C4-FN/CO2 (5%/95%) mixed with different humidities have different effective ionization coefficients (α_{eff}).

Now it is hypothesized that an increase in the operating pressure results in an decrease between the variation of the dry and humid effective ionization coefficients. However, these different α_{eff} coefficients are not constant throughout different electric field configurations.

5.3 Phase B – question 3

The research question is: How does humidity affect the partial discharge behaviour of corona in C4-FN/CO2 (5%/95%)?
This is examined by comparing and analysing the PDIV and the PRPD pattern of corona in dry and humid C4-FN/CO2 (5%/95%).

5.3.1 Measured data

- During the performed experiments the distance between the electrode was kept constant at 10mm. The distance is doubled and the same breakdown strength as the 5mm gap distance is uphold, as an extra safety precaution.
- The pressure of the dry and humid C4-FN/CO2 (5%/95%) gas mixture was for all the experiments 1,00 bar_{abs}.
- The background noise measured below 1pC.
- The PD analyser has been calibrated at 10pC. The PD analyser measured the same applied charge by the calibrator in the range of 5 – 20pC.
- The PD activity of the circuit and test cell without electrodes was measured and proved to be PD free up to 35kV_{peak}. Any PD activity measured is therefore originating from the electrodes.

PDIV of dry and humid C4-FN/CO2 (5%/95%)

The PDIV of corona in dry and humid C4-FN/CO2 (5%/95%) has been measured. The humid C4-FN/CO2 (5%/95%) has a humidity of 9500±300ppmv. The dry C4-FN/CO2 (5%/95%) had a humidity of 35ppmv. The results of the measurements are shown in Figure 5.13. It can be concluded from Figure 5.13 that the PDIV of *dry* and *humid* C4-FN/CO2 (5%/95%) are *both* around 9kV_{peak}.

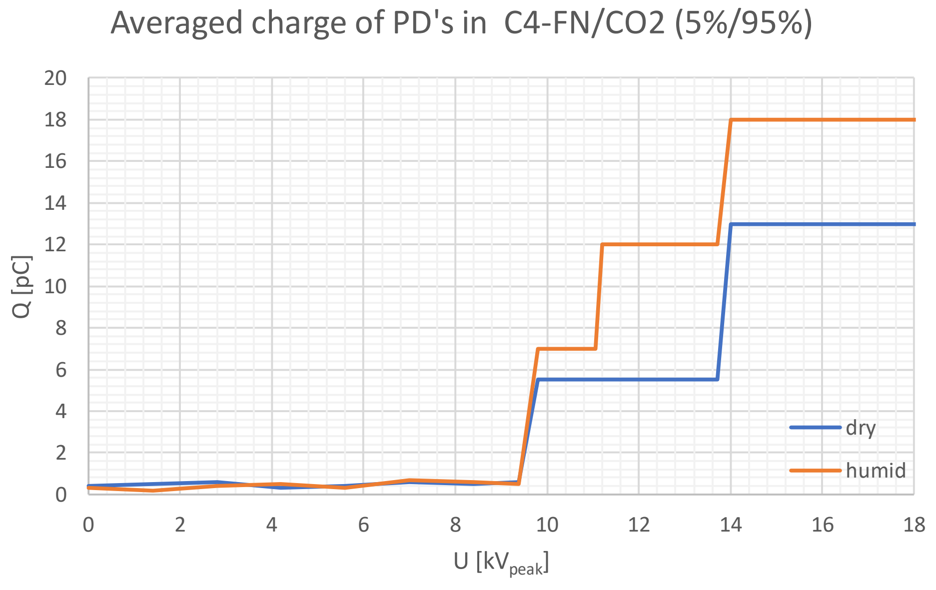

Figure 5.13 The measured average charge at different voltages. Q[pC] is the averaged charge according to the IEC60270.

PRPD pattern of dry and humid C4-FN/CO2 (5%/95%)

Figure 5.13 shows that the averaged charge of the partial discharges in humid C4-FN/CO2 (5%/95%) increases three times, i.e. 0,5pC → 8pC, 8pC → 12pC and 12pC → 18pC. As a consequence, the PRPD pattern is recorded at three different voltages. The PRPD pattern is recorded for a minute at each voltage. An overview of the consecutive PRPD patterns of dry and humid C4-FN/CO2 (5%/95%) are summarized in Table 5.2. The PRPD patterns in Table 5.2 are a direct screenshot of the program "*remote9101*" appurtenant to the PD analyser. The y-axis shows the charge of partial discharges in pC. The x-axis shows the phase of the applied voltage where the partial discharges occur. The colour shows the repetition rate of the partial discharges.

The PRPD pattern of dry and humid C4-FN/CO2 (5%/95%) showed unexpected behaviour. It was expected that the PRPD pattern would be the same PRPD pattern of corona discharges in other gases, like that in air or in SF6. A PRPD pattern of corona in SF6 is visible on Figure 3.4 [14,37]. Instead it took the form of a crescent moon. It was unclear if the different PRPD pattern was caused by the measuring equipment or that the PRPD pattern of corona in C4-FN/CO2 (5%/95%) deviates from the 'standard' PRPD pattern of corona.

$U_{applied}$ [kV_{peak}]	Dry	Humid
10	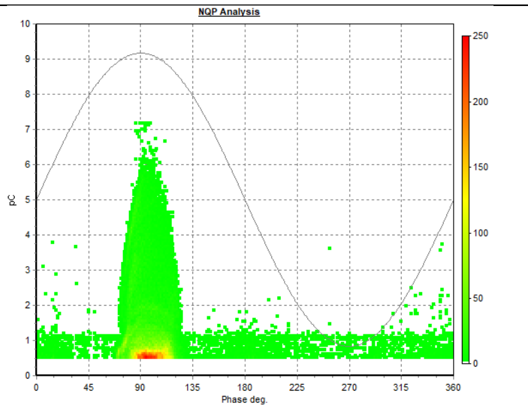	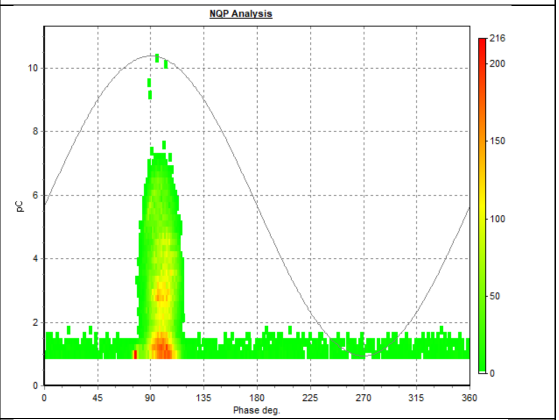
12	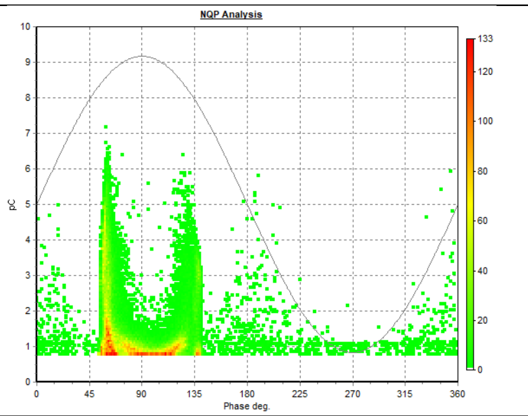	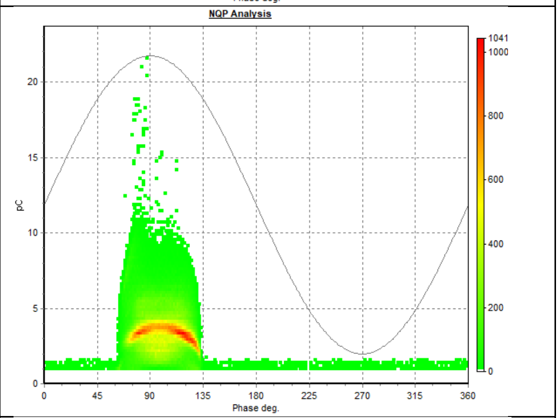
14	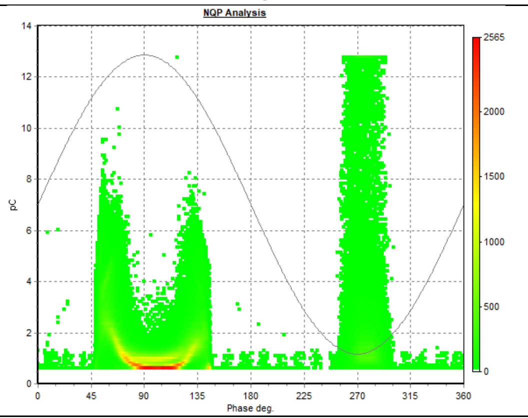	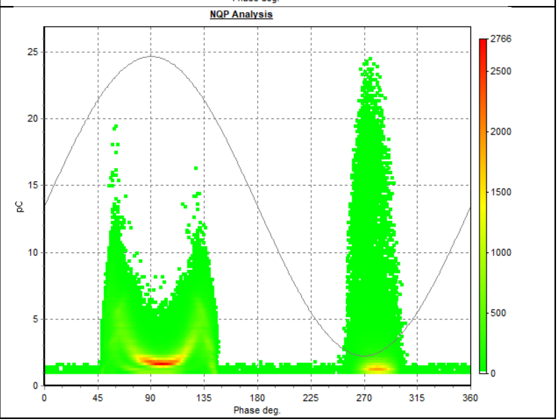

Table 5.2 Multiple PRPD patterns of corona in dry and humid C4-FN/CO2 (5%/95%).

Further investigation into the 'crescent moon' PRPD pattern of corona in C4-FN/CO2 (5%/95%)
The circuit for examining the partial discharge characteristic (section 4.4.3) has been used for investigating the 'crescent moon' pattern. The PRPD pattern can be measured with more detail by using the Tektronix DPO 7354C.

Table 5.3 contains eight screenshots of the oscilloscope during the PD behaviour measurements in *dry* C4-FN/CO2 (5%/95%). Between each screenshot is one minute. The first screenshot was taken immediately after applying a voltage 10% above the PDIV. Table 5.3 summarizes the following sequence of events:

- Screenshot 1 – 5: There is no steady rate of Trichel pulses after applying a voltage which is 10% above the PDIV. The rate of Trichel pulses is irregular.
- Screenshot 6: The rate of Trichel pulses becomes steady after five minutes.
- Screenshot 7: The pattern starts to take the shape of a crescent moon after increasing the applied voltage. The Trichel pulses in the middle appear to have a smaller magnitude compared to the Trichel pulses on the outside.
- Screenshot 8: The pattern still has the shape of a crescent moon after increasing the applied voltage. The discharges of the positive ions appear.

The different Trichel pulses that give the PRPD pattern a crescent moon shape, have been examined. The Trichel pulses had the same shape, the only difference was the height of the Trichel pulses.

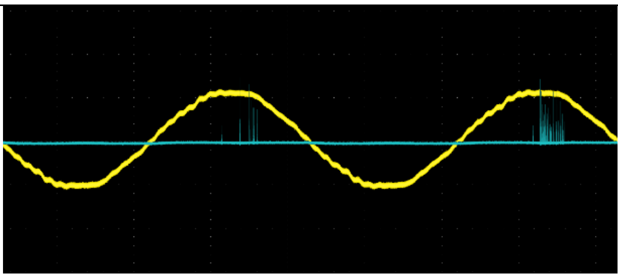 (1) $U_{applied}$ = 10kV$_{peak}$	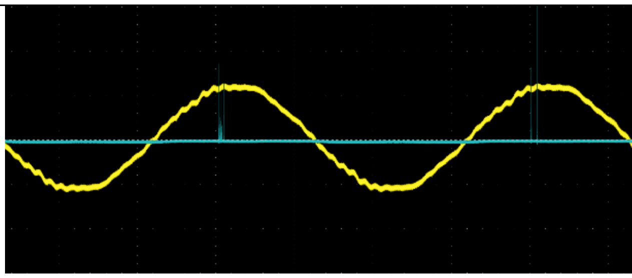 (2) $U_{applied}$ = 10kV$_{peak}$
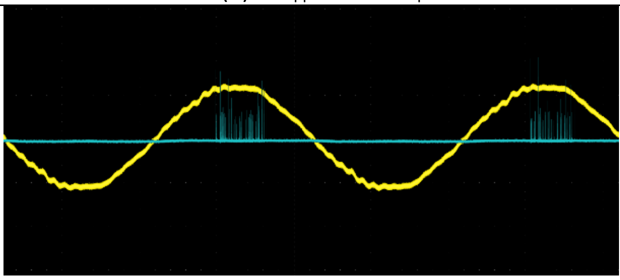 (3) $U_{applied}$ = 10kV$_{peak}$	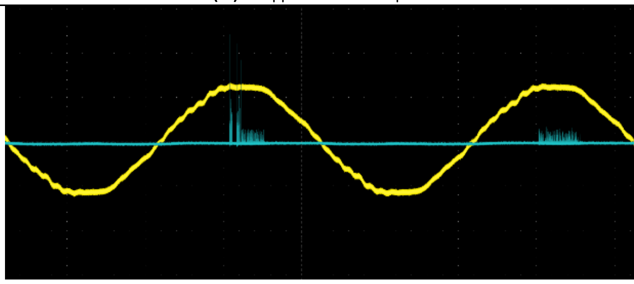 (4) $U_{applied}$ = 10kV$_{peak}$
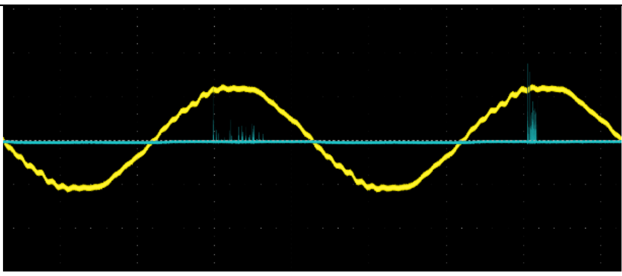 (5) $U_{applied}$ = 10kV$_{peak}$	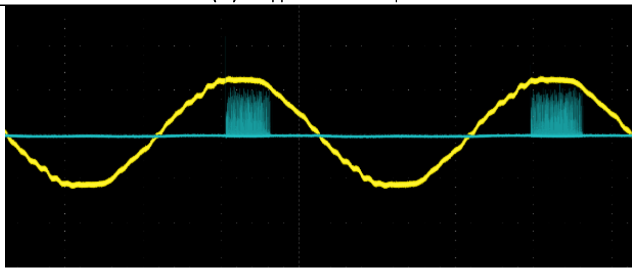 (6) $U_{applied}$ = 10kV$_{peak}$
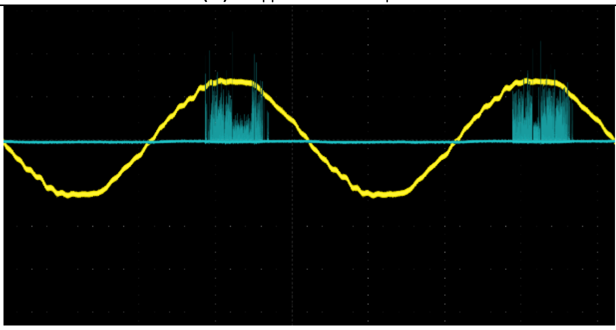 (7) $U_{applied}$ = 12kV$_{peak}$	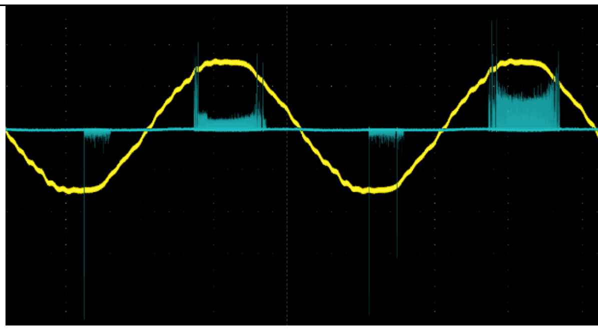 (8) $U_{applied}$ = 14kV$_{peak}$

Table 5.3 Screenshots of the oscilloscope that show the irregular partial discharge behaviour of corona in dry C4-FN/CO2 (5%/95%). The yellow line is the applied voltage. The blue line represents the corona partial discharges.

The PRPD pattern of corona in humid C4-FN/CO2 (5%/95%) also took the form of a crescent moon and is therefore also further investigated. Table 5.4 contains five screenshots of the oscilloscope during the PD behaviour measurements in *humid* C4-FN/CO2 (5%/95%). The first screenshot was taken immediately after applying a voltage 10% above the PDIV. Table 5.4 summarizes the following sequence of events:

- Screenshot 1: There is a steady rate of Trichel pulses after applying a voltage which is 10% above the PDIV.
- Screenshot 2: The pattern starts to take the shape of a crescent moon after increasing the applied voltage. The Trichel pulses in the middle appear to have a smaller magnitude compared to the Trichel pulses on the outside.
- Screenshot 3: The pattern still has the shape of a crescent moon after increasing the applied voltage. The discharges of the positive ions appear.
- Screenshot 4: The rate of Trichel pulses becomes unstable after 20sec after screenshot 3.
- Screenshot 5: The rate of Trichel pulses becomes steady after two minutes. The Trichel pulses have a decreased magnitude.

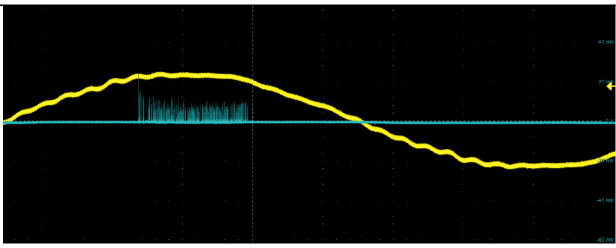

(1) $U_{applied}$ = 10kV$_{peak}$

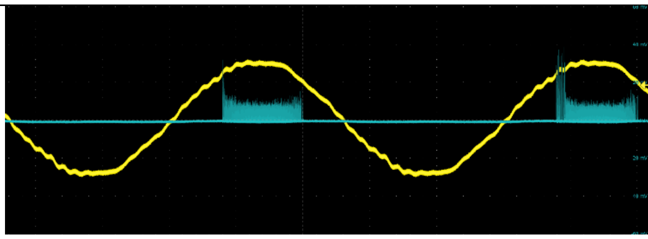

(2) $U_{applied}$ = 11kV$_{peak}$

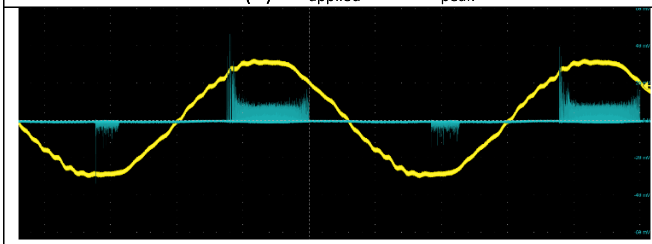

(3) $U_{applied}$ = 14kV$_{peak}$

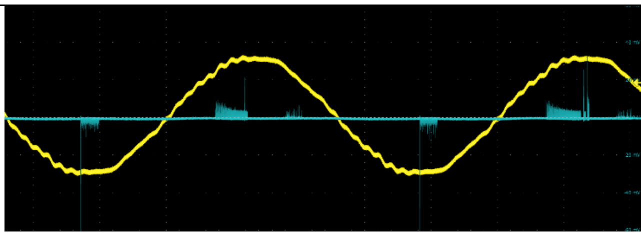

(4) $U_{applied}$ = 14kV$_{peak}$

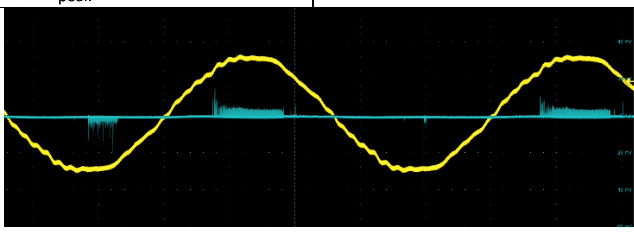

(5) $U_{applied}$ = 14kV$_{peak}$

Table 5.4 Screenshots of the oscilloscope that show the irregular partial discharge behaviour of corona in humid C4-FN/CO2 (5%/95%). The yellow line is the applied voltage. The blue line represents the corona partial discharges.

Investigating the irregular rate of Trichel pulses

The rate of Trichel pulses in both dry and humid C4-FN/CO2 (5%/95%) appear not to be stable. It is hypothesized that the irregular rate of Trichel pulses is caused by the C4-FN molecules. This hypothesis is tested by examining the rate of Trichel pulses of corona partial discharges in pure CO2 gas, as C4-FN/CO2 (5%/95%) has a molar ratio of 5% C4-FN and 95% CO2.

The rate of the Trichel pulses in pure CO2 gas are *stable* in the same range of the applied voltages, i.e. 0V → 14kV$_{peak}$. Therefore it can be concluded that the irregular behaviour of the partial discharges of corona is caused by the 5% C4-FN in C4-FN/CO2 (5%/95%).

5.3.2 Answer to research question B – 3

The PDIV of corona in C4-FN/CO2 (5%/95%) is *unaffected* by the presence of humidity. The PDIV of corona in dry and humid C4-FN/CO2 (5%/95%) are the same, i.e. both are around $9kV_{peak}$.

The PRPD pattern of corona in C4-FN/CO2 (5%/95%) is *affected* by the presence of humidity. The PRPD pattern of corona in dry and humid C4-FN/CO2 (5%/95%) shows similar behaviour, but there are differences;

- The PRPD pattern of corona in dry and humid C4-FN/CO2 (5%/95%) is the same, except for the amount of average charge.
- The average charge of the partial discharges in humid C4-FN/CO2 (5%/95%) is larger compared to the average charge of the partial discharges in dry C4-FN/CO2 (5%/95%).
- The Trichel pulses of the corona partial discharges appear at an irregular rate after applying the PDIV. This applies to both humid and dry C4-FN/CO2 (5%/95%).
- After a certain amount of time the rate of Trichel pulses becomes stable. This applies to both humid and dry C4-FN/CO2 (5%/95%).
- The irregularities of the Trichel pulses of the corona partial discharges are caused by the 5% molar concentration of C4-FN in the C4-FN/CO2 (5%/95%) gas mixture.

5.4 Phase B – question 4

The research question is: How does humidity affect the characteristics of a corona discharge in C4-FN/CO2 (5%/95%)?
The waveforms of 100 partial discharges of corona in dry and humid C4-FN/CO2 (5%/95%) are sampled and analysed in Matlab.

5.4.1 Measured data

- During the performed experiments the distance between the electrode was kept constant at 10mm.
- The dry and humid C4-FN/CO2 (5%/95%) is the same gas from the experiments of research question B - 3. This means that the gas mixtures have exactly the same properties, i.e. humidity and pressure.
- The pressure of the gas mixture during all the experiments was 1,00 bar_{abs}. SF6 had a pressure of 2,4bar_{abs}
- The applied voltage for all experiments was 10% above PDIV, i.e. 10,5kV_{peak}.
- The circuit has a limited bandwidth <1GHz.

Waveform of a corona partial discharge in C4-FN/CO2 (5%/95%)

Figure 5.14 shows 1 out of the 100 sampled waveforms of corona in dry C4-FN/CO2 (5%/95%). Figure 5.15 shows 1 out of the 100 sampled waveforms of corona in humid C4-FN/CO2 (5%/95%). Table 5.5 shows different characteristics of the corona partial discharges in dry and humid C4-FN/CO2 (5%/95%) at an applied voltage of 10kV_{peak}. The characteristics are the average values of the 100 samples. Table 5.5 also contains the partial discharge characteristics of corona in other gases for comparison.

Characteristic	Dry C4-FN/CO2 (5%/95%)	Humid C4-FN/CO2 (5%/95%)	Air	CO2	SF6*
Rise time [ns]	2,55	1,58	2,53	2,42	0,36
Fall time [ns]	2,74	4,86	11,49	23,96	0,34
Bandwidth [MHz]	202	227	145	163	983
PD rate [n/s]	109	54	-	-	-
Average charge [pC]	1,02	5,57	-	-	-

*Table 5.5 Averaged characteristics of 100 corona partial discharge samples in dry and humid C4-FN/CO2 (5%/95%). * The measurement of the characteristics of corona in SF6 is restricted due to the bandwidth of the circuit.*

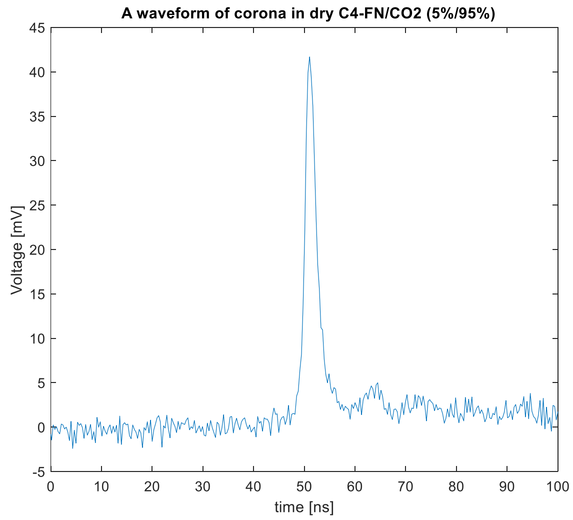

Figure 5.14 A waveform of a corona partial discharge in dry C4-FN/CO2 (5%/95%).

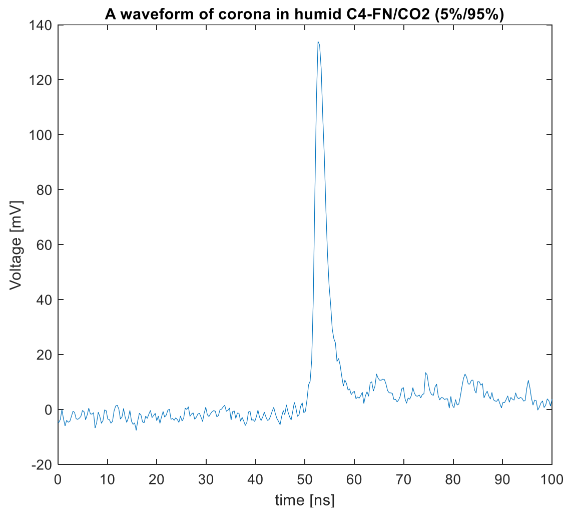

Figure 5.15 A waveform of a corona partial discharge in humid C4-FN/CO2 (5%/95%).

5.4.2 Answer to research question B – 4

The partial discharge characteristics of corona in C4-FN/CO2 (5%/95%) are affected by the presence of humidity. The corona partial discharges in humid C4-FN/CO2 (5%/95%) have a shorter rise time and a larger fall time compared to the corona partial discharges in dry C4-FN/CO2 (5%/95%). This causes that corona partial discharges in humid C4-FN/CO2 (5%/95%) have more charge compared to corona partial discharges in dry C4-FN/CO2 (5%/95%).

6 Answers to the research questions, conclusions & recommendations

SF6 is being phased out of Medium Voltage (MV) and High Voltage (HV) applications as a result of the Paris Agreement (2021). C4-FN/CO2 (5%/95%) shows the most promise as the eco-friendly replacement of SF6 for HV applications. But not everything is known about the gas, including the effect of humidity on the electrical insulation performance. Humidity is always present inside HV equipment as it is primarily caused by the reoccurring moisture ab- and desorption from the materials of HV equipment.

The objective of this master thesis is to examine: *"The electrical behaviour of C4-FN/CO2 (5%/95%) with varying humidities and operating conditions.* The objective of this master thesis is met by answering the four research questions.
It is to be noted that C4-FN/CO2 (5%/95%), in which the percentage ratio is the molar concentration of the gas mixture, is now abbreviated in this chapter to Fluoronitrile to ease the reading.

6.1 Answers to the research question

Question 1: How is the AC breakdown strength of Fluoronitrile influenced by different humidities?
The effect of humidity on the AC breakdown strength of Fluoronitrile depends on two factors;

1. <u>The amount of humidity present in the gas mixture:</u> The breakdown strength of Fluoronitrile shows a decrease with an increase of humidity.
2. <u>The field utilization factor of the electric field configuration:</u> The effect of humidity on the breakdown strength of Fluoronitrile decreases with a decreasing field utilization factor of the electric field.

Question 2: How does humidity affect the AC breakdown strength of Fluoronitrile at different operating pressures?
The effect of humidity on the AC breakdown strength of Fluoronitrile at different operating pressures depends on two factors;

1. <u>The operating pressure:</u> The effect of humidity on the breakdown strength of Fluoronitrile decreases as the operating pressure increases.
2. <u>The field utilization factor of the electric field configuration:</u> The effect of humidity on the breakdown strength of Fluoronitrile at different operating pressures decreases with a decreasing field utilization factor of the electric field configuration.

Question 3: How does humidity affect the partial discharge behaviour of corona in Fluoronitrile?
The partial discharge behaviour of corona in humid Fluoronitrile is examined by comparing the Partial Discharge Inception Voltage (PDIV) and Phase Resolved Partial Discharge (PRPD) pattern of dry and humid Fluoronitrile. The PDIV of corona in Fluoronitrile is *unaffected* by the presence of humidity. The PRPD pattern of corona in Fluoronitrile is *affected* by the presence of humidity, as the average charge of the partial discharges in humid Fluoronitrile is larger compared to the average charge of the partial discharges in dry Fluoronitrile.

Question 4: How does humidity affect the characteristics of a corona partial discharge in Fluoronitrile?
The partial discharge characteristics of corona in Fluoronitrile are *affected* by the presence of humidity. The corona partial discharges in humid Fluoronitrile have a shorter rise time and a larger fall time compared to the corona partial discharges in dry Fluoronitrile. This causes that corona partial discharges in humid Fluoronitrile have more charge compared to corona partial discharges in dry Fluoronitrile.

6.2 Conclusions

There are a number of conclusions that can be drawn from this research, they are;

- The hypothesis of TenneT was correct, humidity can be responsible for an early electrical breakdown.
- Humidity affects the AC insulation performance of Fluoronitrile, i.e. the AC breakdown strength of Fluoronitrile. Three factors determine the extent of the influence of humidity on the AC breakdown strength Fluoronitrile;
    1. The amount of humidity present in the gas mixture.
    2. The field utilization factor of the electric field.
    3. The operating pressure.
- Humidity affects the partial discharge behaviour of corona in Fluoronitrile in different ways;
    1. Humidity does not affect the PDIV of corona in Fluoronitrile.
    2. Humidity affects the PRPD pattern of corona in Fluoronitrile.
    3. Humidity affects the PD characteristics of corona in Fluoronitrile.
- The rate of Trichel pulses of the corona discharges is irregular after applying the PDIV, in both humid and dry Fluoronitrile.
- The rate of Trichel pulses of the corona discharges stabilizes after a certain amount of time, in both humid and dry Fluoronitrile.
- The irregular rate of Trichel pulses is caused by the 5% mole of C4-FN in Fluoronitrile.

6.3 Recommendations

There are six recommendations for future research on the effect of humidity on the electrical insulation performance of Fluoronitrile. The recommendations are prioritized to what the author of this master thesis thinks is most urgent.

Recommendation 1:
The electrical behaviour of Fluoronitrile is in this thesis restricted to AC only. However, HV applications can/will also be subjected to other electrical behaviour/phenomena. Such as: DC, lightning impulses, switching impulses and Very Fast Transients (VFT). It is of utmost important to see what the effect of humidity is on these different electrical behaviour/phenomena to create a complete story on the effect of humidity on the electrical behaviour of Fluoronitrile.

Recommendation 2: (accept or reject the first hypothesis related to research question A – 2)
This hypothesis is based on the conclusion of research question 1. The effect of humidity on the AC breakdown strength of Fluoronitrile at different operating pressures is examined for only one humidity. It is hypothesized that different amounts of humidity cause a different effect on the AC breakdown strength of Fluoronitrile at different operating pressures. A high amount of humidity would decreases the AC breakdown strength of Fluoronitrile at a certain operating pressure more than a small amount of humidity would.

Recommendation 3:
Examine which effect the temperature in combination with humidity has on the AC breakdown strength of Fluoronitrile. The temperature of the insulation gas in a GIS can change a lot depending on the ambient temperature and operating conditions. Therefore it will be interesting to see how the AC breakdown strength of Fluoronitrile, with different humidities, is influenced by different temperatures of the gas.

Recommendation 4:
Examine the partial discharge behaviour of other partial discharge sources in Fluoronitrile. Examine if their discharge behaviour shows the same irregularities that were discovered in this research. It is important to know the complete behaviour of all partial discharge activity in Fluoronitrile as partial discharge activity is a good diagnostic signal and is therefore monitored in HV equipment .

Recommendation 5: (accept or reject hypothesis related to research question A – 1)
It is hypothesized that Fluoronitrile mixed with different humidities have different effective ionization coefficients (α_{eff}). An increase in humidity results in an increase of the effective ionization coefficient, leading to an early breakdown. These different α_{eff} coefficients are however not constant throughout different electric field configurations. This is endorsed by the results of the experimental work performed in this thesis, as the same amount of humidity affected the three electric field configurations differently.

Recommendation 6: (accept or reject the second hypothesis related to research question A – 2)
This recommendation is an addition to recommendation 4. It is hypothesized that an increase in the operating pressure results in an decrease between the variation of the α_{eff} coefficients of dry and humid Fluoronitrile. The decrease of the variation of α_{eff} coefficients is however not constant throughout different electric field configurations. This is endorsed by the results of the experimental work performed in this thesis, as the same amount of humidity at the same operating pressure affected the three electric field configurations differently.

References

1 *Paris Agreement*. (n.d.). Climate Action. https://climate.ec.europa.eu/eu-action/international-action-climate-change/climate-negotiations/paris-agreement_en#:~:text=The%20EU's%20initial%20nationally%20determined,by%20the%20end%20of%202018.

2 CIGRE D1 849. (2021). *Electric performance of new non-SF6 gases and gas mixtures for gas insulated systems*.

3 CIGRE GCC. (2022). *long-term behaviour of c4-fn mixtures in high-voltage equipment*.

4 IEC 60600-1:2010. *High-voltage test techniques – Part 1: general definitions and test requirements*.

5 Zhang, B., Li, C., Xiong, J., Zhang, Z., Li, X., & Deng, Y. (2019). Decomposition characteristics of C_4F_7N/CO_2 mixture under AC discharge breakdown. *AIP Advances*, *9*(11), 115212. https://doi.org/10.1063/1.5115588

6 Purnomoadi, A. P. (2020). *Asset Health Index and Risk Assessment Models for High Voltage Gas-Insulated Switchgear Operating in Tropical Environment*. https://doi.org/10.4233/uuid:d2a3bafb-f39d-49ba-a9c0-bb266a9f9ba5

7 *2016 Electrical Insulation Conference (EIC), Montréal, Qc, Canada, 19-22 June 2016*. (2016).

8 *IEEE Guide for Moisture Measurement and Control in SF6 Gas-Insulated Equipment* (C37.122.5-2013). (2013). IEEE.

9 CIGRE B3.40 723. (April 2018). *SF6 measurement guide.*

10 Suwarno, S. (2016). Partial Discharge in High Voltage Insulating Materials. *International Journal on Electrical Engineering and Informatics*, *8*(1), 147–163. https://doi.org/10.15676/ijeei.2016.8.1.11

11 Kreuger, F. H. (1991). *Industrial High Voltage part 1 & 2*. IOS Press.

12 Zeng, F., Tang, J., Li, Y., Zhou, S., & Pan, C. (2018). Typical Internal Defects of Gas-Insulated Switchgear and Partial Discharge Characteristics. In *InTech eBooks*. https://doi.org/10.5772/intechopen.79090

13 IEC 60270:2000. *High voltage test techniques – partial discharges measurement*.

14 CIGRE D1.33 444. (December 2010). *Guidelines for unconventional partial discharge measurements..*

15 Mor, A. R., Heredia, L. C., Harmsen, D., & Muñoz, F. (2018). A new design of a test platform for testing multiple partial discharge sources. *International Journal of Electrical Power & Energy Systems*, *94*, 374–384. https://doi.org/10.1016/j.ijepes.2017.07.013

16 Owens, J. D., Xiao, A., Bonk, J., DeLorme, M. P., & Zhang, A. (2021). Recent Development of Two Alternative Gases to SF6 for High Voltage Electrical Power Applications. *Energies*, *14*(16), 5051. https://doi.org/10.3390/en14165051

17 IEC 62271-102:2018+AMD1:2022. *High-voltage switchgear and controlgear – Part 102: Alternating current disconnectors and earthing switches*.

18 CIGRE GCC. (2022). *Design Considerations for implementing SF6 alternatives for distribution switchgear applications with focus on toxicity and load break performance.*

19 *Illias, H. A., Chen, G., & Lewin, P. (2010). Modelling of temporal temperature and pressure change due to partial discharge events within a spherical cavity in a solid dielectric material using finite element analysis. https://doi.org/10.1109/ichve.2010.5640716*

20 *Reid, A., Judd, M. D., Stewart, B. G., & Fouracre, R. (2006). Partial discharge current pulses in $SF_6$and the effect of superposition of their radiometric measurement. Journal of Physics D, 39(19), 4167–4177. https://doi.org/10.1088/0022-3727/39/19/008*

21 IEC 60243-1:2013. *Electric strength of insulating materials – Test methods - Part 1: Tests at power frequencies.*

22 VDE. (2020). Influence of humidity on electric strength of CO2 and C4-FN/CO2 gas mixtures. *VDE High Voltage Technology 2020; ETG-Symposium*.

23 Beroual, A., Khaled, U., & Coulibaly, M. B. (2018). Experimental Investigation of the Breakdown Voltage of CO2, N2, and SF6 Gases, and CO2–SF6 and N2–SF6 Mixtures under Different Voltage Waveforms. *Energies*, *11*(4), 902. https://doi.org/10.3390/en11040902

24 P. Ranjan *et al*., "Lightning Impulse and AC Breakdown Characteristics of SF6 and its Alternatives," *2022 IEEE 4th International Conference on Dielectrics (ICD)*, Palermo, Italy, 2022, pp. 672-675, doi: 10.1109/ICD53806.2022.9863486

25 Kumar, S. (2021). *Electrical Breakdown Investigation in CO2: at Room and High Temperatures for High-Voltage Equipment*. [Phd Thesis 1 (Research TU/e / Graduation TU/e), Electrical Engineering]. Eindhoven University of Technology.

26 Kemma, A., Sipahutar, T., Pattanadech, N., Pratomosiwi, F., Suwarno, & Muhr, M. (2013). Ramp Rates Effect in Ramp Method for Partial Discharge Inception Voltage Measurement in Mineral Oil. *Procedia Technology*, *11*, 608–613. https://doi.org/10.1016/j.protcy.2013.12.235

27 Sipahutar, T., Kemma, A., Pattanadech, N., Pratomosiwi, F., Suwarno, & Muhr, M. (2013). Effect of Test Method and Needle Plane Configuration on Partial Discharge Inception Voltage Measurement of Mineral Oil based on Weibull Analysis. *Procedia Technology*. https://doi.org/10.1016/j.protcy.2013.12.210

28 Shin, G., Kim, S. Y., & Kil, G. (2022). Comparison between the PD Characteristics of g3 and Dry Air for Gas-Insulated Switchgears. *Energies*, *15*(19), 7043. https://doi.org/10.3390/en15197043

29 3M™ Novec™ 4710 Insulating Gas. *Safety datasheet.*

30 IEC 62539:2007. *Guide for statistical analysis of electrical insulation data.*

31 Gao, Q., Wang, X., Adamiak, K., Wang, D., Liu, D., Niu, C., & Zhang, J. (2021). Effects of H2O and O2 Impurities on the Trichel Pulses Characteristics of the Negative Point-Plane Corona Discharge in SF6. *Plasma Chemistry and Plasma Processing*, *41*(4), 1101–1119. https://doi.org/10.1007/s11090-021-10166-7

32 Li, B., Li, X., Fu, M., Zhuo, R., & Wang, D. (2018). Effect of humidity on dielectric breakdown properties of air considering ion kinetics. *Journal of Physics D*, *51*(37), 375201. https://doi.org/10.1088/1361-6463/aad5b9

33 Ekram Hussian, M. R. Nandagopal and B. R. Prabhakar (1974). *Effect of humidity on breakdown voltages of gaps and insulators.* Department of High Voltage Engineering, Indian Institute of Science.

34 Wu, D., Asplund, G., Jacobson, B., Li, M., & Sahlén, F. (2005). *Humidity influence on switching-impulse breakdown voltage of air gaps for indoor high-voltage installations.*

35 Xiao, Song & Zhang, Xiaoxing & Han, Y. & Dai, Q.. (2016). *AC breakdown characteristics of CF3I/N2 in a non-uniform electric field*. doi: 10.1109/TDEI.2016.005756.

36 Onal, Emel. (2011). B*reakdown characteristics of gases in non-uniform fields.*

37 Ren, M., Zhou, J., Song, B., Zhang, C., Dong, M., & Albarracín, R. (2017). *Towards Optical Partial Discharge Detection with Micro Silicon Photomultipliers.* Sensors, 17(11), 2595. https://doi.org/10.3390/s17112595

38 Mahdy, A., Anis, H., & Ward, S. A. (1998*). Electrode roughness effects on the breakdown of air-insulated apparatus.* IEEE Transactions on Dielectrics and Electrical Insulation, 5(4), 612–617. https://doi.org/10.1109/94.708280

39 Y. Inagawa, F. Miyazaki, K. Kato, M. Sakaki, H. Ichikawa and H. Okubol, "*Effect of electrode surface roughness on breakdown conditioning process under non-uniform electric field in vacuum,"* XXIst International Symposium on Discharges and Electrical Insulation in Vacuum, 2004. Proceedings. ISDEIV., Yalta, Ukraine, 2004, pp. 72-75, doi: 10.1109/DEIV.2004.1418604.

40 ASTM D2477:2012. *Standard Test Method for Dielectric Breakdown Voltage and Dielectric Strength of Insulating Gases at Commercial Power Frequencies.*

Appendix A Eliminating known-unknowns

This appendix explains what the known-unknowns were and how they were eliminated by converting them in known-knowns. There were four known-unknowns which had to be solved before the experiments to answer the four research questions could start. The known-unknowns can be summarized as the following questions:

1. Are the electrode configurations described CIGRE Brochure 849 D1 feasible for this research? The outcome of this question is given in the first section, A.1.
2. How much damage cause multiple BD's to the electrode and what are the mitigating measures that can be taken? The outcome of this question is given in the second section, A.2.
3. What is the maximum breakdown strength of the enclosure of the test cell? The outcome of this question is given in the third section, A.3.
4. How can the humidity of the gas be altered? The outcome of this question is given in the fourth section, A.4.

A.1 Feasible electric field configurations

The electrode configuration was originally planned to be taken from the CIGRE brochure 849 D1 [2]. This was however not possible since the test cells of the HV lab of TU Delft were not big enough to mount electrodes of the size given in the CIGRE brochure 849 D1. Small test cells have been made in the past by the technician of the HV lab. The materials of those cells were still in the storage of the HV lab. The electrode configurations were adjusted to the materials present in the HV lab, as not to get caught up in multiple and different delivery times. The type of test cell made in the past by the HV lab technician is shown in Figure A.1. These test cells were used for research on partial discharges.

The inner diameter of the transparent cylinder is 48mm, meaning that the diameter of the new electrodes cannot be larger than 44mm. Another starting point for the design of the electrodes was the field utilization factor η for different electric field configurations given in CIGRE brochure 849 D1. The η-factors for different field configurations are given in Table A.1. The field utilization factor can be calculated with Equation A-1, where U = 5kV$_{peak}$ and d = 5mm for the COMSOL simulations of three different electric field configurations. The maximum electric field strength of each electrode configuration is later defined at the relevant section of the electrode configuration.

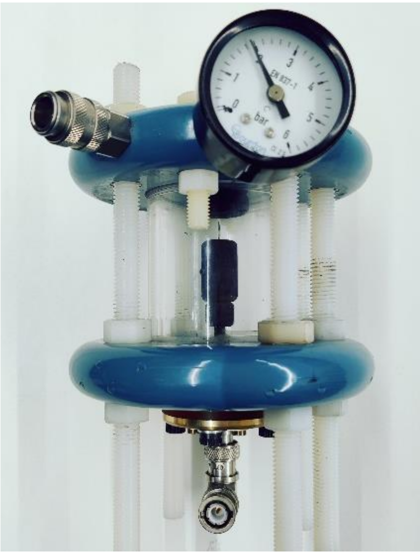

Figure A.1 Photo of the type of test cell that was made in the past the technician of the HV lab.

$$\eta = \frac{\frac{U}{d}}{maximum\ electric\ field\ strength}$$

Equation A-1

Field configuration	Field utilization factor η
Uniform	1
Quasi uniform	0,45 – 0,8
Non uniform	
- Sharp edges	0,05 – 0,15
- Protrusions	0,01 – 0,05

Table A.1 Field utilizations factors according to CIGRE 849 D1 [2] .

Plate – plate configuration

A plate – plate configuration is used to make an uniform field. The designed configuration is visible on Figure A.2. In order for the electric field to be uniform, the plate electrodes are required to have a Rogowski profile. The Rogowski equation is given in Equation A-2. The Rogowski profile is dependent on the gap distance between the electrodes. The designed Rogowski electrodes are designed to produce an uniform field if the gap distance is between 5mm and 10mm. Multiple Rogowski electrodes are made at DEMO, a workshop in TU Delft, which has high end machinery which can cut metal according to a 3D drawing.

As can be read from Figure A.2 the maximum field strength is $1kV_{peak}/mm$, creating η = 1. The top of the upper electrode and the bottom of the lower electrode are not required to have a special radii, as they do not influence the electric field between the electrodes.

$$f(x) = y = \frac{s}{\pi}\left(\frac{\pi}{2} + e^{x\pi/s}\right) \quad \text{with s = gap distance}$$

Equation A-2

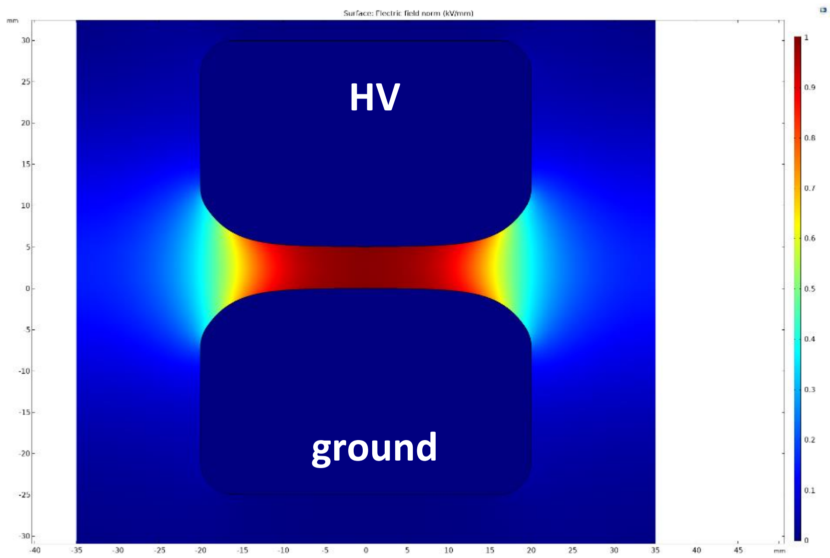

Figure A.2 Designed plate - plate configuration in COMSOL for an uniform electric field.

Sphere – plate configuration

A sphere – plate configuration is used to make a quasi-uniform field. The designed configuration is visible on Figure A.3. The ground plate does not need to have a Rogowski profile. The electric field is now concentrated between the small sphere and ground plate instead of the entire length of the electrodes, this can be seen on Figure A.4. The field is not influenced by the radii of the corners of the plate as long as the ground plate under the sphere has an extended flat part. The maximum electric field strength is circa $1{,}67kV_{peak}/mm$ as can be read from Figure A.3 or Figure A.4, creating a η ≈ 0,6. The radius of the sphere is 2mm.

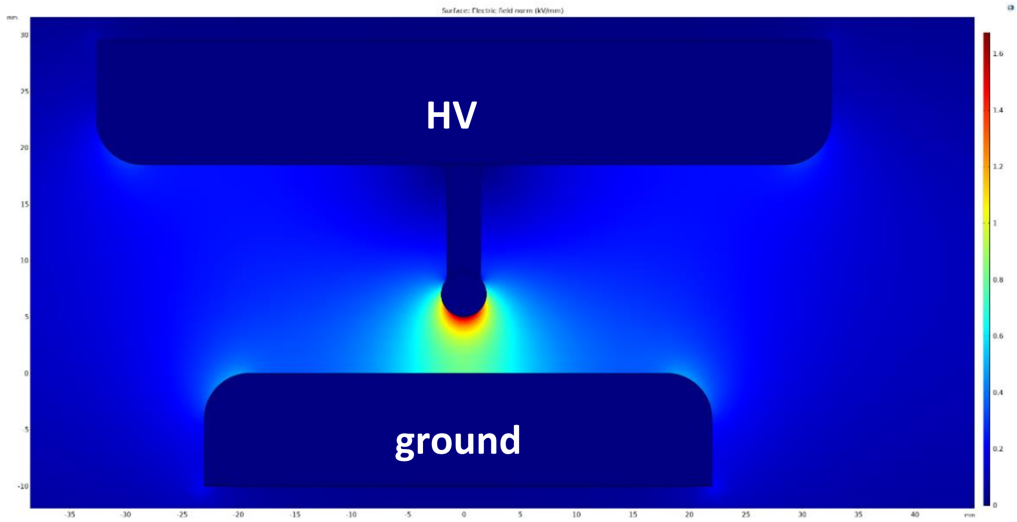

Figure A.3 Designed sphere- plate configuration in COMSOL for a quasi-uniform electric field.

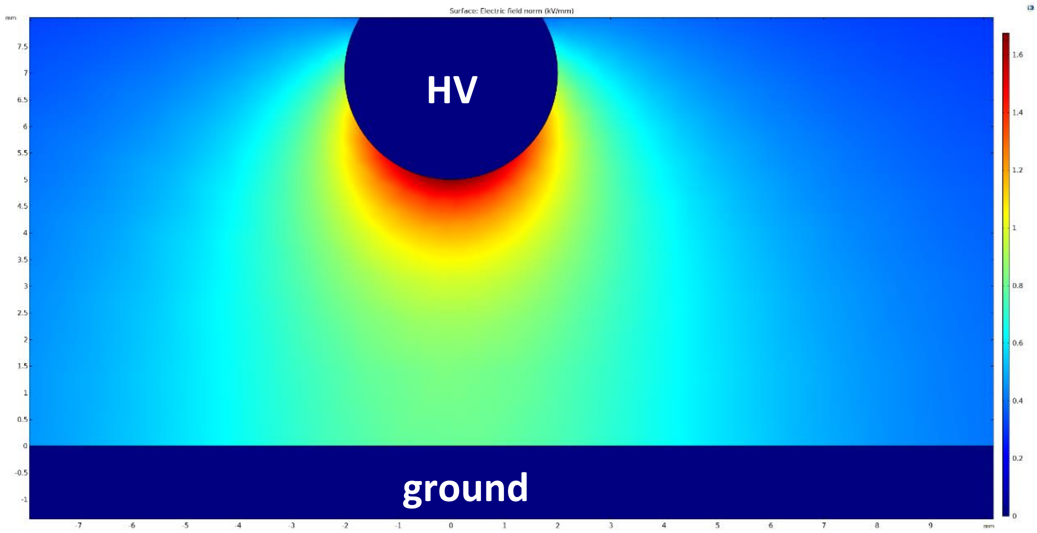

Figure A.4 Close up of the sphere in the sphere - plate configuration.

Needle – plate configuration

A needle – plate configuration is used to make a non-uniform field. The designed configuration is visible on Figure A.5. Figure A.6 shows a close up of the concentrated electric field around the needle. The ground plate does not need to have a Rogowski profile. The electric field is now concentrated between the needle and ground plate instead of the entire length of the electrodes. The field is not influenced by the radii of the corners of the plate as long as the ground plate under the needle has an extended flat part.

The maximum field strength is circa 11,8kV$_{peak}$/mm as can be read from Figure A.5 or Figure A.6, creating a $\eta \approx 0{,}08$. A photo of the created needle is visible on Figure A.7. The crafted needle and designed needle in COMSOL are not a complete match, which makes it difficult to calculate the exact η-factor. The needle is one millimetre thick and has oblique edges of 1 mm at the tip of the needle. The tip is 0,5mm flat as to keep the calculated η-factor as long as possible. A real sharp tip will quickly lose its sharpness as multiple breakdowns can cause the material to erode, thus constantly altering the η-factor.

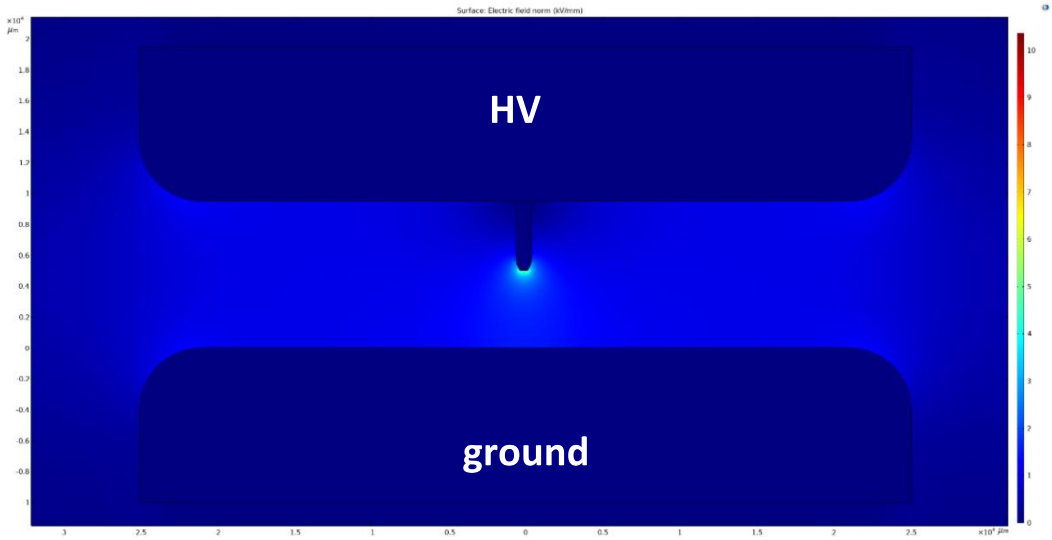

Figure A.5 Designed needle - plate configuration in COMSOL for a non-uniform electric field.

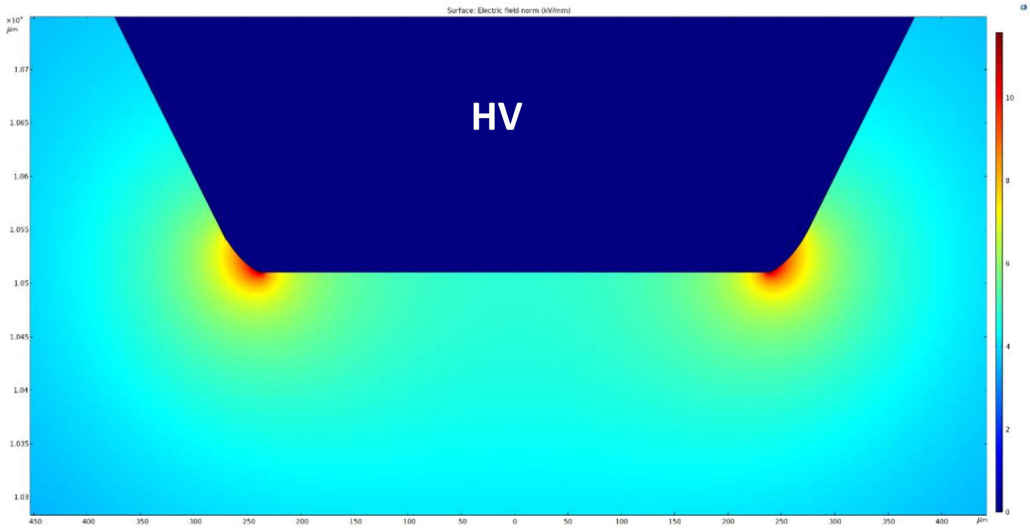

Figure A.6 Close up of the needle in the needle - plate configuration.

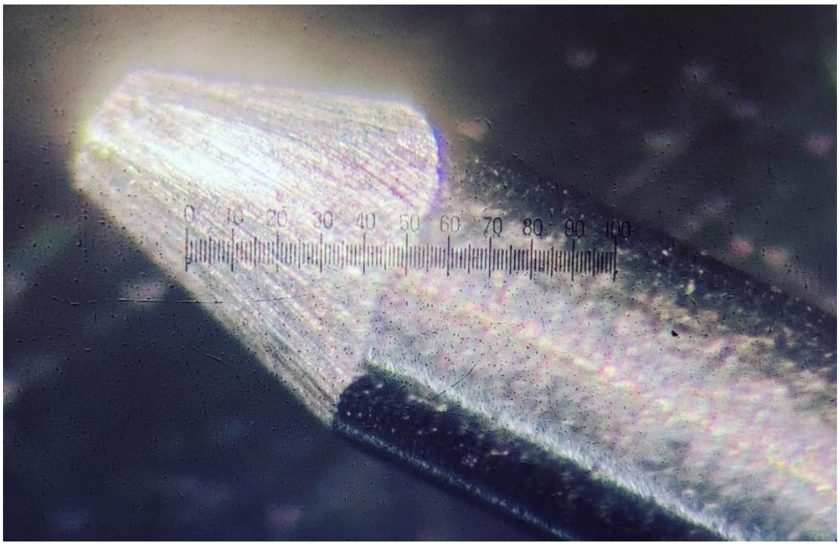

Figure A.7 Photo of the hand crafted needle by HV lab technician under a microscope. 80 on the ruler corresponds to 1mm.

Ensuring a constant gap distance of 5,0mm

There are two problems which allow the gap distance between the electrode to deviate from the 5,0mm:

1. The electrodes; the needle, sphere, plate and Rogowski electrodes all have different heights.
2. Assembling the test cell compresses the test cell and decreases the distance between the top and bottom plate of the test cell. This ultimately decreases the gap distance between the electrodes. Tightening the nuts on the glasfiber reinforced plastic thread with different torque gives a variation in the compression of the test cell, ultimately leading to a variation in the gap distance of the electrodes.

Solution to the two problems:

1. The thread to secure the electrodes to the top and bottom of the test cell is complemented with washers and nuts. This gives all the electrodes effectively the same height.
2. A constant torque is used during the assembly of the test cell. The test cell will have the same constant compression and thus the same gap distance between the electrodes. The torque to tighten the nuts on the glasfiber reinforced plastic thread is 30kgcm. At 30kgcm there is no gas leakage from the test cell when filled with 8 bar_{abs} gas. 8 bar_{abs} is the initial planned maximum test pressure.

Conclusion

Three electrode configurations have been made to simulate three different electric field configurations. The electrode configurations are designed according to the recommended field utilization factors described in the CIRGE brochure 849 D1 [2]. The details of the designed electrodes are summarized in Table A.2. The real field utilization factor can however deviate from the simulated field utilization factor in COMSOL. The reason for a possible deviation is that the handcrafted electrodes by the lab technician are difficult to simulate with high accuracy in COMSOL.

It is extremely important to keep a constant gap distance of 5,0mm, since a deviation of the gap distance greatly affects the breakdown voltage of C4-FN/CO2 (5%/95%). To ensure a constant gap distance of 5,0mm two rules must be followed:

1. Use a constant torque of 30cmkg during assembly. This results in a constant the gap distance between the top and bottom of the test cell.
2. Give all the electrodes the same effective height. Complement, if needed, the thread of the electrodes with washers and nuts.

Electric field configuration	**Electrode configuration**	**Field utilization factor (η)**	**Production**
Uniform	Rogowski – Rogowski	$\eta = 1$	Machined at DEMO
Quasi uniform	Sphere – Plate	$\eta \approx 0{,}6$ (r_{sphere} = 2mm)	Handmade by technician
Non uniform	Needle – Plate	$\eta \approx 0{,}08$	Handmade by technician

Table A.2 Summarized details of the created and used electrodes. The field utilization factor is calculated with a gap distance of 5,0mm and with the same voltage across the electrodes.

A.2 Damage to the electrode caused by breakdown

The damage to the electrodes, caused by the breakdowns, can influence the breakdown voltage [2,38,39]. Therefore it might be required that the electrodes have to be polished after each breakdown. Polishing the electrodes after each breakdown is however a very inconvenient complexity, because of the need for identical properties of the insulation gas.

Polishing the electrodes requires the test cell to be disassembled which entails that the gas has to be removed from the test cell. After the electrodes have been polished, the test cell must be refilled with the correct mixture of humid C4-FN/CO2 (5%/95%). The new humid C4-FN/CO2 (5%/95%) must have *identical* properties with the corresponding pressure as before the test cell was disassembled. This is a fundamental prerequisite for an useful analysis of the experiments. Since an experiment consists out of 10 breakdowns, the gas has to be recreated 10 times. It is an impracticable process to polish the electrodes after each breakdown.

The need to polish the electrodes after each experiment is investigated for all the used electric field configurations.

Examining all the used different electric field configurations

The effect of unpolished electrodes on the breakdown voltage of C4-FN/CO2 (5%/95%) is examined in all three different electric field configurations. The conclusion of the performed experiments is summarized in Table A.3. The cause of the affected breakdown voltages in the uniform electric field configuration is examined and explained in the next section.

Field configuration	Breakdown behaviour of C4-FN/CO2 (5%/95%)
Uniform	Affected by unpolished electrodes
Quasi-uniform	Not affected by unpolished electrodes
Non-uniform	Not affected by unpolished electrodes

Table A.3 Conclusion on the investigation for the need of polishing electrodes.

Results of the experiments in uniform field

The results of the performed experiments in the uniform electric field configuration are shown in Figure A.8, each experiment consisted out of 10 breakdown repetitions.
The experiments of part A were performed to examine how the breakdown voltages of C4-FN/CO2 (5%/95%) are affected by the unpolished electrodes. From the graph it can be concluded that the delta of the measured breakdown voltage increases after each experiment. Delta is the difference between the minimum and maximum measured breakdown voltage of C4-FN/CO2 (5%/95%) during an experiment. The experiments of part B were performed to examine if the delta can be limited by polishing of the electrodes after each experiment. Through the results of the experiments of part A and B, a correlation was found between affected breakdown behaviour of C4-FN/CO2 (5%/95%) and the surface roughness of the electrodes. The experiments of part C examined three different polishing methods to decrease the amplitude of the delta of the breakdown voltages of C4-FN/CO2 (5%/95%).

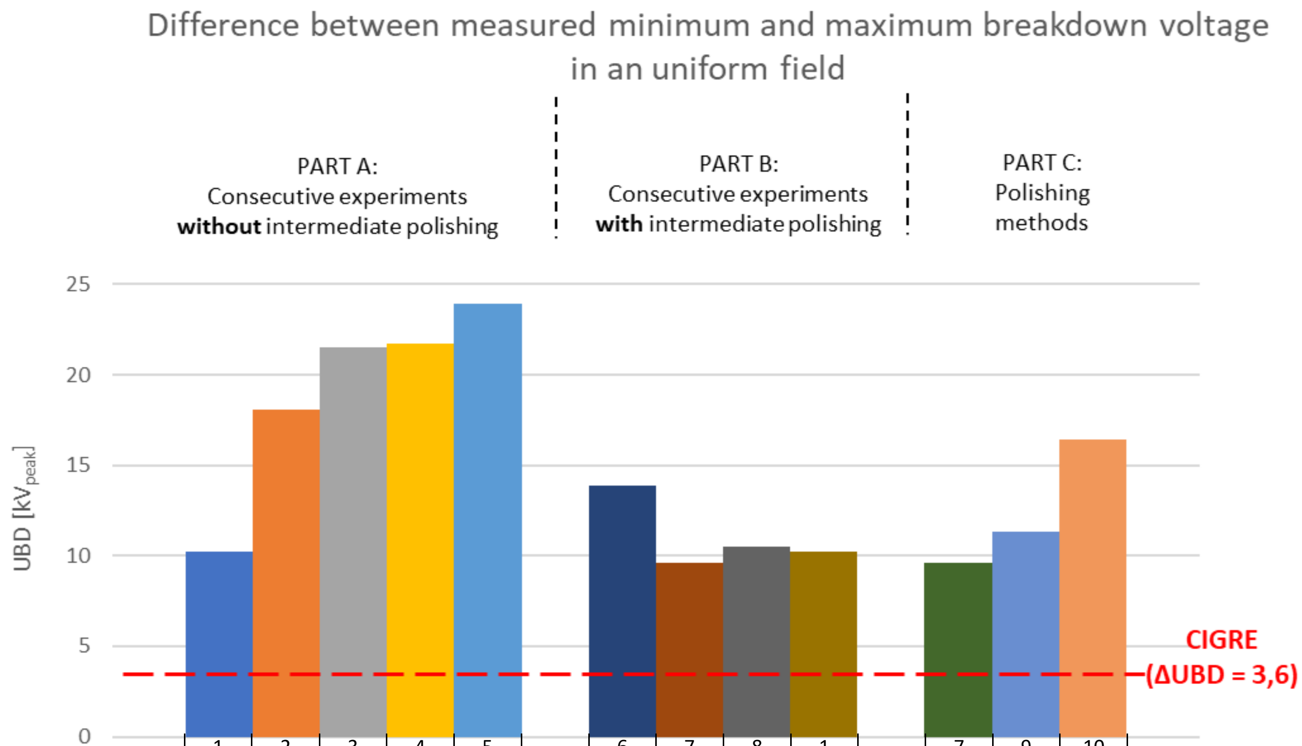

Exp nr.	1	2	3	4	5	6	7	8	1	7	9	10
Gap distance [mm] ±0,05mm	5	5	5	5	5	5	5	10	5	5	5	5
Pressure [bar$_{abs}$]	1,00	2,00	0,60	0,50	0,50	1,00	1,00	0,50	1,00	1,00	1,00	1,00
Average UBD [kV$_{peak}$]	38,1	65,3	28,9	28,9	31,0	41,6	44,6	46,2	38,1	44,6	40,9	38,2
ΔUBD of avg. UBD [%]	27	28	74	75	77	33	22	23	27	22	28	43

Figure A.8 The results of the performed experiments to examine the damage on the electrodes caused by breakdowns and the effect of the damaged electrodes on the breakdown behaviour of C4-FN/CO2 (5%/95%).

Explanation of the results of part A: unpolished Rogowski electrodes cause an increase in the delta of the measured breakdown voltages of C4-FN/CO2 (5%/95%).

Due to the continued use of the electrodes, without intermediate polishing between each experiment, the roughness of the surface of the Rogowski electrodes kept increasing. Figure A.9 and Figure A.10 show a photo of the same electrodes before and after performing experiment 1 through 5 respectively. The dots, visible on Figure A.10, are impact craters caused by the damaging effects of the breakdown. A close-up of an impact crater (imperfection) is shown on Figure A.11.

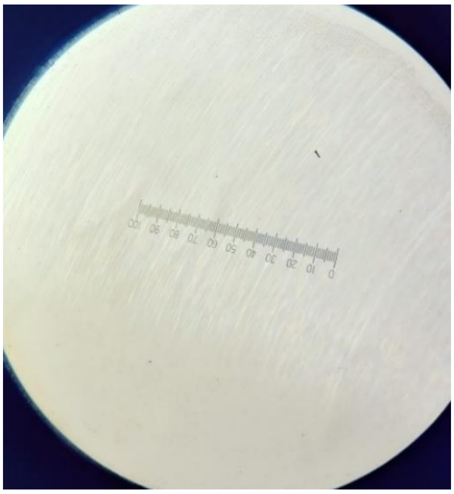

Figure A.9 A photo of the polished electrode before testing under the microscope. (the ruler holds no value)

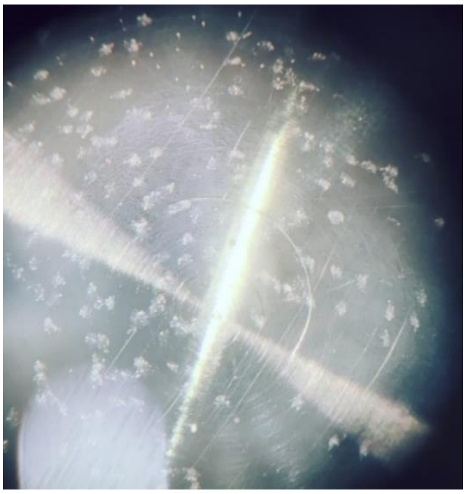

Figure A.10 A photo of the polished electrode after a number of consecutive experiments under the microscope.

The impact craters cause very small imperfections on the otherwise smooth electrode. These impact craters increase the surface roughness of the Rogowski electrodes. These imperfections have a (large) field enhancement factor. The localized electric field around those imperfections can be tens or hundreds of times larger compared to the uniform electric field strength. This will accelerate the (localized) electric field to the critical electric field strength and will eventually lead to an early breakdown.
A breakdown can also destroy the imperfections leading to an increase of the breakdown voltage. The measured breakdown voltage did not have a linear decrease but swinged between a minimum and maximum value. This was observed during all of the performed experiments [2].

The surface of the electrodes before performing experiment 5 is altered with 40+ breakdowns, which created a lot of imperfections. Some of these imperfections can create an even larger field enhancement factor due to the fact that they are close to each other. This will lead to a higher localized electric field and will lead to an early breakdown. This can be seen in the results of experiment 5, visible on Figure A.12. The lowest measured breakdown voltage is $19kV_{peak}$ and the highest measured breakdown is $43kV_{peak}$, this difference creates the largest delta of $24kV_{peak}$.

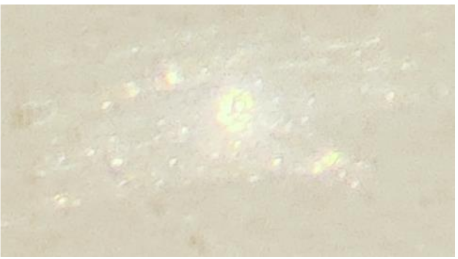

Figure A.11 A zoom in on the breakdown, which causes small imperfections. i.e. the impact crater and the tiny metallic particles around the crater. (the black hazy spots are filth on the lens of the microscope)

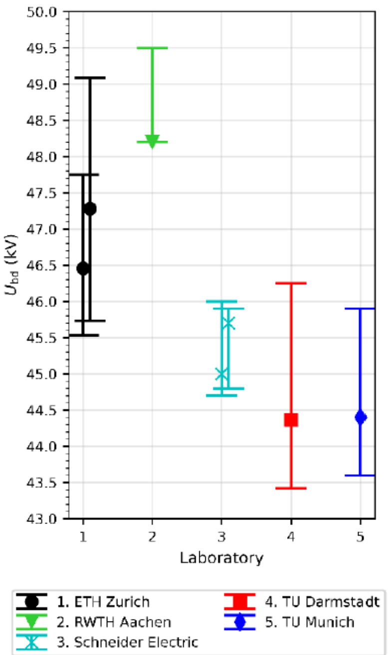

Figure A.13 AC breakdown results of dry C4-FN/CO2 (5%/95%) reported in CIGRE brochure 849 D1 [2].

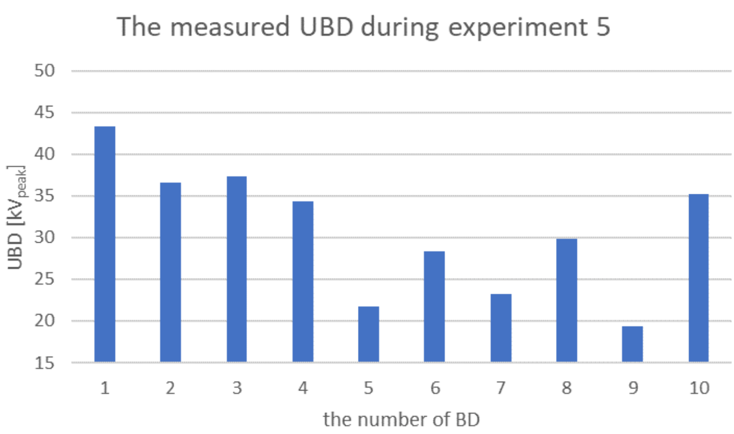

Figure A.12 The measured breakdown voltage during experiment 5.

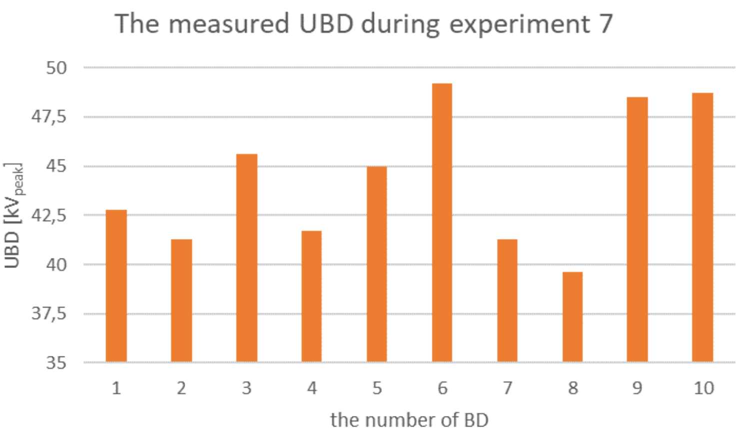

Figure A.14 The measured breakdown voltage during experiment 7.

Explanation of the results of part B: limiting delta of UBD by polishing the electrodes
Part A concluded that the delta of the measured breakdown voltage is correlated with the surface roughness of the Rogowski electrodes. To limit the delta of the measured breakdown voltages the surface roughness of the Rogowski electrodes must be as small as possible. This entails polishing the Rogowski electrodes after each experiment. This section describes the results of the experiments which were performed to investigate the possibility to limit the delta of the measured breakdown voltages by polishing the Rogowski electrodes.

The results of experiment 6 – 8 (and 1) show that the delta of the measured breakdown voltages can be limited if the Rogowski electrodes are polished after each experiment. The results of experiment 7 are shown in Figure A.14 and show that the delta of the measured breakdown voltages can be limited to circa $10kV_{peak}$. Figure A.12 and Figure A.14 shows a clear comparison between the variation in the measured breakdown voltages with unpolished and polished Rogowski electrodes respectively.

Explanation of part C: different polishing methods to decrease delta
Part B concluded that the delta of the measured breakdown voltages can limited by polishing the Rogowski electrodes. This section describes the results of the performed experiments and the investigation into different polishing methods to decrease the delta of the measured breakdown voltages.

<u>Amplitude of delta of the measured breakdown voltages</u>
CIGRE brochure 849 D1 examined the AC breakdown behaviour of dry C4-FN/CO2 (5%/95%) at 1 bar_{abs} [2]. The results of those AC breakdown tests are shown in Figure A.13. Those results and the results of the performed experiments at 1 bar_{abs} were compared to determine if the delta of the measured breakdown voltages can be lower.

The results of experiment 1, 6 – 8 show that the delta of the measured breakdown voltages can be limited to roughly $10kV_{peak}$. However, the delta of breakdown voltages measured by the different laboratories in the CIGRE brochure is roughly $4kV_{peak}$. The difference in the delta of the breakdown voltages between the performed experiments and the experiments done in the CIGRE brochure is visible given in Figure A.8. Through the comparison it is affirmed that the delta of the measured breakdown voltages can be decreased.

<u>Decreasing the delta of the measured breakdown voltages</u>
Decreasing the delta of the breakdown voltages can be achieved by using Rogowski electrodes with an smaller surface roughness. However, achieving Rogowski electrodes with a smaller surface roughness is a difficult process due to multiple aspects:

1. Time: There is only one technician in the HV lab of TU delft whom is responsible for the mechanical constructions of all the research performed at the HV lab of TU Delft. This means that the technician has limited time to perform tasks, including polishing electrodes.
2. Material of the electrodes: the Rogowski electrodes are made out of stainless steel. Stainless steel is a tough material, making it a good choice as to minimize the damaging effects of the breakdowns on the Rogowski electrodes. This however also the downside when it comes to (re)polishing.

The Rogowski electrodes needs to be polished multiple times to get an extremely small surface roughness. The polishing has to be done with increasing steps of finer polishing equipment and material. Reducing the surface roughness of the Rogowski electrodes to an extremely small surface roughness is labour intensive, time consuming and thus not an efficient process for this research.

Three different polishing methods were examined. These different methods were;

- Experiment 7: The Rogowski electrodes are sanded with waterproof sandpaper with a grit of P1200 and finished with a polish of 'brasso koperglans'. Multiple measurement gave a delta between the measured breakdown voltages of <10kV_{peak}.
- Experiment 9: The Rogowski electrodes are sanded with waterproof sandpaper with a grit of P1200. One measurements gave an average delta between the measured breakdown voltages of circa 11,5kV_{peak}.
- Experiment 10: The Rogowski electrodes are sanded with waterproof sandpaper with a grit of P1200 and afterwards sanded again with sandpaper with a grit of P2000. One measurement gave a delta between the measured breakdown voltages of circa 16kV_{peak}.

The conclusion

Different research papers conclude that the electrodes have to be polished after each breakdown as it can affect the breakdown voltage of consecutive breakdown [2,38,39]. This is however not possible because of the very complex and delicate nature of making humid C4-FN/CO2 (5%/95%).

It was examined, through multiple experiments in all the used field configurations, how unpolished electrodes affect the breakdown voltage of C4-FN/CO2 (5%/95%). The experiments concluded the following:

- Unpolished electrodes *do* affect the breakdown voltage of C4-FN/CO2 (5%/95%) in an uniform electric field configuration.
- Unpolished electrodes *do not* affect the breakdown voltage of C4-FN/CO2 (5%/95%) in a *quasi-uniform* electric field configuration.
- Unpolished electrodes *do not* affect the breakdown voltage of C4-FN/CO2 (5%/95%) in a *non-uniform* electric field configuration.

The breakdown voltage of C4-FN/CO2 (5%/95%) in an uniform field is easily influenced by the surface roughness of the Rogowski electrodes. The surface roughness is increased due to the occurrence of the breakdowns. An increased surface roughness can create an enhancement of the localized electric field. This can result in an early breakdown and thus a lower breakdown voltage of C4-FN/CO2 (5%/95%) [38,39].

The Rogowski electrodes need to be polished after each experiment in order to limit the delta of the measured breakdown voltages of C4-FN/CO2 (5%/95%). Delta is the difference between the minimum and maximum measured breakdown voltage.

Different polishing methods to decrease the delta of the measured breakdown voltage of C4-FN/CO2 (5%/95%) were examined. The results from the different polishing methods concluded that the delta of the breakdown voltage of C4-FN/CO2 (5%/95%) can be limited to <10kV_{peak}. This method is: sanding the Rogowski electrodes with waterproof sanding paper with a grit of P1200 and afterwards polishing with 'brasso koperglans'.

A.3 Maximum breakdown voltage of the air around the enclosure of the test cell

For this research a new test cell is created. A photo of the created test cell is shown in Figure A.15. The design is based on the existing test cells (shown in Figure A.1). The initial plan for this research is that the gas inside the cylinder can be tested up to 8 bar_{abs}. Therefore the test cell must be able to withstand 350kV_{peak}. 350kV_{peak} is based on the assumption that the breakdown voltage increases linear with the pressure. The breakdown voltage of C4-FN/CO2 (5%/95%) in an uniform field at 1 bar_{abs} over a gap distance of 5mm is circa 45kV_{peak}, therefore the breakdown voltage at 8 bar_{abs} = 350kV_{peak}. The linearity is based on measurements described in CIGRE brochure 849 D1[2]. The results of that measurement is visible in Figure A.16.

This section explains the investigation that was done into the maximum breakdown strength of the enclosure of the test cell, i.e. when the surrounding air on the outside of the test cell breaks down. The investigation tells which steps were taken to increase the breakdown strength of the test cell. The investigation was performed in the test set-up used to examine the breakdown behaviour of C4-FN/CO2 (5%/95%) as described in 4.4.1. The applied voltage to the test cell was increased in steps of 2kV_{peak}/s until there was a breakdown. The breakdown voltage was noted as the voltage at which the air on the outside of the enclosure of the test cell broke down. Three breakdowns were done in order to get an average breakdown voltage.

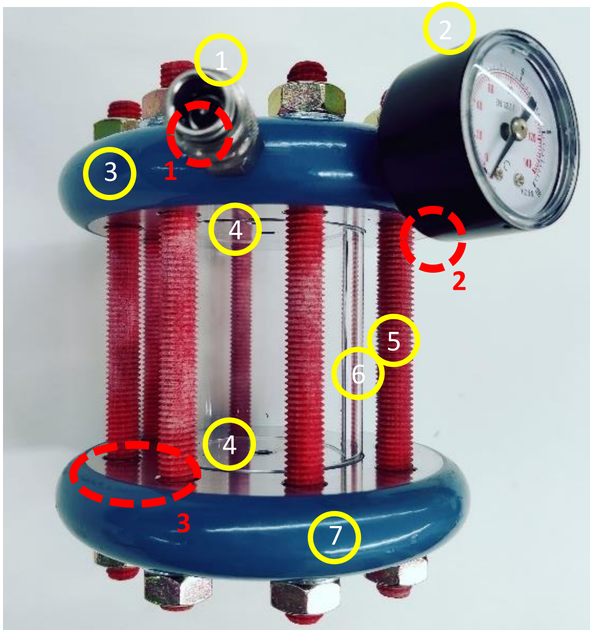

Figure A.15 Initial test cell for this thesis research made by HV lab technician.

Nr.	Description
1	Female DILO connection to serve as in-/outlet for the gas.
2	Relative pressure meter.
3	Top plate of the test cell, made of aluminium.
4	Screw holes for the electrodes.
5	Screw thread to keep the test cell pressure tight. Made of glasfiber reinforced plastic to withstand the pressure range up to 20+$bar_{abs.}$
6	PMMA cylinder to contain the gas and 2 O-rings to prevent leakage of the gas.
7	Bottom plate of the test cell, made of aluminium.

Maximum breakdown voltage of the enclosure of the created test cell

350kV_{peak} cannot be applied to the test cell, as 350kV_{peak} exceeds the maximum output voltage of the used step up transformer. The maximum output voltage of the step up transformer is 280kV_{peak}. Furthermore, the used step up transformer is 70+ years old. Therefore a safety factor of 80% is implemented. This means that the maximum output voltage of the step up transformer is limited to 224kV_{peak}. This entails that it is now investigated if the breakdown strength of the test cell can be 224kV_{peak}.

The distance between the top and bottom container of the test cell is 67mm. The AC breakdown strength of air (in an uniform field) is circa $3kV_{peak}/mm$ for atmospheric pressures. This means that the electric field on the outside of the test cell should theoretically breakdown at circa $3kV_{peak}/mm \cdot 67mm \approx 200kV_{peak}$. This is close to the maximum output voltage of the step up transformer, i.e. $224kV_{peak}$. However, the breakdown voltage of the test cell will not be 200kV since the electric field is distorted by a number of factors. These factors are encircled in red in Figure A.15. The unwanted factors that influence the electric field are:

- The protruding metal of the pressure meter. The sharp edge will give an enhanced localized electric field strength.
- The protruding female DILO connection. The sharp edge will give an enhanced localized electric field strength.
- Multiple triple points on the bottom and top plate. Triple points consist out of the surrounding air, glasfiber reinforced plastic and the metal top/bottom container. The triple points will enhance the localized electric field strength.

The enhanced localized electric fields will cause an accelerated breakdown.

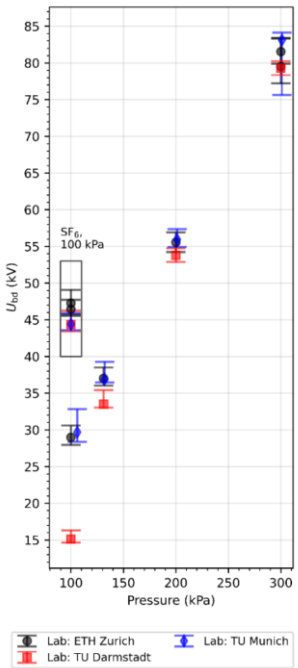

Figure A.16 AC breakdown behaviour of C4-FN/O2/CO2 (5%/5%/90%) against pressure in an uniform field arrangement [14].

Step taken to increase the breakdown voltage of the enclosure of the test cell.

0. High voltage was applied to the initial test cell and the breakdown tests were performed. The breakdown occurred at an average of $53kV_{peak}$, instead of the theorized $200kV_{peak}$. The BD occurred between the pressure meter and the bottom of the container.
1. The first improvement was increasing the distance the two breakdown points. An L-shaped connection piece was placed between the pressure meter and the top of the container. The L-shaped connection was also smoothened to reduce the field enhancement. The physical result of the improvement is visible on Figure A.17. High voltage was applied to the test cell and the breakdown tests were performed. The breakdown occurred at an average of $70kV_{peak}$. Making this a first *improvement* of $17kV_{peak}$. The breakdown still occurred between the pressure meter and the bottom of the container. The BD occurred at the smoothened corner of the L-shaped piece. The location of the breakdown is indicated with a red dotted circle on Figure A.17.

2. The second step was trying to shield the two attachments on the top plate of the test cell, i.e. the DILO connection and the L-shaped connection of the pressure meter. The shielding was achieved through electrode grading by attaching a corona disk to the bottom of the top plate of the test cell. A photo of the used corona disk is visible on Figure A.18. Any sharp edges or screws were covered with smooth aluminium tape. The DILO connection and the L-shaped connection of the pressure meter were both above the corona disk. The corona disk was electrically connected to the top plate of the test cell to ensure the same potential on the corona disk and attachments. High voltage was applied to the test cell and the breakdown tests were performed. The breakdown occurred at an average of 65kV$_{peak}$. Making this a *degradation* of 5kV$_{peak}$. The breakdown occurred at the inner edge of the corona disk and the bottom of the container, location is indicated with a red dotted circle on Figure A.18. Because of the degradation the corona disk is not integrated into the test cell.

Figure A.17 Improvement of the cell with a smoothened L-shaped connection to the pressure meter. Red dotted circle is where BD occurred.

Figure A.18 Corona disk used for electrode grading. Red dotted circle is where BD occurred.

3. The third step concerned the removal of the pressure meter, thereby eliminating the strongest interference of the electric field. High voltage was applied to the test cell and the breakdown tests were performed. At two of the three breakdown tests, the breakdowns occurred at the DILO connection at an average of 83kV$_{peak}$. The last BD did not occur at the DILO connection, but occurred between random places between the top plate and bottom plate of the test cell. Three new breakdown test were performed. All the breakdowns occurred between the top plate and bottom plate of the test cell. The breakdown occurred at an average of 90kV$_{peak}$. Making this a second *improvement* of 20kV$_{peak}$ and a total *improvement* of 37kV$_{peak}$, with regard to the initial test cell of Figure A.15.
4. The fourth step to improving breakdown strength of the cell was increasing the distance between the top plate and bottom plate of the test cell. Multiple measurements have been performed to get an understanding of the correlation between the height of the test cell and the breakdown voltage of the test cell. High voltage was applied to the test cell and the breakdown tests were performed. After three breakdown tests, the height of the test cell was increased with the height of one 'standard' test cell, which is circa 80mm. Figure A.19 shows a photo of the test cell with four stacked cylinders. The results of the multiple breakdown tests are presented in Figure A.21.

5. Figure A.21 shows that increasing the test cell beyond circa 40cm gives a reduced increase in breakdown strength. The main reason as to not go beyond the circa 40cm is that the available remaining tube length is circa 41cm. These reasons led to the creation of another test cell with a height of circa 40cm. The long test cell, of 40cm, has an breakdown voltage of circa $190kV_{peak}$. The large test cell has a total *improvement* of $131kV_{peak}$ with regards to the initial test cell. $190kV_{peak}$ is close to the maximum output voltage of the step up transformer which is $224kV_{peak}$. This test cell will be used for experiments that require the application of a higher voltage.

Extra steps taken for the investigation into the breakdown voltage of the enclosure of the test cell.

6. Toroids were attached to the top plate and bottom plate of the test cell to mitigate any disturbances to the electric field. This was now possible as the height of the test cell was sufficient enough to place the toroids. A photo of the test cell with toroids can be seen on Figure A.20. However, attaching the toroids to the test cell decreased the effective distance between the high voltage and ground. A decreased distance of the test cell corresponds to a lower breakdown voltage of the test cell. The results of the measurements with the toroids are shown in Figure A.21.
7. The threads connecting the top and bottom of the test cell are removed to investigate the effect the triple points on the electric field. The top plate of the test cell is connected with rope to a beam to make it float directly above the bottom plate of the test cell. The results of the measurements without the triple point is also visible on Figure A.21.

Figure A.19 Test cell with stacked cylinders, this test cell contains 4 cylinders.

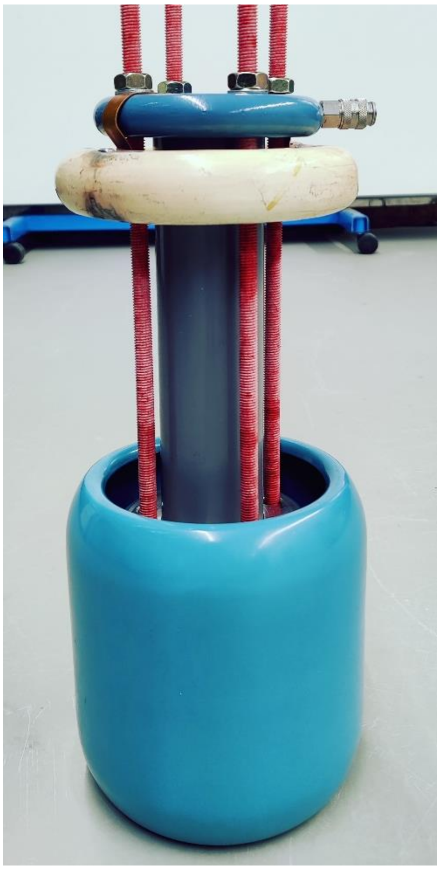

Figure A.20 Test cell with attached toroids to mitigate the disturbance of the electric field.

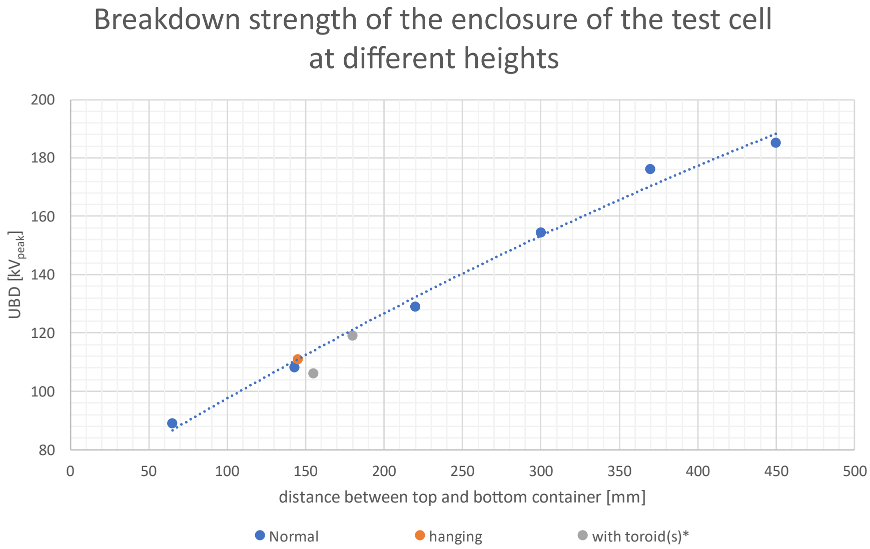

Figure A.21 Results of the investigation on the breakdown strength of the test cell.

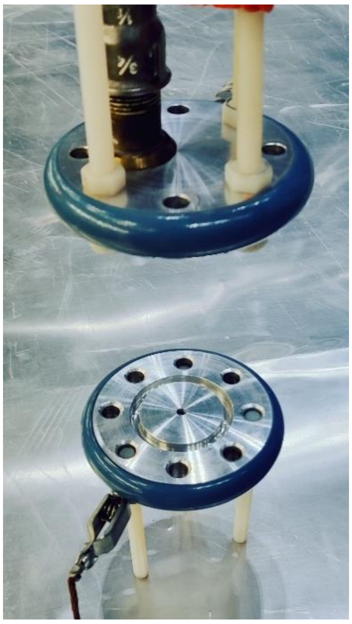

Figure A.22 The test cell without any triple points to see the effect of the triple points. This is done by floating the top of the test cell.

Figure A.23 The test cell after all the other adjustments were made.

Other adjustments made to the test cell

There were now two test cells with an improved maximum breakdown voltage of the enclosure of the test cell. Two components were however still missing, i.e. an extra female DILO connection and a pressure meter.

- The extra DILO connection is needed to make it possible to flush the test cells with other gases to remove any humidity.
- The pressure meter is needed to be able to check if the test cell leaks any gas.

A photo of the test cell with these adjustments is visible on Figure A.23.

Conclusion

The initial test cell had an initial breakdown strength of circa $53kV_{peak}$, i.e. the air on the outside of the enclosure of the test cell broke down at an applied voltage of $53kV_{peak}$. After several improvements the initial (small) test cell had an increased breakdown voltage of $90kV_{peak}$. A second version of the test cell was made with an height of roughly 40cm and a breakdown strength of circa $190kV_{peak}$.

A.4 How to alter the humidity of C4-FN/CO2 (5%/95%)

The humidity of C4-FN/CO2 (5%/95%) is altered in a 'mixing' vessel, visible on Figure A.24. The humidity of C4-FN/CO2 (5%/95%) is altered by combining gaseous water with dry C4-FN/CO2 (5%/95%). Gaseous water is water vapor which has a certain humidity. Combining both gases results in a changed humidity as that of the water vapor.

Procedure to create humidity

The humidity is altered through the following procedure:

1. Flush the test cell and mixing vessel with N2. This is done to ensure the equipment does not have any (remaining) humidity.
2. Flush the test cell and mixing vessel with dry C4-FN/CO2 (5%/95%) to ensure there is no other gas mixed with the to-be-created humid C4-FN/CO2 (5%/95%).
3. Evacuate the mixing vessel to 0,4$mbar_{abs}$. (The equipment in the lab could not vacuumize but evacuate to as low 0,4$mbar_{abs}$)
4. Inject a desired amount of water into the mixing vessel. This was done through the means of a switch, a connection piece and a small syringe. Photos of those components are given as Figure A.25, Figure A.26 and Figure A.27 respectively. Water vaporizes in 0,4$mbar_{abs}$ at circa -30 °C. This creates the water vapor.
5. Add the required amount of dry C4-FN/CO2 (5%/95%) until desired pressure is reached.
6. Wait circa 20 minutes until the mixing is saturated.
7. Transfer the humid C4-FN/CO2 (5%/95%) to vacuumized the test cell, by connecting the male DILO connection of the mixing vessel to the female DILO connection of the test cell.

There were however problems with step 4 and step 7. The problem and their solution are explained in the next sections.

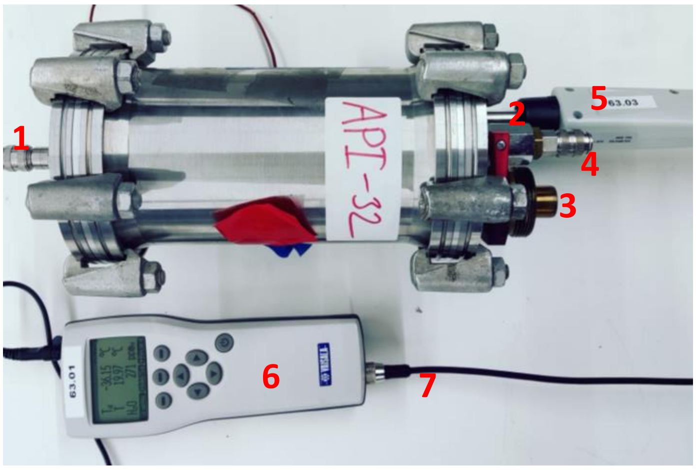

Figure A.24 Mix vessel to alter the properties of C4-FN/CO2 (5%/95%).

Nr.	Description
1	A male DILO connection, to act as outlet for the gas.
2	The red switch can be opened and closed to control the flow of the gas into the mixing vessel.
3	Connection for a pressure sensor.
4	A female DILO connection, to act as inlet for the gas.
5	Humidity probe DMP74B.
6	Handheld Dewpoint meter DM70.
7	Connection from probe to sensor.

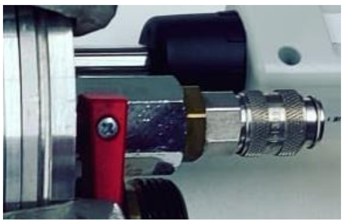

Figure A.25 A zoom-in of the red switch controlling the inlet flow of the gas on the mixing vessel.

Figure A.26 The connection piece which enables the syringe to inject the water into the mixing vessel.

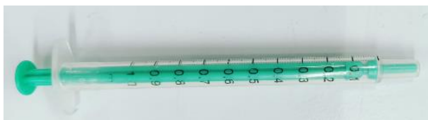

Figure A.27 The syringe used to inject the water. 1,0mL syringe with 100 marks.

Problem with step 4
The problem of step four was that not all of the injected water was evaporated, this was discovered through a lot of trial and error. A large part of the injected water was left behind in the connection piece, visible on Figure A.26. The connection piece and the syringe with the water needed to be weighed with precision, before and after the injection. This is required to get an accurate reading on how much water is evaporated and the humidity it would create. Performing multiple measurements by weighing the syringe and connection piece created a graph with the correlation between the water vaporized and the humidity in ppmv. The graph is shown in Figure A.28. Less than 0,01ml needs to be evaporated to get a humidity <5000ppmv at 1 bar_{abs}!

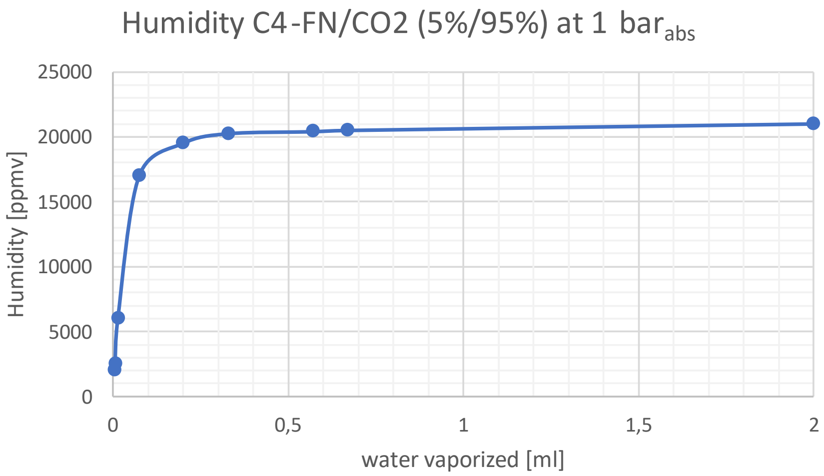

Figure A.28 Correlation between injected amount of water and created humidity in C4-FN/CO2 (5%/95%) at 1 bar_{abs}.

Figure A.29 Added grey switch to prevent problems occurring at step 7.

Problem with step 7
The problem of step seven was that during the coupling of the mixing vessel and test cell the gas mixture got polluted. Besides the humid C4-FN/CO2 (5%/95%), air got sucked into the vacuumized test cell as well. This ultimately created a gas mixture with unknown properties. Another problem was that during the decoupling of the mixing vessel and test cell some of the gas mixture escaped, resulting in a random small unknown reduction of pressure. This reduction was too small to be read of the mechanical pressure meter which was mounted on the test cell. Both problems had to be eliminated in order to do measurements where the only variable is the humidity.

Both these problems were solved by attaching a switch to female DILO connection of the test cell. A photo of the switch is given Figure A.29. The entire set-up for mixing the gas and monitoring the pressure and humidity is visible on Figure A.30.

<u>Solving the problem of the coupling procedure</u>
The test cell and mixing vessel will be connected before any flushing or vacuuming. This ensures that there is already a connection from the mixing vessel to the test cell for the transfer the humid C4-FN/CO2 (5%/95%). There is no possibility for air to get mixed into the created humid C4-FN/CO2 (5%/95%) as there is already a connection between the test cell and mixing vessel.

<u>Solving the problem of the decoupling procedure</u>
The grey switch is closed to prevent the gas mixture from leaving the test cell during the decoupling procedure. This prevents an unknown random amount of gas mixture leaving the test cell. It is now possible to perform all the experiments with a constant known pressure.

Figure A.30 The entire set-up for mixing the gas and monitoring the properties of C4-FN/CO2 (5%/95%)

A detailed explanation of injecting water in order to create humidity

This section explains how the humidity of the gaseous water is altered and controlled. The most common and used unit to indicate humidity is ppmv, which stands for parts per million by volume. This unit depends on the dewpoint temperature and pressure [7].

The following steps show how the humidity can be altered as desired [7].

- Humidity in ppmv can be calculated according to Equation A-3. The operating pressure will be constant, enabling the water vapor partial pressure (e) as the variable.
- The water vapor partial can be calculated according to Equation A-4. Equation A-4 shows that the water vapor partial pressure is a function of the dewpoint temperature.
- The dewpoint temperature can be calculated according to Equation A-5. The dewpoint temperature is a function of the temperature (T) and relative humidity (RH) of the gas.

This concludes that humidity can be altered through either the temperature or Relative Humidity. Injecting water into the mixing vessel increases the Relative Humidity. The increase in Relative Humidity increases the Dewpoint Temperature. The Dewpoint Temperature increases the water vapor partial pressure, which increases the humidity (in ppmv).

$$ppmv = \frac{e}{p - e} \cdot 10^6$$ *Equation A-3*

where
ppmv = humidity expressed in parts per million by volume
e = water vapor partial pressure [Pa]
p = total pressure at which e is measured [Pa]

$$e = 611{,}2 \exp\left(\frac{17{,}62 \cdot T_d}{243{,}12 + T_d}\right)$$ *Equation A-4*

where
e = water vapor partial pressure [Pa]
Td = Pew Point Temperature [°C]

$$T_d = \frac{237{,}7 \cdot \gamma(\mathrm{T,RH})}{17{,}27 - \gamma(\mathrm{T,RH})} \quad \text{with} \quad \gamma(\mathrm{T,RH}) = \frac{17{,}27 \cdot T}{237{,}7 + T} + \ln(RH/100)$$ *Equation A-5*

where
T = temperature of the gas [°C]
RH = relative humidity of the gas [%]

Choosing a suitable sensor
The literature review revealed that there are two measurement principles for measuring humidity, which is chilled mirror or capacitive sensor technology [7].

Chilled mirror technology
Light is aimed at a chilled mirror and a sensor measures the intensity of the direct reflected light. A chilled mirror with water vapor condensed on its surface scatters the light, resulting in a reduced signal intensity compared to a clean and dry mirror. By cooling the mirror to the temperature at which the detected light signal is constant, the dewpoint temperature of a gas mixture can be determined.

Capacitive sensor technology
These sensors use a hygroscopic polymer film. The capacitance of the hygroscopic polymer film is altered by the humidity surrounding the sensor. By measuring the capacitance of the hygroscopic polymer film the dewpoint temperature of a gas mixture can be determined.

By weighing the advantages against the disadvantages the chosen technology for the sensor is the capacitive sensor technology. A paper from the literature study listed the different advantages and disadvantages of the two technologies [7].

Possible sensors which have capacitive sensor technology
- The ‘C4-Analyser 3-in-1 (D-C4-3-039R-R301) of DILO’ is a device which can analyse C4-FN gas mixtures. This includes measuring the humidity of any C4-FN gas mixture. As of 3 November 2022 the price is 21.866 euro with a delivery time of 12 weeks.
- The ‘handheld dewpoint meter DM70 with probe DMP74B of Vaisala’ is a device which can measure the humidity of gas mixtures in a very broad temperature range. These gas mixtures included the used gas mixture for this research, i.e. C4-FN/CO2 (5%/95%). As of 4 November 2022 the price is 2.458 euro with a delivery time of 1 week.

The handheld dewpoint meter DM70 with the probe DMP74B is chosen as humidity sensor for this research based on the price and delivery time.

Conclusion
The humidity of C4-FN/CO2 (5%/95%) is altered by combining gaseous water with dry C4-FN/CO2 (5%/95%). Gaseous water is created by evaporating water in a hermetically sealed mixing vessel. Evaporating water inside the hermetically sealed mixing vessel increases the Relative Humidity. This increases the dewpoint temperature, which increases the water vapor partial pressure. The water vapor partial pressure increases the measured humidity. The humidity of C4-FN/CO2 (5%/95%) is measured with the handheld dewpoint meter DM70 with the probe DMP74B.

Altering the humidity of C4-FN/CO2 (5%/95%) is done with the following (improved) procedure:
1. The grey switch is mounted on top of the test cell.
2. The test cell with the grey switch is connected to the mixing vessel.
3. The grey switch and the red switch (near the inlet of the mixing vessel) are opened.
4. The entire set-up is evacuated to 0,4$mbar_{abs}$. The *Dilo Economy Series L057R01 service cart* is used for evacuating. The minimum evacuation limit for non-SF6 gases is 0,4$mbar_{abs}$.
5. The entire set-up is flushed with N2 to dry the set-up.
6. The entire set-up is evacuated to 0,4$mbar_{abs}$.
7. The entire set-up is flushed with dry C4-FN/CO2 (5%/95%). A lot of N2 particles are still present in the entire set-up because the entire set-up is evacuated to 0,4$mbar_{abs}$ and not 0bar_{abs}. Flushing with C4-FN/CO2 (5%/95%) replaces the remaining N2 particles with C4-FN/CO2 (5%/95%).
8. The entire set-up is evacuated to 0,4$mbar_{abs}$.
9. The grey switch is closed.

10. A certain amount of demineralized water is sucked into the syringe.
11. The syringe with water is weighed up to 3 decimals.
12. The connection piece is weighed up to 3 decimals.
13. The syringe is tightly connected to the connection piece. Both are connected to the inlet of the mixing vessel.
14. The red switch is opened allowing water to get sucked into the evacuated mixing vessel of 0,4$mbar_{abs}$. Water vaporizes in 0,4$mbar_{abs}$ at circa -30 °C, creating the gaseous water.
15. The syringe with water is weighed up to 3 decimals.
16. The connection piece is weighed up to 3 decimals.
17. Check if the required amount of water is evaporated. If not repeat steps 10 to 14.
18. C4-FN/CO2 (5%/95%) is added until the desired pressure is reached.
19. Wait until the mixing is stabilized, circa 20 minutes.
20. Check the final humidity on the handheld dewpoint meter DM70 measured by the DMP74B probe. If the desired humidity is not achieved restart the procedure at step 3.
21. Open the grey switch to transfer the created humid C4-FN/CO2 (5%/95%) from the mixing vessel to the test cell.
22. Close the grey switch.
23. Decouple the test cell *with* the closed grey switch from the mixing vessel.
24. Gas mixture is ready for testing.

Appendix B Measurement notes

Date: Exp. Nr.:

Uniform / quasi / non uniform	Gap distance: 5mm	Experiment at room temperature (~20°C)
Status electrode before testing:	Status electrode after testing:	

PREPERATION

Checklist (tick off if it is done. Humidity after briefly flushing with C4-FN must be <60ppmv)

	1. Vacuum	2. Flush N2	3. Vacuum	4. Flush C4-FN	5. Vacuum
Mixing vessel					
Test cell					
Inlet piece					
After mix vessel and test cell are both 3. Vacuum, connect everything together and briefly 2. Flush N2.					
Test cell connected with mixing vessel					

What pressure is needed in the test cell?

Pressure wanted in test cell		bar
$P_{mix\ vessel} = \frac{P_{test}(V_{mix\ vessel} + V_{test\ cell - xxxx})}{(V_{mix\ vessel}}$	$(P_1V_1 = P_2V_2)$	
$P_{mix\ vessel}$ =		bar

$V_{mix\ vessel}$	1,8876	dm^3
$V_{test\ cell\ -\ needle}$		dm^3
$V_{test\ cell\ -\ sphere}$		dm^3
$V_{test\ cell\ -plate}$		dm^3

The creation of humid gas:

mL syringe	Syringe + water **before** weight [g]	Syringe + water **after** weight [g]	Δ weight	Weight inlet piece **before** [g]	Weight inlet piece **after** [g]	Δ weight	Total water evaporated [mL]
Humidity at ______ bar setting C4-FN = ppmv				Humidity at _______ bar setting C4-FN = ppmv			
Waiting time between H2O and injecting C4-FN				min	Saturation time		min

Information of the gas in mixing vessel before filling test cell:

Temperature [T]		°C		Dewpoint temperature [Td]		°C
Pressure [P] $_{mix\ \vert\ test\ cell}$		bar		Relative Humidity [RH]		%
Humidity [H2O]		ppmv	(Recalculated with magnus law (see excel file))			

TESTING

Estimate UBD through short time test, no waiting time: Method of testing: rate-of-rise test

U_1		kV
U_2		kV
U_3		kV

80% UBD		kV
Rate of rise		kV/s

Rate of rise **before** 80% UBD		kV/s
Rate of rise **after** 80% UBD		kV/s
Waiting time consecutive tests		min

Test results

U_1		kV
U_2		kV
U_3		kV
U_4		kV
U_5		kV
U_6		kV
U_7		kV
U_8		kV
U_9		kV
U_{10}		kV
U_{11}		kV
U_{12}		kV

Remarks:

Appendix C Risk Assessment of Fluoronitrile

TUDelft	Safety Report Sheet	Version name: EEMCS-062022 Version number: V.0-2022 Page 1 of 4

Experiment Title: Electrical behaviour of C4-FN/CO2 mixture

Report number & Date: 2023-1 30 januari 2023

Name of the experimental unit: High Voltage Technology

User/Author & e-mail: Ewout van Veldhuizen - E.J.vanVeldhuizen@student.tudelft.nl
Paul van Nes - P.V.M.vanNes@tudelftnl

Section/Research Group: HVT

Location: High voltage laboratory

Supervisor/Approval: Mohamad Ghaffarian Niasar

Area Supervisor: Wim Termorshuizen

Review by: Paul van Nes

Researcher Phone Number in case of Emergency: 0624497200

1.1 Experiment Objective:

Breakdown strength of the gas mixture

1.2 Hazardous Materials Used (chemicals, gases, biological agents) & risk groups:

#	Material Name & formula	CAS#	Quantity	Unit	Chemwatch Hazard Ratings*			
1	2,3,3,3-tetrafluoro-(trifluormethyl)propane nitrile	42532-60-5	5	%	Flammability		Reactivity	
					Toxicity	x	Chronic	
					Body contact			
2	CO_2		95	%	Flammability		Reactivity	
					Toxicity		Chronic	
					Body contact			
3					Flammability		Reactivity	
					Toxicity		Chronic	
					Body contact			
4					Flammability		Reactivity	
					Toxicity		Chronic	
					Body contact			
5					Flammability		Reactivity	
					Toxicity		Chronic	
					Body contact			

* For MSDSs please visit "Chemwatch GoldFX" database through TUDL Database. Minimum = 0 ; Low = 1 ; Moderate = 2 ; High = 3 Extreme = 4.

- **Is there any CMR agents:** ?

- **Precautions for handling hazardous materials:** yes, see below

1.3 Equipment Safety:

Equipment name and description: Fume hood

Manufacturer, Model, Serial number:

CE Certified:

Equipment Owner (unit):

Main User/Administrator & email:

Safety instruction are given to users by:

Last safety inspection & inspection frequency:

Main findings:

Maintenance is carried out by who? and in what frequency?

More information:

1.4 Experiment main steps and HSE risks analysis:

	Explanation about the experiment (by steps)	Risk involved	Safety measures to be taken	Risk Evaluation
1)	**Storage / Preparation stage:** gas cylinder	Toxic	Handle with care	Low
2)	**Experiment stage 1**: Filling test cell	Toxic	In fume hood	low
3)	**Experiment stage 2**: Electrical breakdown test	Electrocution	Test as per HV lab rules	Low
4)	**End of the experiment stage:** Emptying of test cell	Toxic	In fume hood & use safety gloves	low

1.5 Emergency Readiness

General

Before you begin a practical research phase, please make sure the Emergency Response Team (BHV) coordinator of your unit/building is aware of the risks involved in your experiment. The emergency scenarios should be covered by the BHV emergency protocol and their capabilities to provide first aid assistance in case of an injury.

ERT coordinator name and email: Remco Koorneef

General (expected) emergency response to users:

(Please update those general statements together with the BHV coordinator, if necessary)

In case of evacuation / siren alarm:

- Evacuate the area, follow the escape route signs to the gathering point outside the building. Help others on your way out if it possible and safe;
- Close the doors after you if possible (do not lock them);
- If you have information about the reason for evacuation, please call TU Delft Emergency Control Room 015-2788888.

In case you noticed smoke or fire:

- Press the 'Emergency Machine Off (EMO)' button, if available;
- Evacuate the area (as described above), if relevant press the nearest 'Fire Alarm' manual button on your way out of the room/area;
- Contact TU Delft Emergency Control Room 015-2788888 as soon as possible.

In case of injury including exposure to hazardous materials:

- Immediately contact TU Delft Emergency Control Room 015-2788888, the Emergency response team (BHV) will be notified and provide first aid to the victim.
- If possible, in case of exposure to hazardous material, follow the following instructions (*instructions based on the material safety data sheet (MSDS) sections 4 should be added here*):

____
____
____
____

Emergency response to Emergency Response Teams (BHV & external rescue teams):

Please mention the relevant instructions from the Materials Safety Data Sheet (MSDS, sections 4,5,6, 10) for emergency response team:

Inhalation: place person in fresh air.
Skin contact: flush frosted skin with lukewarm water.
Eye contact: immediately flush with large amounts of water.
If swallowed: rinse mouth.
If still feeling unwell get medical attention

Additional information in case of emergency:

See 3M™ Novec™ 4710 Insulating Gas safety datasheet